

# Investigation of Hybrid Digital/Analog Pre-Distortion of GaN Power Amplifier

by

Marwa MGADMI

THESIS PRESENTED TO ÉCOLE DE TECHNOLOGIE SUPÉRIEURE  
IN PARTIAL FULFILLMENT OF A MASTER'S DEGREE  
WITH THESIS IN ELECTRICAL ENGINEERING  
M.A.Sc.

MONTREAL, MARCH 30, 2021

ÉCOLE DE TECHNOLOGIE SUPÉRIEURE  
UNIVERSITÉ DU QUÉBEC



Marwa Mgadmi, 2021



This Creative Commons license allows readers to download this work and share it with others as long as the author is credited. The content of this work cannot be modified in any way or used commercially.

**BOARD OF EXAMINERS**

**THIS THESIS HAS BEEN EVALUATED  
BY THE FOLLOWING BOARD OF EXAMINERS**

Mr. Ammar B. Kouki, Thesis supervisor  
Department of Electrical Engineering, École de technologie supérieure ÉTS

Mr. Naïm K. Batani, President of the board of examiners  
Department of Electrical Engineering

Mr. Handy Fortin Blanchette , External examiner  
Department of Electrical Engineering

**THIS THESIS WAS PRESENTED AND DEFENDED  
IN THE PRESENCE OF A BOARD OF EXAMINERS AND THE PUBLIC  
ON "MARCH 24, 2021"  
AT ÉCOLE DE TECHNOLOGIE SUPÉRIEURE**





## **ACKNOWLEDGEMENTS**

First and foremost, I extend my wholehearted thanks to professor Ammar B. Kouki, my supervisor, for his invaluable guidance, insight, and encouragement throughout this thesis. As well, I would like to thank Mr. Normand Gravel for his patience and help during my research work in the LACIME laboratory.

My gratitude also goes out to all the students and LACIME lab members for their generous support during this research project.

In addition, I offer tremendous thanks to Libya's Ministry of Education for their financial support of my studies and to their academic manager at the CBIC office in Canada.

As always, I am grateful to my family for being there for me. I thank my fantastic sisters and brothers, especially my brother Mustafa.

Thank you, too, to my father, for your brilliant advice and constant supervision. You have given me confidence and strength always to take one step further and challenge myself. Mom, your unconditional love and wisdom have helped me survive the difficult times. My parents: this thesis is dedicated to you.

I also dedicate this thesis to my husband, Aimen Zekri, and my sons, who have always stood by me and without whom the completion of this work would not have been possible.

I am pleased to be studying at ETS. I was motivated by the international environment at ETS to highlight my technological skills, and my knowledge and awareness have increased substantially.



# **Enquête Sur La Pré-Distorsion Hybride Numérique/Analogique De L'Amplificateur De Puissance GaN**

Marwa MGADMI

## **RÉSUMÉ**

De nos jours, les gens profitent de plus en plus des avantages du développement rapide des communications sans fil. Cependant, le nombre croissant de ces applications conduit à une augmentation de la demande de services de spectre qui font concurrence aux ressources à bande étroite. Une solution est d'augmenter les ressources de bande de disponibilité, mais une meilleure utilisation de la bande passante serait plus efficace. La technique de multiplexage par répartition orthogonale de la fréquence (OFDM) est utilisée dans les réseaux sans fil de quatrième génération (4G) et le Wi-Fi standard. Dans un signal OFDM, le signal d'enveloppe est non constant et il a généralement un rapport de puissance crête et puissance moyenne (PAPR) en hausse le rendant très sensible à la distorsion induite par la réponse non linéaire des composants des systèmes de transmission.

La puissance est un problème dans les applications sans fil où les amplificateurs de puissance (APs) sont un contributeur à la consommation électrique au stade de la transmission; les APs sont également un facteur important de la distorsion du signal. Les systèmes sans fil modernes nécessitent généralement un signal à large bande passante et un débit de données rapide, ce qui en contribue à une consommation accrue d'énergie. Ces exigences conduisent également à la nécessité de convertisseurs analogique-numérique (CAN) de plus haute précision et convertisseurs numérique-analogique (CNA). En conséquence, la complexité du système augmente en raison de l'augmentation des exigences matérielles.

Les techniques de linéarisation pré-distorsion sont non seulement les plus efficaces mais aussi les plus prometteuses des technologies de communication sans fil. Cependant, la pré-distorsion analogique et la pré-distorsion numérique, lorsqu'elles fonctionnent seules, présentent des avantages et des inconvénients complémentaires, alors que lorsqu'elles fonctionnent ensemble, elles se complètent. Plus précisément, la pré-distorsion analogique peut être très large bande mais ses performances limitées, tandis que la pré-distorsion numérique peut fournir d'excellentes performances mais ne peut pas gérer des signaux très large bande.

Pour surmonter ces problèmes, l'approche hybride de pré-distorsion est une solution bien connue, mais seules quelques études dans la littérature ont montré les performances de cette technique. De ces quelques études, aucune n'a examiné les exigences matérielles pour CAN et CNA. Dans ce contexte, la méthode de linéarisation combinée est proposée dans cette thèse. La méthode s'appelle un hybride de pré-distorsion numérique / analogique du GaN PA sélectionné basé sur une pré-distorsion analogique classique et une pré-distorsion numérique polynomiale à mémoire pour un signal à large bande.

Les principaux objectifs de cette approche sont d'obtenir des performances de linéarisation optimales et réduire les exigences matérielles en utilisant CAN et CNA à basse précision. Cette

méthode permet d'utiliser des longueurs de mot plus courtes dans l'algorithme de pré-distorsion numérique, économisant à la fois de la puissance et de la surface. Cela donne également une charge de fréquence d'échantillonnage plus élevée pour tout l'algorithme de pré-distorsion numérique. Dans le travail proposé, un système de conception avancé (ADS) et un modèle Simulink / MATLAB sont utilisés. Les résultats obtenus montrent un excellent accord avec l'approche hybride proposée pour les signaux à large bande, et une meilleure amélioration rapport de puissance de canal ajusté et troisième produit d'intermodulation là où elles sont supprimées. De plus, la résolution de l'CAN dans le modèle proposé est réduite à 8 bits.

**Mots-clés:** Hybride, APD, DPD, linéarité, exigences matérielles, GaN PA

# **Investigation of Hybrid Digital/Analog Pre-Distortion of GaN Power Amplifier**

Marwa MGADMI

## **ABSTRACT**

People all over the world are increasingly enjoying the benefits of the rapid development of wireless communication. However, the rising number of these applications is leading to an increase in demand for spectrum services that compete with narrow band resources. One solution is to increase the availability band resources, but better use of the current bandwidth would be more efficient. The orthogonal frequency division multiplexing (OFDM) technique is used in fourth generation (4G) wireless networking and standard Wi-Fi. In an OFDM signal, the envelope signal is non-constant and it typically has a rise peak-to-average power ratio (PAPR), making it highly susceptible to distortion induced by nonlinear inline component response in transmission systems.

Power is a concern in wireless applications where power amplifiers (PAs) are a primary contributor to power consumption at the transmission stage; PAs are also a significant factor in signal distortion. Modern wireless systems generally require a wide-band signal and a faster data rate, making them a significant issue for increased power consumption. These requirements also lead to the need for higher precision analog-to-digital converters (ADCs) and digital-to-analog converters (DACs). As a result, the system's complexity increases due to increases in the hardware requirements.

Pre-distortion linearization techniques are not only the most efficient but also the most promising of wireless communication technologies. However, both analog pre-distortion (APD) and digital pre-distortion (DPD), when working alone, have complementary advantages and disadvantages, whereas when they work together, they complement each other. Specifically, analog pre-distortion can be very wide-band but limited in performance, while digital pre-distortion can provide excellent performance but cannot handle very wide-band signals.

To overcome these problems, the hybrid pre-distortion approach is a well-known solution, but only a few studies in the literature have shown the technique's performance. Of these few studies, none have examined the hardware requirements for ADC and DAC. In this context, a combined linearization method is proposed in this thesis. The method is called a hybrid digital/analog pre-distortion of the selected GaN PA based on conventional analog pre-distortion and memory polynomial digitalpre-distortion (DPD) for a wide-band signal. The main aims of this approach are to achieve better linearization performance and to reduce the hardware requirements by using low-precision ADCs and DACs. This method enables shorter word-lengths to be used in the digital pre-distortion algorithm, saving both power and area when the technique is implemented. It also gives a higher sample rate for the entire digital pre-distortion algorithm (DPD). Advanced design system (ADS) and Simulink/MATLAB are used to perform this work. The results obtained show excellent agreement with the proposed wide-band signals hybrid approach, achieving the strongest third order intermodulation products (IMD3) and adjusted channel power

ratio (ACPR) enhancement where they are suppressed. Additionally, the bit resolution of the target ADC in the proposed model is reduced to 8 bit.

**Keywords:** Hybrid, APD, DPD, linearity, hardware-requirements, GaN PA

## TABLE OF CONTENTS

	Page
INTRODUCTION .....	1
CHAPTER 1    NONLINEARITY AND LINEARIZATION FUNDAMENTALS .....	7
1.1    Introduction .....	7
1.2    Nonlinear behaviour of PA .....	7
1.3    Harmonic distortion and Intermodulation distortion .....	8
1.3.1    AM/AM and AM/PM conversion .....	10
1.3.2    Linearity versus efficiency .....	11
1.4    Power amplifier performance-evaluating metrics .....	13
1.4.1    Error vector magnitude (EVM) .....	13
1.4.2    Adjacent channel power ratio (ACPR) .....	14
1.5    PA linearization techniques .....	15
1.5.1    Feedback .....	15
1.5.2    Feedforward .....	15
1.5.3    Pre-distortion .....	16
1.6    Conclusion .....	18
CHAPTER 2    STATE OF THE ART .....	19
2.1    Digital pre-distortion .....	19
2.2    Comparison between analog and digital pre-distortion .....	25
CHAPTER 3    GAN AMPLIFIER LINEARIZATION .....	27
3.1    Modeling of selected GaN PA/ ADS software .....	28
3.1.1    Specification of GaN PA .....	28
3.1.2    ADS model of selected GaN PA .....	29
3.2    Proposed analog pre-distortion circuit/ADS software .....	33
3.3    Requirements of the proposed APD circuit .....	35
3.3.1    Characterization and simulation of ADP circuit's linear control path .....	35
3.3.1.1    3 dB hybrid coupler .....	36
3.3.1.2    Wilkinson divider/combiner .....	38
3.3.2    Characterization and simulation of ADP circuit's nonlinear control branch .....	40
3.3.2.1    Simulation of Schottky diode .....	42
3.3.3    Simulation and linearization results of APD circuit .....	43
3.4    Proposed digital pre-distortion (DPD) model/Simulink-MATLAB .....	45
3.4.1    Workflow of proposed DPD circuit .....	46
3.4.2    Implementation and linearization results of proposed DPD system .....	49
3.4.3    Hardware requirements .....	54
3.4.4    Basics of analog-to-digital converters (ADCs) .....	56
3.4.5    Converting proposed DPD model to fixed-point design .....	58

3.5	Conclusion .....	65
CHAPTER 4 HYBRID DIGITAL/ANALOG PRE-DISTORTION METHOD .....		67
4.1	Comparison of results between hybrid approach, DPD only, and APD only .....	71
4.2	Conclusion .....	78
CONCLUSION AND RECOMMENDATIONS .....		79
APPENDIX I SELECTED GAN POWER AMPLIFIER .....		83
APPENDIX II SCOTTKY DIODE SMS392X SERIES OF DIODES .....		85
APPENDIX III LMS AND RPEM ALGORITHM .....		87
APPENDIX IV CONVERTING DPD SIMULINK MODEL TO FIXED-POINT DESIGN MODEL .....		89
APPENDIX V SIMPLE FAST-FITTING PROCEDURE/ MATLAB-CODE .....		91
APPENDIX VI CALCULATING THE COEFFICIENT OF PA/ MATLAB-CODE .....		95
APPENDIX VII POWER GAIN TRANSFER FUNCTION AND ITS FITTING .....		97
BIBLIOGRAPHY .....		98



## LIST OF TABLES

	Page
Table 0.1      Comparison Between APD and DPD .....	3
Table 0.2      Comparison Between APD and DPD .....	3
Table 1.1      Coefficients Corresponding to Each Order for Distortion Product of Two-Carrier Excitation .....	9
Table 1.2      PA Classification .....	12
Table 1.3      Comparison of PA Linearization Techniques for System Level Approach .....	18
Table 3.1      Electrical Specifications of GaN PA .....	28
Table 3.2      GaN PA Model Parameters for ADS .....	29
Table 3.3      Comparison of 3dB Hybrid Coupler Specification and Simulation Results .....	38
Table 3.4      Comparison of Wilkinson Divider/Combiner Specification and Simulation Results .....	40
Table 3.5      The linearity result of the cascade (APD + GaN PA) .....	45
Table 3.6      Compression Results of ACPR Improvement and IMD3 Improvement for the Various Suggested Bandwidths .....	53
Table 3.7      ADC Requirements for Various Applications .....	55
Table 3.8      Standard Bit Depth, Number of Levels and Step Size for 5v Reference .....	58
Table 3.9      Precision of Target ADC in Each Model for Various Proposed Word- lengths/DPD Technique .....	59
Table 3.10     Visualization of Simulation Data Using Proposed Data Type of 16 bit for Proposed Bandwidth/DPD Model Only .....	60
Table 3.11     Visualization of Simulation Data Using Proposed Data Type of 12 Bit for Proposed Bandwidth/DPD Model Only .....	61
Table 3.12     Visualization of Simulation Data Using Proposed Data Type of 10 Bit for Proposed Bandwidth/DPD Model Only .....	62

Table 3.13	Visualization of Simulation Data Using Proposed Data Type of 6 Bit for Proposed Bandwidth/DPD Model Only .....	62
Table 3.14	Pipeline (high-speed) ADCs Available in the Market for Suggested Model with Applying DPD Only .....	64
Table 3.15	Pipeline (high-speed) ADCs for Proposed Hybrid Digital/Analog Pre-Distortion Model .....	64
Table 4.1	Compression Results Between DPD Only, APD Only, and Hybrid Digital/Analog Pre-Distortion (ACPR and IMD3 Improvement) .....	72
Table 4.2	Precision of Target ADC in Proposed Hybrid Digital/Analog Pre-Distortion Model for Various Proposed Word-Lengths .....	74
Table 4.3	Visualization of Simulation Using Proposed data type for Target ADCs with Proposed Bandwidth of 100MHz/Hybrid Digital/Analog Pre-Distortion Model .....	75
Table 4.4	Visualization of Simulation Using Proposed Data Type for Target ADCs with Proposed Bandwidth of 1GHz/Hybrid Digital/Analog Pre-Distortion Model .....	76
Table 4.5	Pipeline (high-speed) ADCs Available in the Market for Proposed Hybrid Digital/Analog Pre-Distortion Model .....	77
Table 4.6	Pipeline (high-speed) ADCs for Proposed Hybrid Digital/Analog Pre-Distortion Model .....	77

## LIST OF FIGURES

	Page
Figure 1.1      Distortion product of two-carrier excitation Pozar (2000) .....	8
Figure 1.2      Illustration of third-order intercept point excitation Pozar (2000) .....	9
Figure 1.3      AM/AM and AM/PM characteristics of model PA Colantonio, Giannini & Limiti (2009) .....	11
Figure 1.4      Linearity vs efficiency .....	12
Figure 1.5      Error vector magnitude of QPSK .....	13
Figure 1.6      Definition of adjacent channel power ratio (ACPR) .....	14
Figure 1.7      Feedback linearization technique .....	15
Figure 1.8      Feedforward linearization technique .....	16
Figure 1.9      Pre-distortion linearization technique .....	17
Figure 1.10     Scenario of pre-distortion .....	17
Figure 1.11     Operation region .....	18
Figure 2.1      Block diagram of baseband digital pre-distortion .....	23
Figure 2.2      Transmitter using indirect learning architecture estimator for DPD .....	24
Figure 2.3      Block diagram of full-band DPD simulation performed .....	24
Figure 3.1      GaN vs other technologies .....	27
Figure 3.2      S-Parameters of GaN PA .....	29
Figure 3.3      ADS simulation model of GaN amplifier at 6GHz .....	30
Figure 3.4      Variations in output power of GaN amplifier at 6GHz .....	31
Figure 3.5      AM-AM conversion of GaN amplifier at 6GHz .....	32
Figure 3.6      Power-added efficiency (PAE) of GaN amplifier at 6GH .....	32
Figure 3.7      Intermodulation products of two-tone simulations .....	33

Figure 3.8	Structure of proposed APD (cubic pre-distortion) .....	34
Figure 3.9	Operation of APD circuit (cubic pre-distortion) of two carrier signals .....	35
Figure 3.10	Schematic diagram of 3dB hybrid coupler .....	36
Figure 3.11	Parameters of transmission lines for characteristic impedance $50\Omega$ and $35.3553\Omega$ of 3dB hybrid coupler .....	37
Figure 3.12	Simulation of S-parameters of 3dB hybrid coupler .....	38
Figure 3.13	Wilkinson divider/combiner .....	39
Figure 3.14	Parameters of transmission lines for characteristic impedance $50\Omega$ and $70.71\Omega$ of Wilkinson divider/combiner .....	40
Figure 3.15	Simulation of S-parameters of Wilkinson divider/combiner .....	41
Figure 3.16	Structure of distortion generator (GD) .....	41
Figure 3.17	Characteristic I (V) simulation of pair of Schottky SMS 3922 diodes .....	42
Figure 3.18	Schematic of APD circuit with GaN PA model .....	43
Figure 3.19	Comparison between responses of simulation GaN PA without and with APD (AM/AM) .....	44
Figure 3.20	Comparison between responses of simulation GaN PA without and with APD (output power) .....	44
Figure 3.21	Proposed baseband DPD circuit model .....	46
Figure 3.22	Input and output complex measurement of I/Q data for various proposed sample rates (25MHz, 100MHz and 1GHz) .....	47
Figure 3.23	Absolute value of output and fitting output signals for sample rate of 25MHz .....	48
Figure 3.24	Simulation DPD Block .....	48
Figure 3.25	DPD operation point .....	50
Figure 3.26	EVM without applying DPD algorithm .....	50
Figure 3.27	EVM with applying DPD technique for various proposed sample rates (25MHz, 100MHz and 1GHz) .....	51

Figure 3.28	Spectrum analyzer for input and output signal of PA with and without applying DPD algorithm for suggested sample rates (100MHz and 1GHz) .....	52
Figure 3.29	Comparison of PA output signal without/with applying DPD technique for bandwidth of 25MHz and 1GHz .....	52
Figure 3.30	Comparison of PA output signal without/with applying DPD technique for bandwidth of 100MHz .....	53
Figure 3.31	(AM/AM) with and without applying DPD .....	54
Figure 3.32	Output power (transfer function) with and without applying DPD .....	54
Figure 3.33	Bandwidth/resolution relationship for different applications Taken from Tex (2018) .....	55
Figure 3.34	Bandwidth/resolution for different topologies of ADC and DAC Taken from Tex (2018) .....	56
Figure 3.35	Converting suggested 100MHz double floating-point design model to fixed-point mode .....	61
Figure 3.36	Converting suggested 1GHz double floating-point design model to fixed-point model .....	63
Figure 4.1	Implemented DPD and APD series in proposed model .....	67
Figure 4.2	Block diagram of proposed hybrid digital/analog pre-distortion system .....	70
Figure 4.3	Spectrum analyzer for baseband signal, nonlinear PA applying pre-distortion methods (APD, DPD, and hybrid approach) for signal envelope bandwidth of 100MHz .....	71
Figure 4.4	Spectrum analyzer for applying pre-distortion methods (APD, DPD, and the hybrid approach) for signal envelope bandwidth of 100MHz .....	72
Figure 4.5	Spectrum analyzer for baseband signal and nonlinear PA, applying pre-distortion methods (APD, DPD, and hybrid approach) for signal envelope bandwidth of 1GHz .....	73
Figure 4.6	Spectrum analyzer for applying pre-distortion methods (APD, DPD, and hybrid approach) for signal envelope bandwidth of 1GHz .....	74

Figure 4.7	Sample rate as function of resolution bits of the target (high-speed ADC) in the proposed model with applying DPD only and Hybrid digital/ analog pre-distortion .....	78
------------	--	----

## LIST OF ABBREVIATIONS

AM/AM	Amplitude-to-Amplitude conversion
PAE	Power Added Efficiency
AM/PM	Amplitude-to-Phase conversion
EVM	Error Vector Magnitude
ACPR	Adjacent Channel Power Ratio
PAR	Power-Average-Ratio
FB	FeedBack
FF	FeedForward
PD	Pre-Distortion
VS	Volterra Series
GMP	Generalized Memory Polynomial
DDR	Dynamic Deviation Reduction
MP	Memory Polynomial
M	Memory depth
K	Linearity Order
LUT	Lookup Table
LS	Least Squares algorithm
LMS	Least Mean Squares algorithm
RSL	Recursive Least Squares algorithm

XX

RPEM	Recursive Predictor Error Method
LTE	Long-Term-Evolution
DPA	Doherty Power Amplifier
HEMT	High-Electron-Mobility-Transistor
PA	Power Amplifier
RF	Radio Frequency
GaN	Gallium Nitride
TWTA	Traveling Wave Tube Amplifier
GaAs	Gallium Arsenide
ILA	Indirect Learning Architecture
BB	Baseband
DPD	Digital Pre-Distortion
APD	Analog Pre-Distortion
DSP	Digital Signal Processing
IMD	Intermodulation Product
ADC	Analog-to -Digital Converter
DAC	Digital-to-Analog Converter
IM3	Third-Order Intermodulation
IIP3	Input Third Intercept Point
OIP3	Output Third Intercept Point



GD	Distortion Generator
S	S-parameters
PAR	Peak to Average Ratio
SNR	Signal-to-Noise Ratio
LO	Local Oscillator
$\eta_{added}$	Power Added Efficiency



## **LIST OF SYMBOLS AND UNITS OF MEASUREMENTS**

<b>dBm</b>	Decibels relative to one milli watt
<b>dBc</b>	Decibels relative to the carrier
<b>MHZ</b>	Mega Hertz
<b>GHZ</b>	Giga Hertz
<b>mm</b>	Millimeter
<b>W</b>	Watt



## INTRODUCTION

In recent years, wireless applications, along with mobile and wireless communication devices, have experienced exponential growth both in industry and development. As wireless technologies become more and more powerful, in order to satisfy the demands of current and future wireless communication systems, design engineers and research groups are involved in three main development aspects. The first of these aspects is reducing wasted power consumption to save energy in order to reduce wasted cost. The second development aspect is providing faster data transmission to offer better service to more users, and the third is reducing hardware requirements to lower power consumption and decrease the carbon footprint of the wireless communication system.

A major essential component in wireless communication systems is the radio frequency (RF) power amplifier (PA). In the radio transmitter chain, PAs are responsible for amplifying the communication signal to power levels sufficient for transmission Hsia, Kimball & Asbeck (2011). PAs are also a primary contributor to energy consumption at the transmission stage as well as a significant factor in signal distortion. If left unchecked, distortions may lead to increased losses and possible interference with other radio channels. Thus, there are two aspects that PAs in RF transmitters must have: good linearity and high efficiency. Specifically, PAs should be sufficiently linear to ensure a good quality of transmitted signals from an RF transmitter and be highly efficient to extend the battery life in handset applications.

The gallium nitride (GaN) power amplifier has contributed significantly to improving the output of RF PAs, with GaN transistors providing higher power densities, more bandwidth, and improved dc-to-RF efficiencies Walt (2016). GaN-based transistor can quickly produce tens to hundreds of watts at RF frequencies of around 10 GHz Walt (2016). Travelling wave tube (TWTA) amplifiers can be substituted in satellites and radar. For instance, in Walt (2016), travelling wave tube (TWT) devices and TWT amplifiers were replaced by GaN-based X-band

amplifiers capable of 8 KW pulsed output power Woo, Miller & Kenney (2005). Compared to Gallium arsenide (GaAs) equipment, GaN device designers have developed an interest in RF power because it supports very high operating voltage up to 80 V (three or five times higher GaAs). Furthermore, GaN has a power density ranging from 2 to 5  $W/mm^2$ , while GaAs has a power density of around 1.5  $W/mm^2$ . Overall, GaAs power equipment is generally considered to be more linear compared to GaN devices but has less efficiency Katz & Dorval (2012). In recent years, the most researched topic in relation to RF power amplifier designer has been linearized GaN power amplifiers.

In the design of a power amplifier, the efficiency versus linearity trade-off is a critical aspect. Unfortunately, the high efficiency and good linearity of PAs are complicated to implement because of the different problems related to the type and operation of PAs. In this case, designers usually emphasise the efficiency of PAs in the design process and then use linearization methods to restore linearity.

To reach high efficiency and a good linearity trade-off, there are two significant research approaches. The first approach is to increase the power efficiency by developed PA techniques, such as envelope-tracking Braithwaite (2015) and Doherty amplifier methods Srirattana, Raghavan, Heo, Allen & Laskar (2005). The second approach lengthens PA's linear range through applying some linearization techniques. Several studies cover the linearization of power amplifiers, the main techniques of which are feedback, feedforward, and pre-distortion.

Pre-distortion linearization is the most efficient and promising of the three mentioned techniques. It is classified into two types: digital pre-distortion (DPD) and analog pre-distortion (APD). APD circuits are much simpler than DPD ones and are also much smaller. However, APD has a few disadvantages which have resulted in less improvement in performance. In addition, APD cannot be used to suppress the memory effect impact. On the other hand, DPD has shown superior performance compared to APD. For instance, DPD is faster and more flexible in handling data

than analog signal processing. But, like APD, DPD also has drawbacks, the main one being its limited bandwidth at the start of the signal chain (the digital baseband). As channel bandwidth of an RF signal becomes wide, this becomes more and more a significant problem. Also, to correct distortion up to the fifth-order IMD product, the sampling rate must be at least five times greater than the RF signal bandwidth. High sampling rates burden the entire DPD system, leading to high power consumption and system complexity. With the trend of endlessly increasing the bandwidth of RF signals

The following tables show a simple comparison of the main features of ADP and DPD.

Table 0.1 Comparison Between APD and DPD

<b>Type of Pre-Distortion</b>	<b>Power Consumption</b>	<b>Complexity</b>	<b>Linearization Performance</b>
APD	Low	Low	Low
DPD	High	High	High

Table 0.2 Comparison Between APD and DPD

<b>Type of Pre-Distortion</b>	<b>Support</b>	<b>Bandwidth</b>
APD	Memoryless	High
DPD	Memory effect	Low

Digital pre-distortion is known as a block that has reverse transfer characteristics compared to those of PA. DPD is inserted in front of a PA, resulting in the linear behavior of the full model. There are two critical steps to realizing DPD: The first step is the PA behavioural modelling, and the second step is the identification pre-distortion algorithm. The most popular approach for determining the pre-distortion is Indirect Learning Architecture (ILA) Braithwaite (2015), due to its ease of implementation and fast convergence. In ILA, a post-PA feedback path after the PA is needed, which has a down-converter and analog-to-digital converter (ADC) Katz, Wood & Chokola (2016). In a wideband signal, the ADC sampling rate has to be swift.

Particularly for mobile applications, cost and power are an issue. A way to deal with this problem may be to employ ADC with low precision to reduce the complexity of the system. This is one reason to choose a hybrid digital/analog pre-distortion method, which is a relatively new research area Xie (2017). In the hybrid approach, the DPD algorithm is implemented using word-lengths that are relatively shorter, thus saving on both energy usage and area. At the same time, it is worth noting that ADCs that have low precision typically use less energy compared to higher precision devices and also support faster sampling rates.

In the best of all possible worlds, digital pre-distortion and analog pre-distortion complement each other. It is because APD can be very wideband but tends to be limited in performance, while DPD can provide excellent performance but cannot handle very wideband signals. A hybrid approach may offer superior performance, such as reducing hardware requirements with larger bandwidth.

### **Problem statement**

Pre-distortion is well-suited as a linearization technique to provide optimum power amplifier output with sufficient linearity, due to the advantages and disadvantages of digital pre-distortion (DPD) and analog pre-distortion (APD). On the one hand, APD can be very wideband but limited in performance, while on the other hand, DPD can provide outstanding output but cannot handle a wideband signal. This becomes a drawback when a wideband signal is needed in the modern system. Moreover, it can at times become a major problem, requiring higher number of bits for the resolution of (ADCs) and digital-to-analog converters (DACs), leading to increased system complexity as well as increased power consumption.



## **Thesis objective**

The main aim of this project is combining the advantages of both APD and DPD linearization methods to create a hybrid digital/analog pre-distortion of the selected GaN PA. In order to reduce resolution bit of ADCs and DACs as a function of signal bandwidth. result in the DPD algorithm having a word-length that is relatively short, thus saving on energy and area required. Besides, it would achieve better performance of the APD linearization.

## **Thesis organization and contribution**

The remainder of the chapters are arranged as follows:

**Chapter 1** introduces and highlights the different parameters that quantify the nonlinearity of a PA. As well, the different linearization techniques are described.

**Chapter 2** presents a literature review, which includes existing information, theoretical findings, and methodological limitations related to the thesis topic.

**Chapter 3** covers the modelling of a GaN PA at 6 GHz and obtaining its nonlinear model in ADS. It presents a conventional analog pre-distortion (APD) circuit in ADS, and combines it with the PA to obtain a linearized response. A digital pre-distortion (DPD) with memory effect is presented and discussed, which models it using Simulink/MATLAB, and the requirements of bandwidth and level of nonlinearity for the selected PA are quantified. Additionally, the simulation model is converted to a fixed-point design to define the number of bits for the resolution that the DPD algorithm requires, which helps to select the right ADC and DAC for our model, where we focus on ADC.

**Chapter 4** covers the proposed hybrid digital/analog pre-distortion approach and quantifies the performance improvement and resource requirements reducing compared to the DPD system. This work may help decrease the carbon footprint of wireless communication systems.

Finally a conclusion, and recommendation for future works complete the report.



## CHAPTER 1

### NONLINEARITY AND LINEARIZATION FUNDAMENTALS

#### 1.1 Introduction

Power Amplifiers (PAs) for Radio Frequency (RF) are critical importance in today's communication infrastructure. The task of a power amplifier (PA) is to amplify the transmission signal and produce the required RF power that authorizes the signal to be transmitted over a suitable range or spectrum. However, the nonlinearity distortion phenomenon in PAs can lead to unwanted effects that may result in increased losses, signal distortion, and possible interference with other radio channels. PA linearity vs. efficiency are relatively recent considerations in this technology, so designers have typically prioritized the efficiency of power amplifiers (PAs) in the design process and later recovered the linearity using linearization methods. The purpose of this chapter is to represent the linearity problem of the amplifier in general and to highlight the different parameters that quantify the nonlinearity of a PA. Various methods for improving the linearity of amplifiers are discussed at the end of the chapter.

#### 1.2 Nonlinear behaviour of PA

Due to nonlinear phenomena caused by semiconductor restrictions in PAs, the output signal becomes a different version of the input signal. Nevertheless, if a PA produces an approximation of the 5th order power series, the output voltage of the PA is calculated as a function of the input voltage, as follows:

$$V_{out} = a_1 V_{in} + a_2 V_{in}^2 + a_3 V_{in}^3 + 4V_{in}^4 + 5V_{in}^5 \quad (1.1)$$

where:

$V_{out}$  is PA output voltage.

$V_{in}$  is the input voltage.

$a_1, a_2, a_3, a_4, a_5$  are amplifications coefficients.

Let us consider a two-tone signal as input to the PA. Assuming that the two carriers have the same amplitude  $A$  and frequencies  $\omega_1$  and  $\omega_2$ , respectively, we can write:

$$V_{in} = A(\cos(\omega_1 t) + \cos(\omega_2 t)) \quad (1.2)$$

The PA output can be expressed as in Figure 1.1 below, which illustrates the coefficients corresponding to each order.

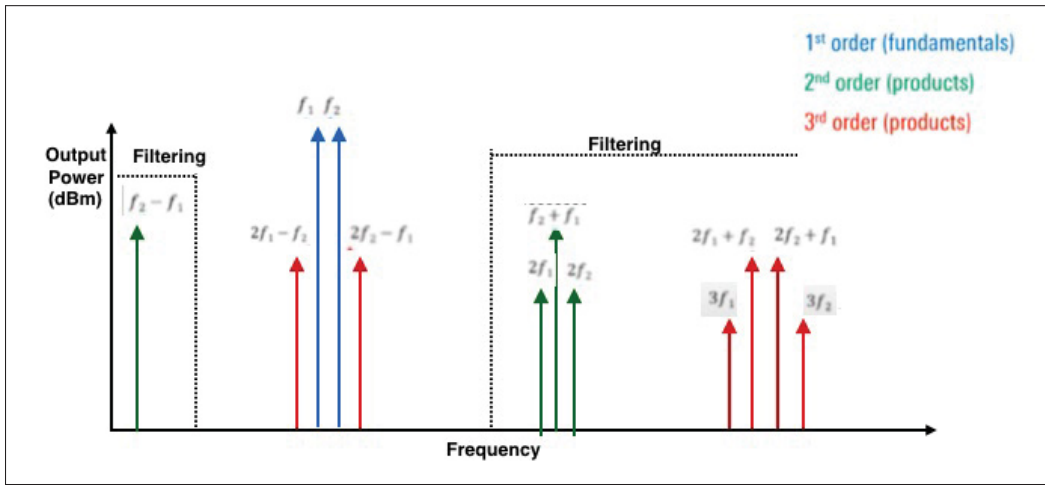


Figure 1.1 Distortion product of two-carrier excitation  
Pozar (2000)

### 1.3 Harmonic distortion and Intermodulation distortion

According to Table 1.1, the produced frequency components can be classified in two categories: Intermodulation (IM) components and harmonic components. Figure 1.1 presents an output spectrum of a two-carrier excitation.

Harmonic components: Since the harmonic components occur at frequencies high above the desired frequency, this is not a significant problem, so the filtering can be carried out quite easily where the harmonics interfere with another system within the communication system.

Table 1.1 Coefficients Corresponding to Each Order for Distortion Product of Two-Carrier Excitation

Frequency	Amplitude
0(dc)	$A^2 a_2$
$w_1$	$\frac{Aa_1+9A^3a_3}{4}$
$w_2$	$\frac{Aa_1+9A^3a_3}{4}$
$2w_1$	$\frac{A^2a_2}{2}$
$2w_2$	$\frac{A^2a_2}{2}$
$w_1 \pm w_2$	$A^2a_2$
$2w_1 \pm w_2$	$\frac{3A^3a_3}{4}$
$2w_2 \pm w_1$	$\frac{3A^3a_3}{4}$
$3w_1$	$\frac{A^3a_3}{4}$
$3w_2$	$\frac{A^3a_3}{4}$

Intermodulation components: These are produced as  $f_{IM} = nf_1 \mp mf_2$ . On the one hand, even-order IM products are far from the useful band, which will not cause a problem. But, on another hand, odd-order IM products are close to the fundamental components, especially IM3 (third-order) products because they have large amplitude and are almost impossible to filter out. As well, they can cause interference with another radio channel Pozar (2000).

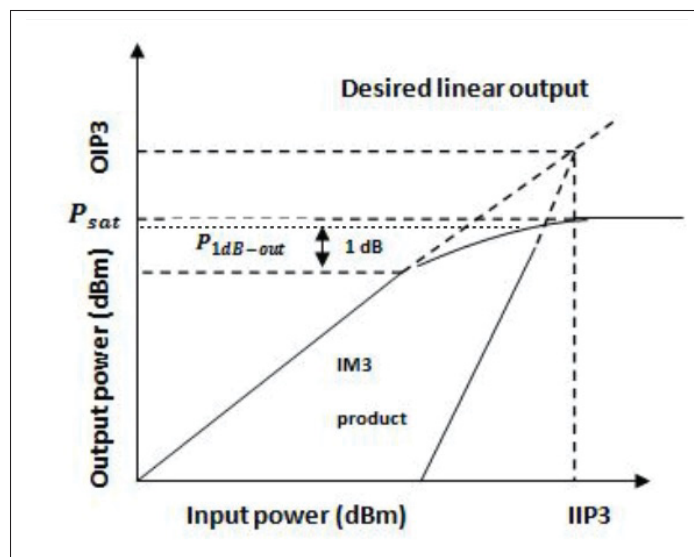


Figure 1.2 Illustration of third-order intercept point excitation  
Pozar (2000)

The input third intercept point (IIP3) is a theoretical point at which the desired output signal is equal to the third-order IM3, and its corresponding output known as output third intercept point (OIP3). IIP3 is also used to evaluate PA linearity, where a higher IIP3 means lower distortion generation and better linearity performance Pozar (2000). The following function (1.4) derives the IIP3, as shown in Figure 1.2:

$$a_1 A = \frac{3a_3 A^3}{4} \quad (1.3)$$

$$A_{IIP3} = \sqrt{\frac{4|a_1|}{3|a_3|}} \quad (1.4)$$

### 1.3.1 AM/AM and AM/PM conversion

Because of the nonlinear characteristic of PA (as shown in the previous section and Table 1.1), the amplification of the signal is  $a_1 + 3a_3 A^3/4$ . Thus, as the input signal increases  $3a_3 A^3/4$ , it is clear that gain is decreased not only by  $a_1$  but also by  $a_3$  and  $A$ . It is therefore important to note that for most RF circuits,  $a_1 a_3 < 0$ , which leads to compression behaviour. This gain compression phenomenon is called AM/AM distortion and causes compression of fundamental voltage gain, as illustrated in Figure 1.2. 1-dB is a common measure used to measure the linearity of the PA. AM/PM distortion is a phenomenon where the phase of the output depends on the level of the input signal due to the variability of the capacitance. Figure 1.3 shows AM/AM and AM/PM characteristics of model PA Colantonio *et al.* (2009).

AM/AM is thus a nonlinear gain behaviour, which mainly arises from nonlinear transconductance. In comparison, in transistor models, AM/PM nonlinear behaviour in phase arises from nonlinear behaviour in internal capacitors and inductors. In communication systems, however, AM/AM and AM/PM distortions are troublesome because they have a negative effect on the constellation diagram of the system.

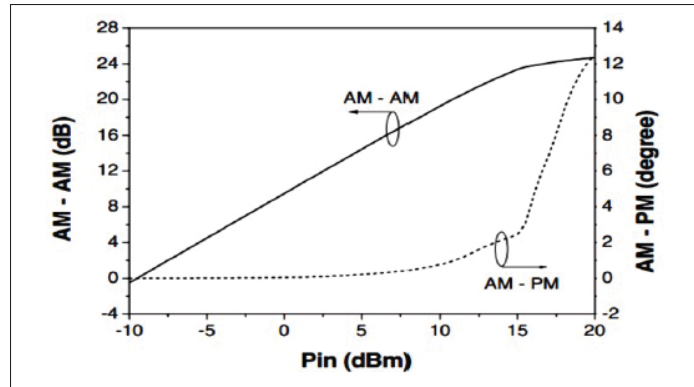


Figure 1.3 AM/AM and AM/PM characteristics of model PA  
Colantonio *et al.* (2009)

### 1.3.2 Linearity versus efficiency

Scientists are deeply concerned about the power efficiency of PAs in modern wireless communication systems because it directly affects the entire transmitter's power efficiency. PAs can amplify an input signal by the DC source, which is the added power. Therefore, a power-added efficiency (PAE) is a convenient parameter that is used to define how much the DC input power contributes to the amplification of the input signal. PAE is typically calculated as (1.6) Iwamoto, Williams, Chen, Metzger, Larson & Asbeck (2001):

$$PAE(\eta_{add}) = \frac{P_{out} - P_{in}}{P_{DC}} \quad (1.5)$$

where:

$PAE(\eta_{add})$  is power- add efficiency.

$P_{out}$  is output power.

$P_{in}$  is input power.

$P_{DC}$  is DC power.

When designing an amplifier, the efficiency vs linearity trade-off is a critical aspect. Specifically, there is an inversely proportional relationship between energy efficiency and amplifier linearity. This relation is shown in Figure (1.3).

As can be seen in Figure 1.4, using a less linear amplifier will be more power-efficient. In this

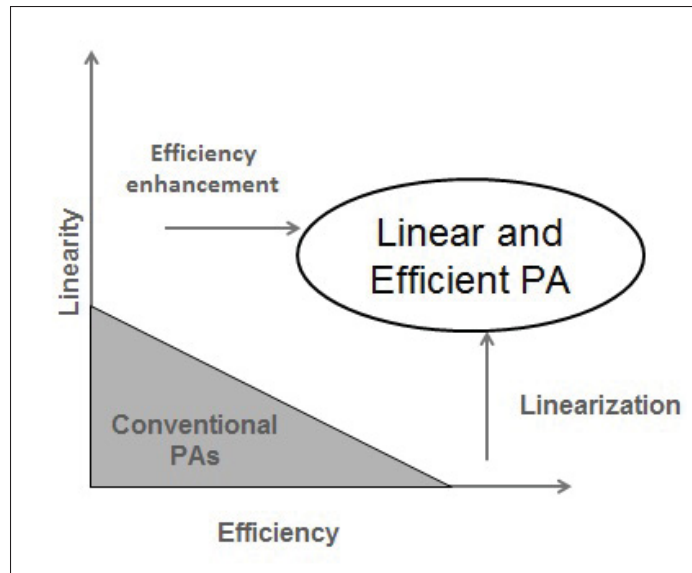


Figure 1.4 Linearity vs efficiency

case, however, it leads to distortion (i.e., the data gets distorted because the signal is not original), which means the data rate will fall and non-useful information will result. A solution to this problem is high linearity. However, a designer first needs to recommend high efficiency and then recover the linearity. So the designer chooses PA that has high efficiency and then improves linearity by using the linearization techniques. Table 1.2 shows the relation between the linearity and efficiency of a PA classification Bortoni, Noceti Filho & Seara (2002).

Table 1.2 PA Classification

Class	Output power	Ideal Efficiency	Gain	Linearity
A	Moderate	50%	Large	Excellent
AB	Moderate	50%~ 78%	Moderate	Good
B	Moderate	78%	Moderate	Moderate
C	Small	78%~ 100%	Small	Poor
D	Large	100%	Small	Poor
E	Large	100%	Small	Poor
F	Large	100%	Small	Poor



## 1.4 Power amplifier performance-evaluating metrics

PA linearities lead to distortion of both the in-band and the out-of-band. Current RF waveforms are digitally modulated signals which use complex modulations and vary in single-tone or two-tone statistics. This section presents two standard performance metrics to evaluate the PA linearity for an in-band and an out-of-band distortion.

### 1.4.1 Error vector magnitude (EVM)

EVM is used to evaluate the model's in-band performance. It is dominated by the in-band error, which represents any difference arising between the symbol received value and an expected value of a complex voltage demodulated symbol. As formulated below, we can write the EVM as:

$$EVM = \sqrt{\frac{P_{error}}{P_{reference}}} \times 100 \quad (1.6)$$

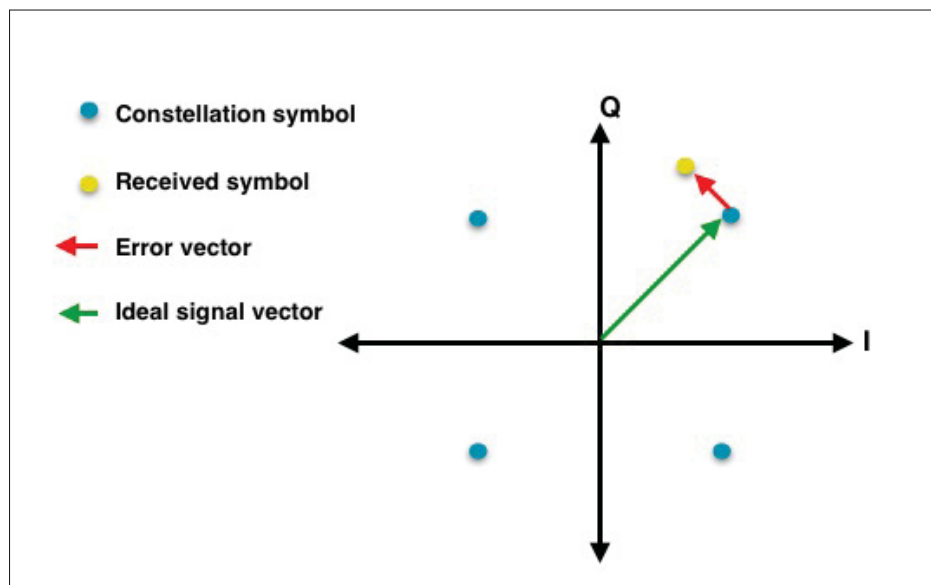


Figure 1.5 Error vector magnitude of QPSK

### 1.4.2 Adjacent channel power ratio (ACPR)

ACPR is another PA indicator. It is a measure of the out-of-band modelling's capacity and determines the power ratio for the adjacent and main channels. Further, it measures the leakage power in adjacent channels caused by nonlinearities in PAs, as described in Figure 1.5 and Equations (1.7) and (1.8), where poor ACPR results reduced signal transmission efficiency.

$$ACPR_1(dBc) = \frac{\text{Power in main channel}}{\text{Power in Adjacent channel}_1} \quad (1.7)$$

$$ACPR_2(dBc) = \frac{\text{Power in main channel}}{\text{Power in Adjacent channel}_2} \quad (1.8)$$

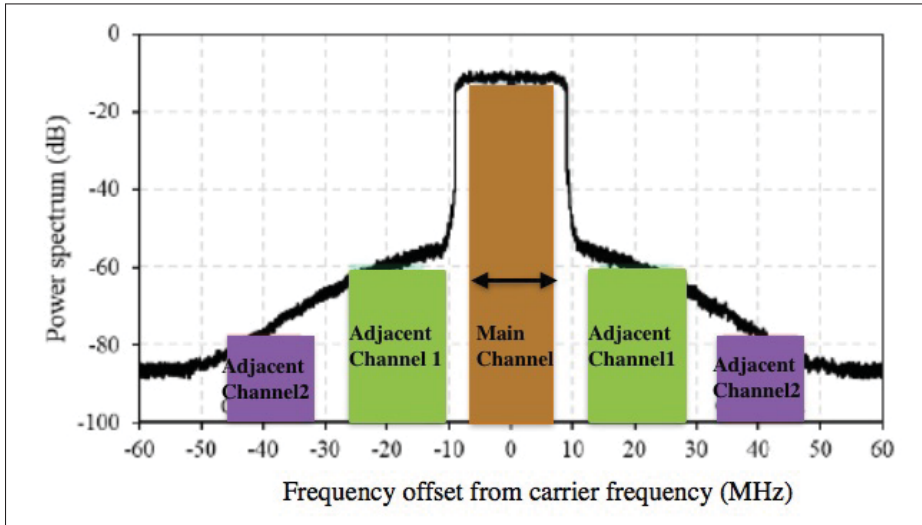


Figure 1.6 Definition of adjacent channel power ratio (ACPR)

## 1.5 PA linearization techniques

Modern wireless communication systems require high efficiency and a high data rate. At the same time, satisfactory linearity is also required. However, operating a PA at near saturation levels can be challenging when the aim is to achieve high efficiency for extended battery life. Many linearization techniques were devised in the past few decades that use a variety of applications, with the aim of improving the linearity of PAs. Moreover, linearization techniques have system-level approaches, which are suitable for linearizing PAs with high PAR signal. System-level approaches are classified into three categories: feedback, feed-forward and pre-distortion.

### 1.5.1 Feedback

Feedback (FB) is the most straightforward linearization technique. Its limitations are shown when the RF bandwidth increases, because more correction bandwidth is needed in PA linearization where the electrical delay around the feedback loop limits the correction bandwidth Cho (2016). Figure 1.7 illustrates the feedback approach.

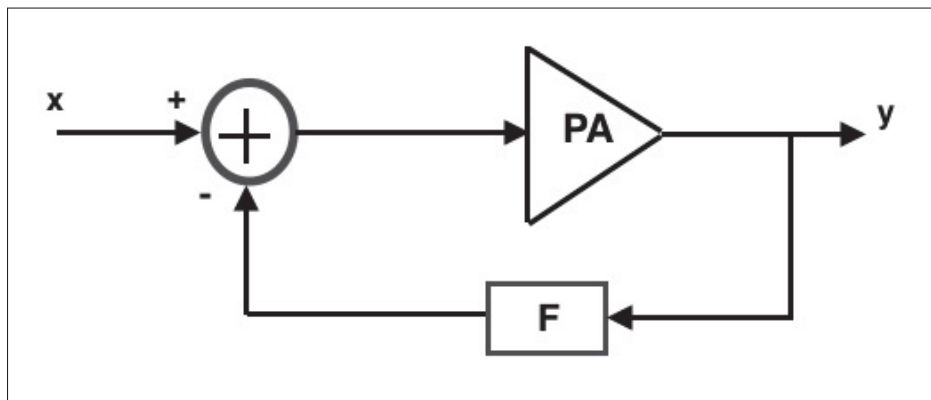


Figure 1.7 Feedback linearization technique

### 1.5.2 Feedforward

Feedforward (FF) offers better correction than FB by subtracting an estimate of nonlinearity-induced artifacts from the output. Figure 1.8 shows the feedforward technique in block diagram

form. This technique requires a linear auxiliary PA to amplify the error signal. It also requires the matching of delays and attenuation gain behaviours in order to function correctly. However, efficiency is low due to losses in the output delay line and output power combiner. As well, the auxiliary amplifier is sensitive to parameter variations over temperature and time Kenington (2000).

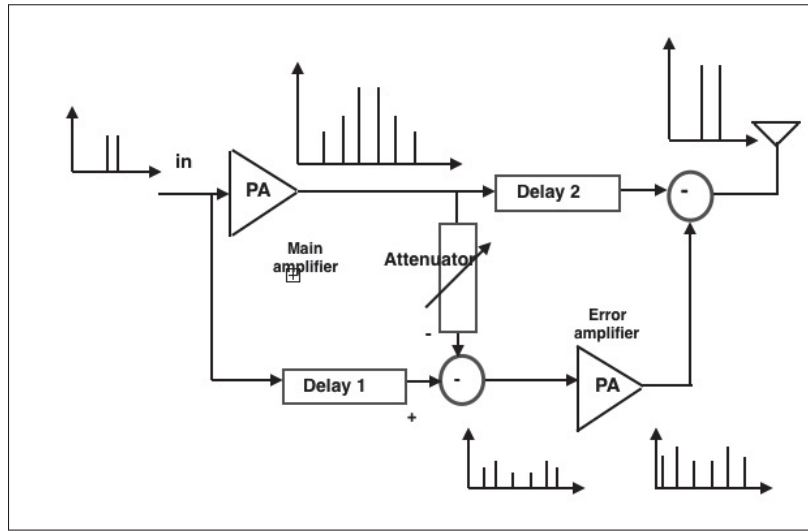


Figure 1.8 Feedforward linearization technique

### 1.5.3 Pre-distortion

Predistortion (PD) is the most efficient and promising linearization technique. It compensates for amplifier gain and phase variation over power range by applying an inverse nonlinearity to the input signal entering the amplifier Wik (2020).

A pre-distortion technique scenario is shown in Figure 1.9, assuming  $P_{in}$  is the input signal amplitude, and,  $P_{out}$  is the output signal. As shown in Figure 1.10, the relation of  $P_{in}$  and  $P_{out}$  is nonlinear. Thus, the desired output signal is  $P_{desired-out}$  from the linear response. The value of the desired output is used to search through the output characteristic of the PA. The suitable input amplitude to PA is determined by  $P_{pd}$ . The task of PD is to adjust the origin input amplitude to be the correct amplitude of  $P_{pd}$ . So, the correct output amplitude is produced and

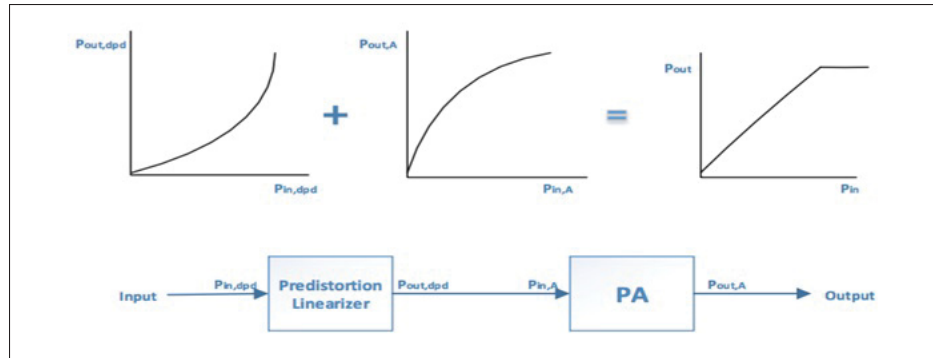


Figure 1.9 Pre-distortion linearization technique

the linear response is achieved. The phase is also pre-distorted. The different operating regions are illustrated in Figure 1.11 for a power amplifier in the general case.

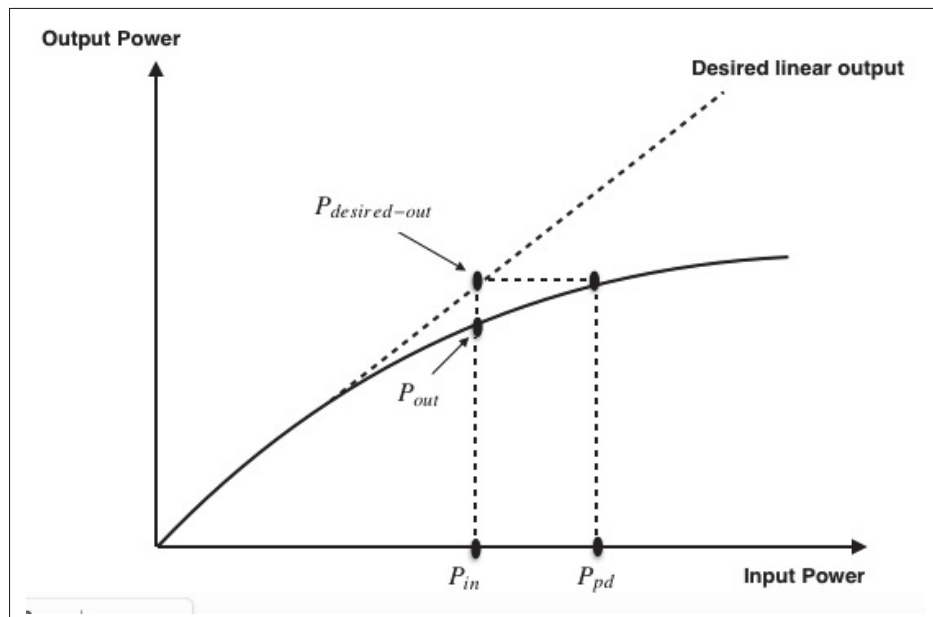


Figure 1.10 Scenario of pre-distortion

Predistortion can be separated into two groups: analog pre-distortion (APD) and digital pre-distortion (DPD). The next section describes comparisons between them, while Table 1.3 illustrates a comparison of the system-level PA linearization technique.

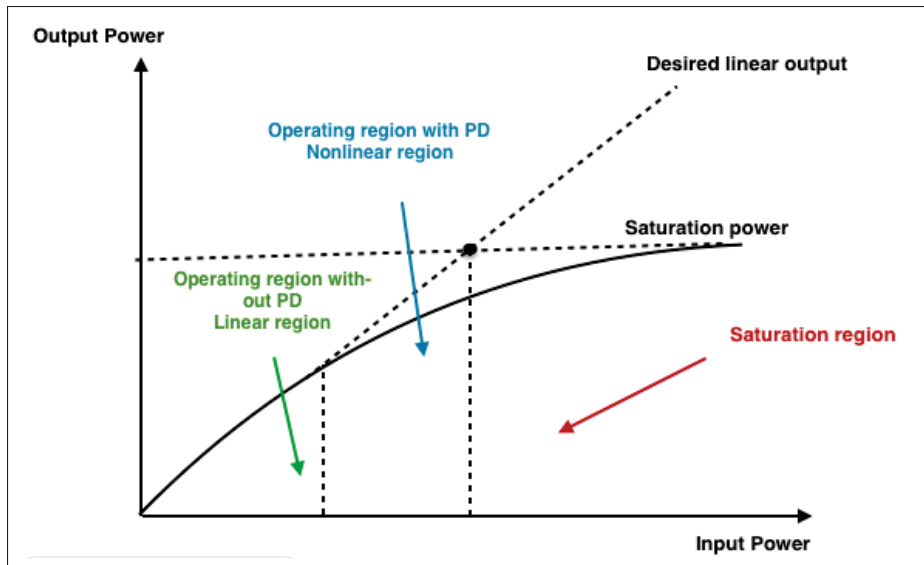


Figure 1.11 Operation region

Table 1.3 Comparison of PA Linearization Techniques for System Level Approach

Technique	Bandwidth	Size	Efficiency	Distortion correction
Feedback	Small	Moderate	Moderate	Poor
Feedforward	Large	Big	Poor	Good
Predistortion	Moderate/Large	Little	Good	Moderate

## 1.6 Conclusion

This chapter represented the amplifier's linearity problem in general and also highlighted the various parameters that quantify a PA's nonlinearity. The different methods for enhancing amplifier linearity were discussed as well. We concluded that the pre-distortion linearization technique is the most effective and promising. In the following chapter, a literature review will be represented.

## **CHAPTER 2**

### **STATE OF THE ART**

In the wireless application as a mobile device, power is a concern when power amplifiers (PAs) are a primary contributor to energy consumption at the transmission stage. In modern systems, a wide-band signal is required, but this becomes a significant issue which then leads to requiring higher precision in digital-to-analog converters (DACs) as well as in analog-to-digital converters (ADCs). Hence, designers need to focus on achieving high performance in both efficiency and linearity to reduce the distortion effect and power consumption of the system.

One option for reducing power consumption and achieving better performance is lowering the system's complexity. Using low-precision ADCs and DACs enables the use of shorter word-lengths in DPD algorithms, saving on energy as well as space during implementation. It also gives a higher sample rate burden for the entire DPD algorithm. Extensive research has been performed on various linearization techniques to define the hardware requirements to achieve better performance. The following is a review of the most promising and relevant results in the literature.

#### **2.1 Digital pre-distortion**

As transmission rates increase in communication systems, the requirement for accuracy is also increased. However, digital pre-distortion (DPD) methods have been developed over the years. DPD and PA behavioural modelling are two closely related areas of study. To account for the distortion that PA has created, it is essential to find a way to characterize its nonlinear behaviour as well as the inverse of that behaviour. Several models have been reported in the literature, as presented in this section.

The memory effect, among all distortion effects, is not essential in the early stages of the DPD. So, several models are reported as memoryless. These models are based on amplitude-to-phase conversion (AM/PM) and amplitude-to-amplitude conversion (AM/AM), which represent the

amplitude and phase distortion of the output signal as a function of the input signal amplitude. The polynomial model is one of the simplest memoryless models. In Gutierrez, Gard & Steer (1999), it is used in pre-distortion. Other authors Guo & Cavallaro (2002) and Nordsjo (2002) have used this model in the context of particular regrowth approximation, while still others have used it for the identification and modelling of Winner systems. Although this model is simple, its accuracy is low.

The Salah model is another option of a memoryless model. It is a quasi-memoryless model. The model is fitted to measurement data using four parameters, and it is composed of AM/AM and AM/PM functions. It is used to model the behaviour of TWTA Mathews & Sicuranza (2000). In most research studies, such as Costa, Midrio & Pupolin (1999), Aschbacher & Rupp (2003) and Santella & Mazzenga (1998), the Salah model has been applied in the context of pre-distortion and characterizing the nonlinearity of PA. However, the Salah model is not an optimal option for composing the SSPA or other devices. Therefore, additional models have been reported, including the Rapp model Rapp (1991), the Ghorbani model Ghorbani & Sheikhan (1991), and others. All memoryless models are frequency-independent because they are unable to model distortion based on frequency.

The high carrier frequency and wideband signals are among the most critical specifications in a modern wireless communication system. As a result, the memory effect is apparent in these and the memoryless model provides poor performance. Numerous models with memory effects have been reported in the literature, including: the Volterra Series (VS), the Generalized Memory Polynomial (GMP) model, the Dynamic Deviation Reduction (DDR) model, the Memory Polynomial (MP) model, the Hammerstein model, the Winner model, and others Chang & Ogunfunmi (1998).

Because the linear memory effect model cannot handle the complex nonlinear memory effect influenced by the input signal and each frequency's instantaneous signal, the researchers used the Volterra Series (VS) to construct their model. The most comprehensive model for nonlinear



PAs with memory effect is the Volterra series (VS) model. It is a Taylor series extension with varying time results. In mathematics, it is expressed as:

$$\begin{aligned}
 y(t) &= \sum_{m_1=0}^M h_1(m_1)x(t-m_1) \\
 &+ \sum_{m_1=0}^M \sum_{m_2=0}^M h_2(m_1, m_2)x(t-m_1)x(t-m_2) \\
 &+ \sum_{m_1=0}^M \sum_{m_k=0}^M h_2(m_1, \dots, m_2)x(t-m_1)\dots x(t-m_k) \\
 &= \sum_{k=0}^K \sum_{m_1=0}^M \dots \sum_{m_k=0}^M h_k(m_1, \dots, m_k) \prod_{j=1}^k x(t-m_j)
 \end{aligned} \tag{2.1}$$

Where  $h_k(m_1, \dots, m_k)$  are the kernels of Volterra series,  $M$  is the memory depth, and  $K$  is the linearity order. As shown in Equation (2.1), the number of coefficients of the model increases with nonlinearity order and memory depth; hence, it raises the system complexity and makes the inverse PA model hard to measure Ding, Zhou, Morgan, Ma, Kenney, Kim & Giardina (2004).

Several different mathematics research projects have focused on the Volterra series Chang & Ogunfunmi (1998). One of these projects produced the Memory Polynomial (MP), which is the simplest model of the Volterra series Ding *et al.* (2004). The MP model can be used in most nonlinear devices in communication systems. It is expressed as:

$$y(t) = \sum_{k=1}^K \sum_{m=0}^M a_{km} x(t-m) |x(t-m)|^{k-1} \tag{2.2}$$

DPD has been widely investigated and has become one of the most fundamental building blocks in modern wireless communication systems. A considerable number of DPD techniques have been published in the literature. For baseband, DPD can be divided into three groups: Look-Up Table (LUT)-based methods Ai, Yang, Pan, Tang & Zhang (2007) Barradas, Cunha, Lavrador & Pedro (2014); polynomial-based methods Ding *et al.* (2004) Morgan, Ma, Kim,

Zierdt & Pastalan (2006); and neural network-based methods Mkadem & Boumaiza (2011) Aguilar-Lobo, Garcia-Osorio, Loo-Yau, Ortega-Cisneros, Moreno, Rayas-Sánchez & Reynoso-Hernández (2014).

In comparing LUT and neural networks with model-based pre-distortion, LUT-based pre-distortion is easy to implement in hardware and has low complexity. However, in LUT, the problem caused by quantification needs to be solved. Further, while model-based pre-distortion can be more accurate than LUT-based pre-distortion, many mathematical operations are needed. Today's neural network-based pre-distortion has been developed Aguilar-Lobo *et al.* (2014). Neural network-based pre-distortion can be used to mimic the nonlinear behaviour of pre-distortion. However, the implementation of its structure is difficult in hardware, and the training process is complicated and time-consuming.

Model-based DPD Raich, Qian & Zhou (2004) Liu, Zhou, Chen & Zhou (2013) is also called memory polynomial-based DPD, which is mainly used to linearize PA. Similarly, the pre-distortion is a nonlinear system, and the polynomial approach can be used for pre-distortion modelling. Nothing is wrong with that, as the model's input and output have different meanings between modelling the PA and modelling the pre-distortion.

DPD has another essential step, which is the identification of the pre-distortion algorithm. In order to identify the post-distorter, many algorithms are proposed. Some identification algorithms have been reported, such as Least Square (LS), Least Mean Square (LMS), and Recursive Least Squares (RSL) Abi Hussein, Bohara & Venard (2012). Baseband Digital Pre-Distorter (BB-DPD) is the most widely adopted, as shown in Figure 2.1.

Several authors have studied a different behaviour model configuration of the baseband DPD of GaN power amplifiers, as well as different architectures of DPD coefficient estimation. In Madero-Ayora, Barataud, El Dine, Neveux, Nebus, Reina-Tosina, Allegue-Martinez & Crespo-Cadenas (2011), the authors showed three different baseband DPD models of a 10W GaN PA. Of the models presented, one is based on memory polynomial (MP) and the others are based on DVBW. Braithwaite (2015) emphasized that the indirect learning architecture (shown in Figure

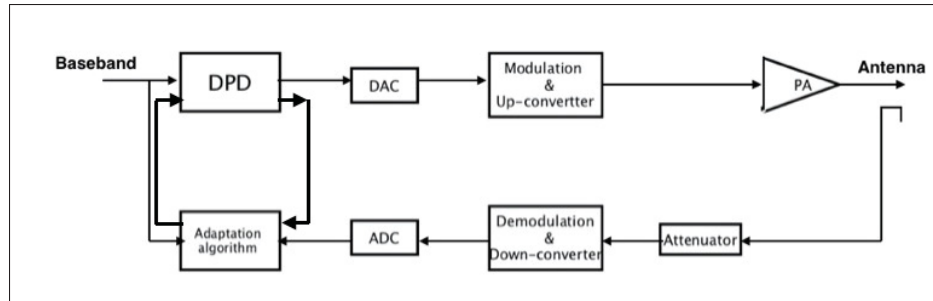


Figure 2.1 Block diagram of baseband digital pre-distortion

2.2) has been a good option in estimating DPD coefficients due to fast convergence as well as relatively easy implementation. However, limitations like coefficient offset (due to EVM/PA saturation) and high rates of ADC sampling have led to challenges. To resolve these issues, low-precision ADCs and DACs could potentially be used in modern applications as a means to lessen complexity in a system and to lower energy requirements of the components. For example, in Massive MIMO resolution, researchers have investigated using only a single bit in order to lower throughput requirements in cases where dozens or more antennas have to function at the same time. For mmWave, there is currently availability of sizeable band-widths to ensure data rate speed. However, in this case, ADCs with swift sampling rates would have to be used.

The following studies were conducted to determine the bits of resolution for DACs and ADC needed in the DPD circuit. Tarver & Cavallaro (2017) looked at low-precision ADCs as a means to determine the amount of precision required for full-band DPD setups that have only 6 bits. The method employed in this study uses two tone-signals each per 5MHz of band-width. Figure 2.3 shows the simulation with the nonlinear PA with memory effect implemented in MATLAB. Fixed-point tools are used to quantize the feedback input to DPD learning, where the word-lengths are varied as low as 6 bits.

Tarver & Cavallaro (2017) concluded that a lower resolution ADC may cost less and allow for lower computationally complexity in digital processing. The drawback of DPD occurs in wide-band signals, which can become a significant problem. The sample rate must be faster and

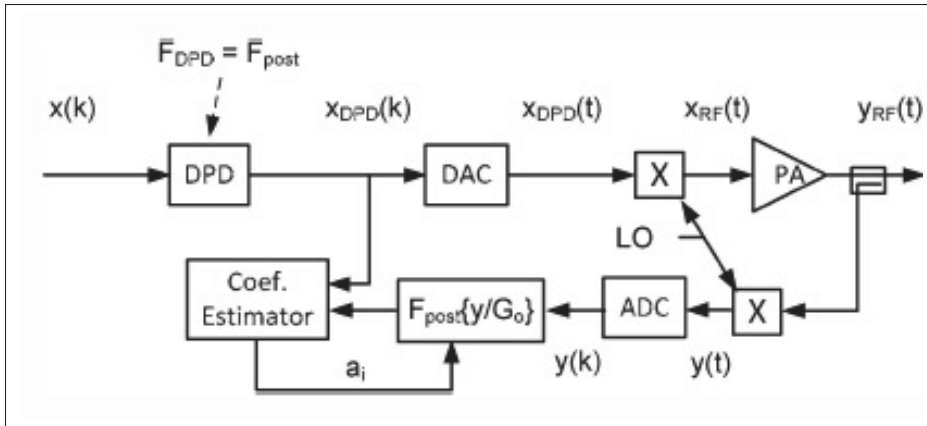


Figure 2.2 Transmitter using indirect learning architecture estimator for DPD

lead to an increase in system complexity and power consumption, and this has been discussed by numerous authors in the literature.

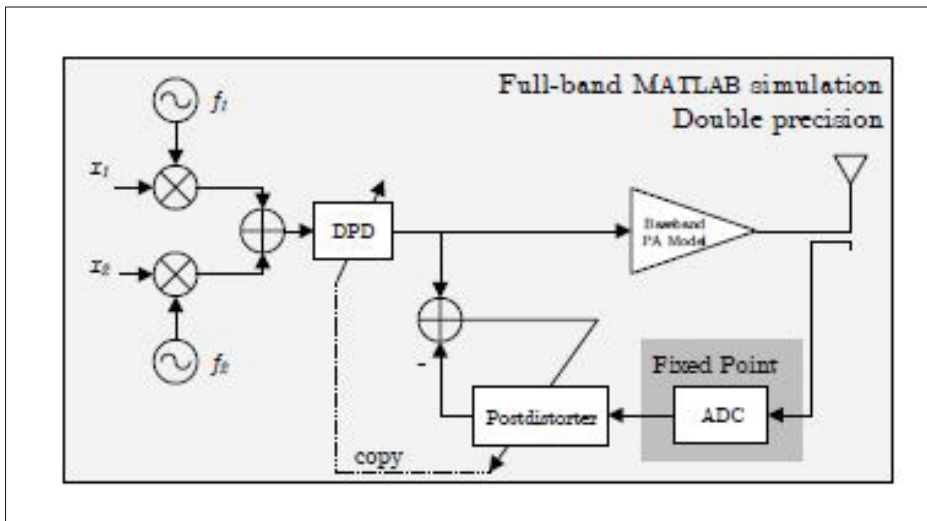


Figure 2.3 Block diagram of full-band DPD simulation performed

Wu, Xia, Zhai, Tian, Yang, Zhang & Zhu (2012) addressed a high-performance wide-band DPD with instantaneous bandwidth up to 100 MHz (five carrier each 20 MHz of bandwidth) that is suitable for LTE advanced systems with an RF frequency of 1.95 GHz GaN Doherty power amplifier. The researchers mentioned that the processing bandwidth is about three to five times

the Nyquist bandwidth. In this case, the ADC and DAC are operated under a high speed of 400 MHz, where ADC has 14 bits in resolution and DAC has 16 bits. Wu *et al.* (2012) offered a platform with an effective method correcting the nonlinearity and memory effect in PA, which has reached ACLR of -50dBc, for an improvement of about 15 dB.

## 2.2 Comparison between analog and digital pre-distortion

In comparing analog pre-distortion (APD) with BB-DPD, we can see that APD is realized in RF bands and requires a complicated analog circuit design. The basic concept of APD is to use dedicated nonlinearity components, such as a diode or field-effect transistor, to create a certain nonlinearity that can compensate for a PA. Although the odd order of intermodulation distortion (IMD) is generally compensated by the APD device, they cannot repair the memory effect caused by PA. This leads, as mentioned earlier, to low precision linearization performance. Hence, APD is less used.

In contrast, BB-DPD has a good performance. It has the lowest operating frequency bands because it is processed at baseband frequency, where the signal rate is relatively low and the hardware requirement is not high. The drawback of BB-DPD occurs in a wide-band signal, which can become a significant problem. As a result, the sample rate must be faster, which can cause an increase both in system complexity and power consumption. This thesis proposes a hybrid digital/analog pre-distortion to handle the best linearization performance and reduce hardware requirements. To address better linearization efficiency with a wideband signal, the current work focuses on a combination of linearization techniques. Recent research, such as Tomé, Barradas, Cunha & Pedro (2018), described hybrid digital and analog pre-distortion in a GaN HEMT (i.e., high-electron-mobility transistor)-based PA featuring GMP (i.e., conventional generalized memory polynomial) DPD and analog feedback circuits. The authors achieved a level of intermodulation distortion of -65 dBc. Although other research also found comparable outcomes, their digital approaches resulted in DPD structures which were difficult to implement due to their complexity. The present research proposes an approach that helps to obtain similar results by applying a standard GMP DPD and an analog circuit. As shown above, the modern

wireless system requires a wideband signal and faster data rate. That is a significant issue for increased power consumption and hardware requirements. On the one hand, only a few studies of a hybrid pre-distortion have shown the technique's performance. However, no study to date has examined and studied the hardware requirements needed (ADC and DAC) for a system with a wide-band signal.

The proposed research investigates a hybrid digital/analog pre-distortion linearization scheme of a GaN power amplifier based on a conventional analog pre-distortion and memory polynomial DPD for a wideband signal. The aim here is to reduce hardware requirements and achieve better linearization performance.

## CHAPTER 3

### GaN AMPLIFIER LINEARIZATION

In this chapter, the first section illustrates the model of the selected GaN PA in ADS to obtain a nonlinear model. The frequency of operation is chosen to be 6GHz. In the second section, the conventional APD circuit is designed in ADS and combined with the selected PA to obtain the linearization response. The last section illustrates the proposed DPD model using Simulink/MATLAB and quantifying DPD requirements as a function of bandwidth and level of nonlinearity for the selected PA. It takes into account the hardware requirements (i.e., how many bits for DAC and ADC are needed in the DPD circuit).

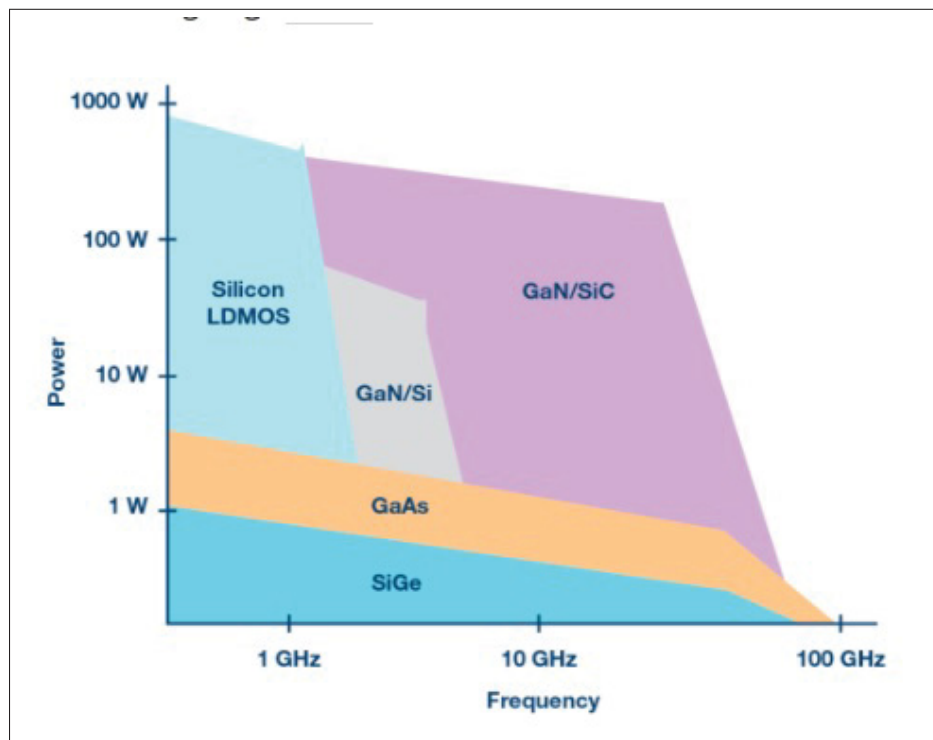


Figure 3.1 GaN vs other technologies

### 3.1 Modeling of selected GaN PA/ ADS software

Gallium nitride (GaN) technology can be used to achieve higher power and extended frequencies better than other technologies, as shown in Figure 3.1 Keith (2017). GaN also allows higher and higher frequencies for more complex applications, such as 5G base transceiver station and radar. The selected GaN PA is made from Quarvo (QPA2213 2-20GHz 2 Watt GaN Amplifier). Appendix I outlines the data-sheet.

#### 3.1.1 Specification of GaN PA

In PA design, the process begins by defining the requirements and specifications. The process is completed when the newly designed PA has been validated, meaning that it has met all or most of the stated requirements and specifications. The electrical specifications displayed in Table 3.1 below show the operating frequency set to 6GHz, while the S-parameters of the selected GaN PA are shown in Figure 3.2. The next sections provide a detailed outline of the design process.

Table 3.1 Electrical Specifications of GaN PA

Parameters	Value	Unit
Operation frequency	6	Ghz
Power-added efficiency Pin= 18 dBm	22.5	%
Output power for Pin= 18 dBm	35.5	dBm
Small signal gain	26	dB
Input return loss	16	dB
Output return loss	15	dB
Noise figure	4.4	dB



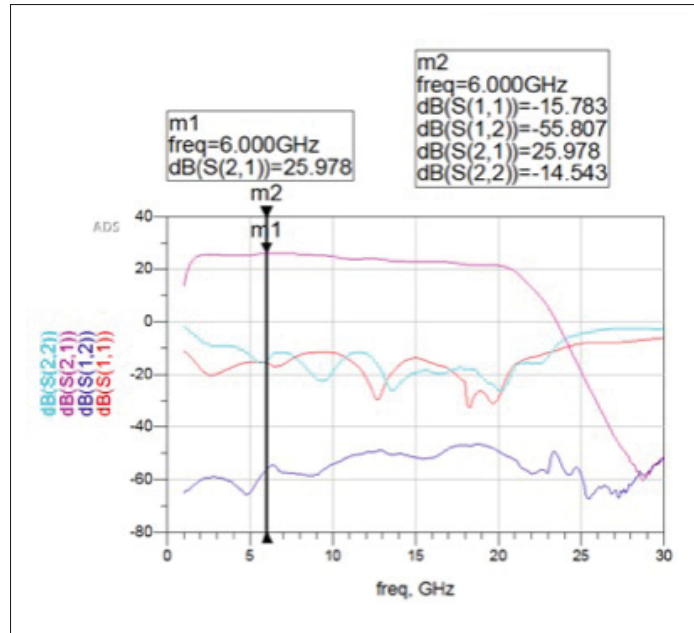


Figure 3.2 S-Parameters of GaN PA

### 3.1.2 ADS model of selected GaN PA

Until presenting and testing the design of the pre-distortion circuits to be built, modelling of the selected GaN amplifier in ADS is required to obtain the amplifier's nonlinear model. This simulation will also require a deduction of the order of distortion that GaN PA will produce. We have built a model of the ADS amplifier, as shown in Figure 3.3. The GaN PA model parameters for ADS are given in Table 3.2.

Table 3.2 GaN PA Model Parameters for ADS

Parameters	Value	Unit
Operation frequency	6	Ghz
Power-added efficiency $P_{in}= 18$ dBm	63.7	%
Output power for $P_{in}= 18$ dBm	35.8	dBm
Small signal gain	26	dB
Input return loss	16	dB
Output return loss	15	dB
$P_1$ dB	9.8	dBm

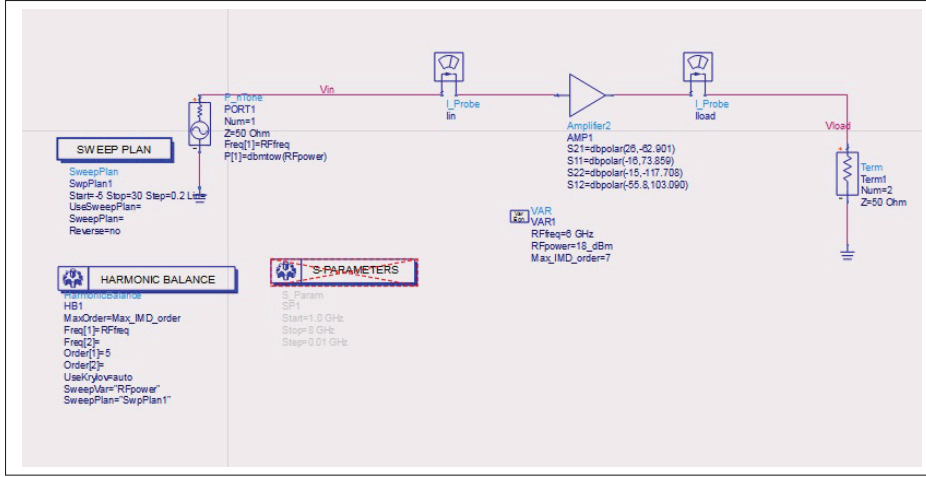


Figure 3.3 ADS simulation model of GaN amplifier at 6GHz

The simulated variation of the output power as a function of input power is shown in Figure 3.4. The PA starts to compress at  $7\text{dBm}$  (m4). Note that  $1\text{dB}$  power, which is approximately equal to  $9.8\text{dBm}$ , corresponds to input power. The compression points correspond to the input power where the PAE is maximum at  $P_{input} = 18\text{dBm}$  is  $8.146\text{dB}$ . As illustrated in Figure 3.5 (AM-AM conversion), the small-signal gain of the modelled GaN PA is approximately equal to  $26\text{dB}$ .

As described in Chapter 1, PAE is a convenient parameter used to evaluate how much DC input power contributes to an input signal amplification. As shown in Figure 3.6, at  $P_{input} = 18\text{dBm}$  the PAE is maximum, which is approximately  $63.7\%$ .

Two-tone test analysis is performed to define the IMD performance of the modelled GaN power amplifier. IMD occurs when an input of the PA shows more than one input frequency. As given in the specifications of the selected Qurvo GaN PA, the tone spacing is  $100\text{MHz}$ . In a two-tone test, the frequency spacing is swept between the input tones. We can define the two tones as in the following equations where  $RF_{frequency}$  is an operating frequency which is equal to  $6\text{GHz}$ .

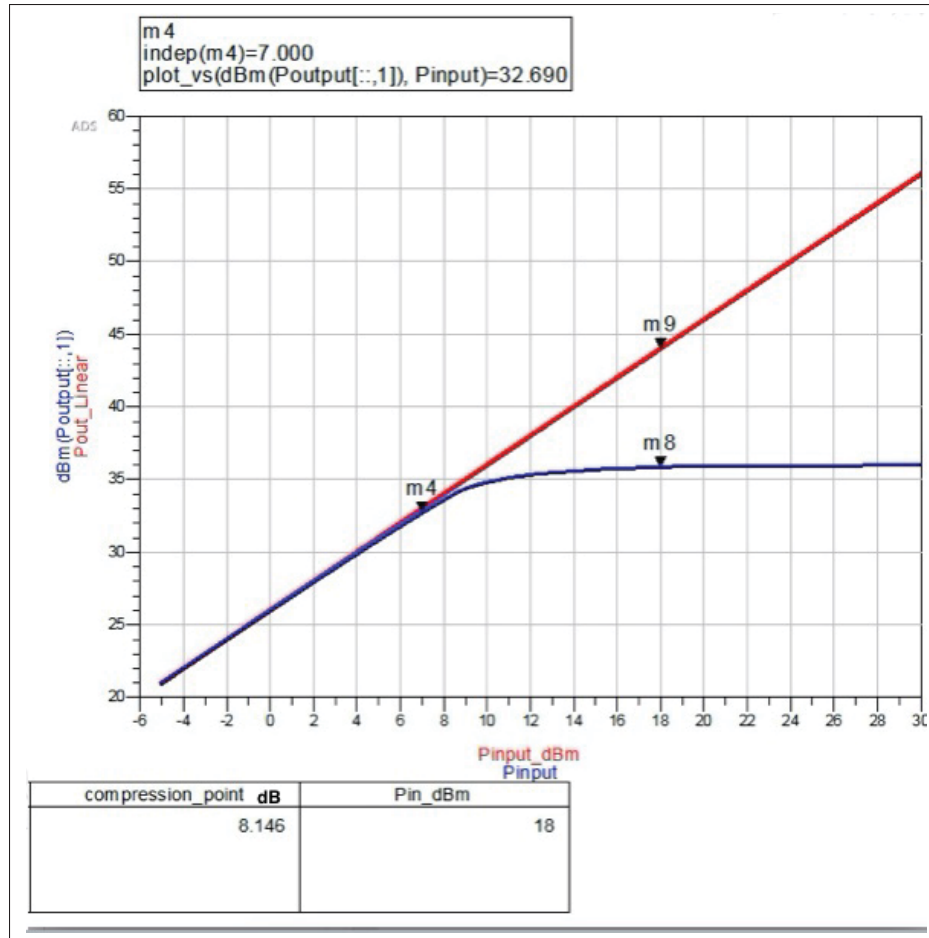


Figure 3.4 Variations in output power of GaN amplifier at 6GHz

$$F_1 = RF_{frequency} + (F_{spacing}/2) = 6.05GHz \quad (3.1)$$

$$F_2 = RF_{frequency} - (F_{spacing}/2) = 5.95GHz \quad (3.2)$$

From Figure 3.7 below, we can define IMD as:

$$IMD = m1 - m2 = 10.274(-10.274dBc) \quad (3.3)$$

Besides, we can define the IIP3 the third intercept. Additionally, we can define IIP3 as the third intercept point, as in Equation (3.4). IIP3 is a theoretical point at which the desired output signal

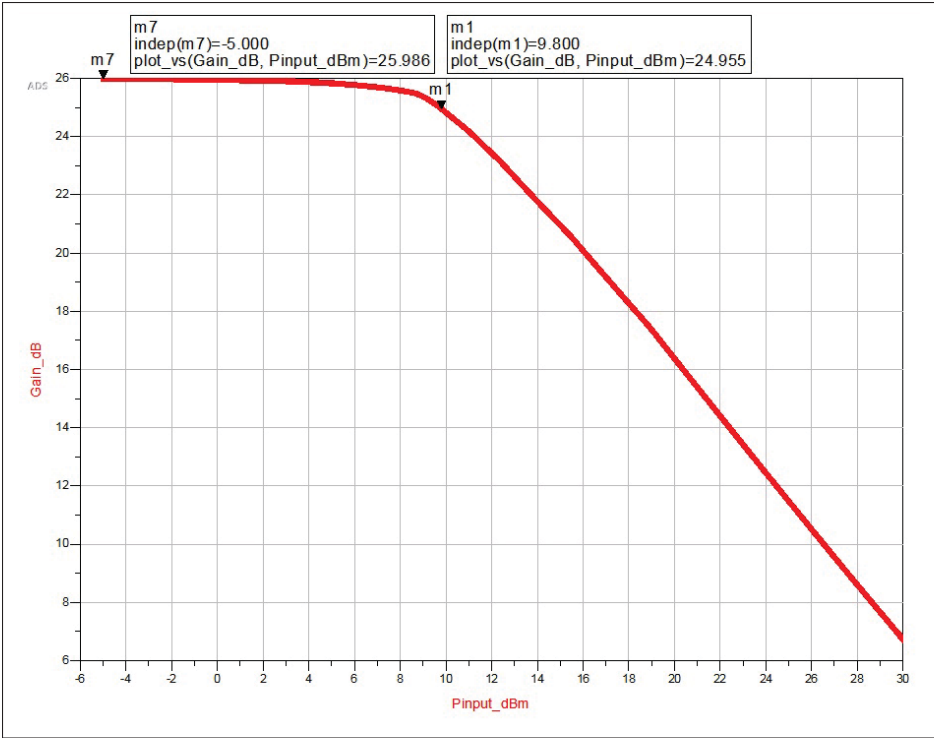


Figure 3.5 AM-AM conversion of GaN amplifier at 6GHz

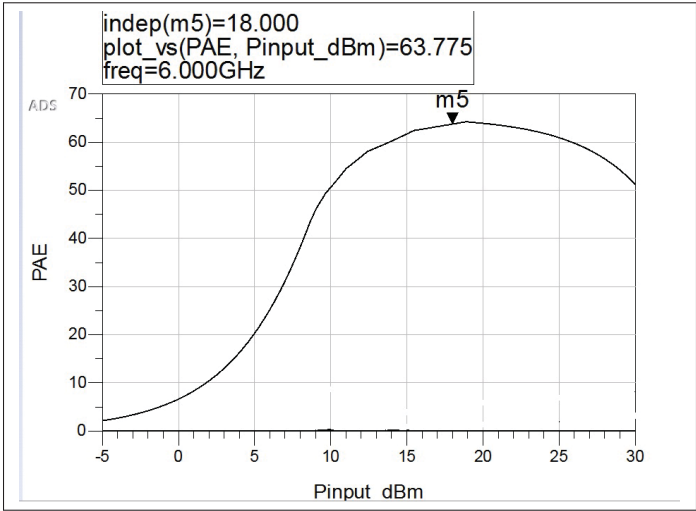


Figure 3.6 Power-added efficiency (PAE) of GaN amplifier at 6GHz

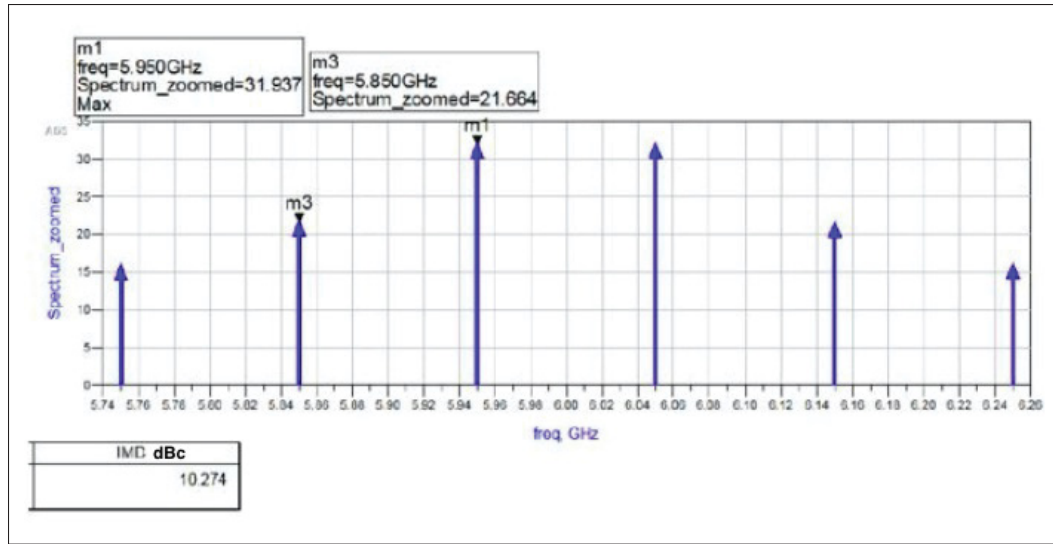


Figure 3.7 Intermodulation products of two-tone simulations

is equal to the 3rd-order IMD. Figure 3.7 illustrates that the IM3 is around  $-21.7\text{dBc}$

$$IIP3 = P_{input} + IMD/2 = 23.137\text{dBm} \quad (3.4)$$

As we explained above, the model of the selected GaN power amplifier is successfully modelled in ADS since the modelled parameters are approximate meet the specification of that selected power amplifier.

In the next section, the proposed analog pre-distortion (APD) and its linearized function will be presented.

### 3.2 Proposed analog pre-distortion circuit/ADS software

Several pre-distortion circuit configurations have been designed to minimize the effect of ACPR of the 3rd-order element of the amplifier. The most conventional analog pre-distortion circuit used the idea of splitting the input signal into two linear and nonlinear branches with nonlinear path control circuits and a distortion generator Hadouej (2013). This linearization form is called cubic pre-distortion. Numerous methods exist for creating inverse distortion. The proposed

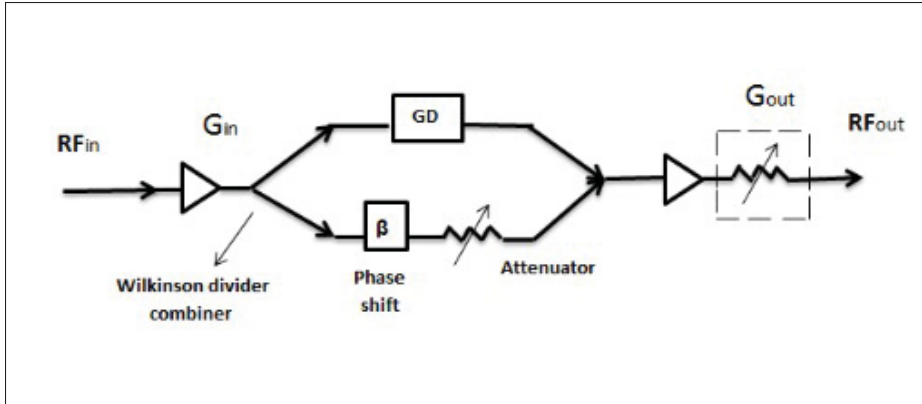


Figure 3.8 Structure of proposed APD (cubic pre-distortion)

ADP circuit (block diagram), outlined in Figure 3.8, is based on the model used by Hadouej (2013) and a variant of the one suggested by Imai, Nojima & Murase (1989). Hadouej (2013) added a bias circuit for the Schottky diodes as Figure 3.16 is shown a structure of distortion generator, with the author following the classical structure in order to limit the ACPR of the 3rd-order element of the amplifier.

In the following steps, we present a summary of the operation of the proposed APD circuit in detail by following Hadouej (2013) structure shown in Figure 3.8.

- The operation of the GD depends on the level of the signal at the input. At low input values, its output is linear, and the original signal is obtained at the output.
- With increases to the input signal, we will have a nonlinear component from the GD, which is added to the linear branch's fundamental components.
- In the linear branch, we introduce a variable attenuator and phase shift to control the expansion/compression generated by GD, as shown in Figure 3.8.
- The  $G_{in}$  amplifier stage at the entrance allows us to adjust the expansion obtained at the same level of the input power range as the obtained nonlinear response of modelled GaN PA.
- According to the phase shift value of the linear branch, the shape obtained by the GD can be modified to obtain an expansion, which is the shape of the desired (inverse function).
- At the output of the circuit, an amplifier and attenuator were introduced to control the level of linearity obtained in return for variations in the system's overall gain.

Figure 3.9 represents the operation of a cubic pre-distortion in the case of a two-carrier signal. In an ideal case, the GD should generate a signal containing only a GaN PA distortion. That summed with the initial input signal gives us the signal pre-distortion.

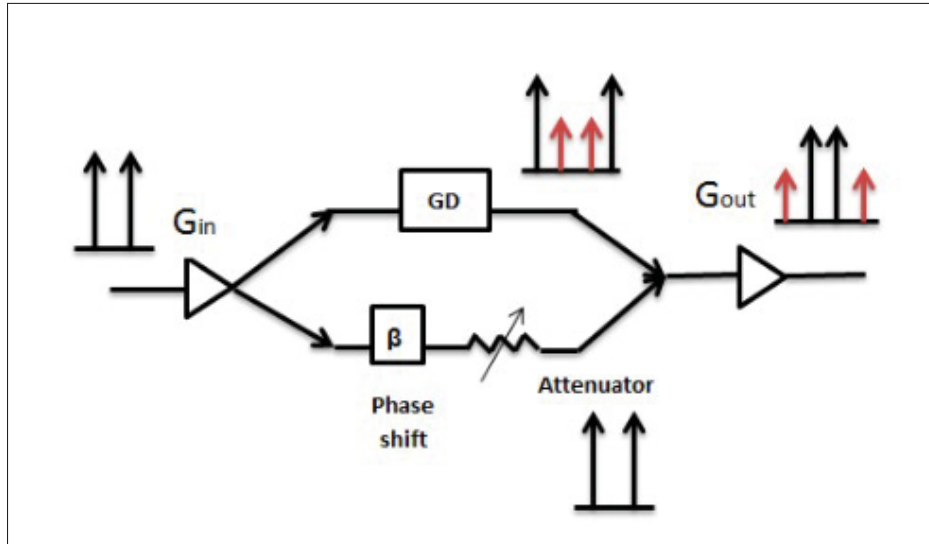


Figure 3.9 Operation of APD circuit (cubic pre-distortion) of two carrier signals

### 3.3 Requirements of the proposed APD circuit

The previously presented architecture of the proposed APD (cubic pre-distortion) circuit consists of two paths – linear and nonlinear. The contents of the nonlinear path control circuits and the distortion generator (GD). In the following section, the characterization and simulation of these requirements are presented.

#### 3.3.1 Characterization and simulation of ADP circuit's linear control path

The characterization of the ideal structures of ADP circuits consist of different control components, as listed below:

- 3dB hybrid coupler.
- Wilkinson divider combiner.
- Phase Shift.

- Attenuator.

This section also describes the 3dB hybrid coupler and Wilkinson divider/combiner simulation circuit in ADS at an operating frequency of 6GHz.

### 3.3.1.1 3 dB hybrid coupler

The balanced structure of the proposed APD (cubic pre-distortion) circuit is based on a 3dB hybrid coupler. Using ADS simulation, we designed the structure of the 3dB hybrid coupler at 6GHz to meet theoretical requirements.

#### Theory of 3dB hybrid coupler

A 3dB hybrid coupler is a directional coupler (4 ports) with a coupling of -3dB and a phase shift of  $90^\circ$  between the direct port and the coupled port Pozar (2005). Therefore, it allows the input power to be divided and distributed to the two output ports. Microstrip and coplanar line technologies are often used to achieve this process. Figure 3.10 shows the schematic diagram of a 3dB hybrid coupler.

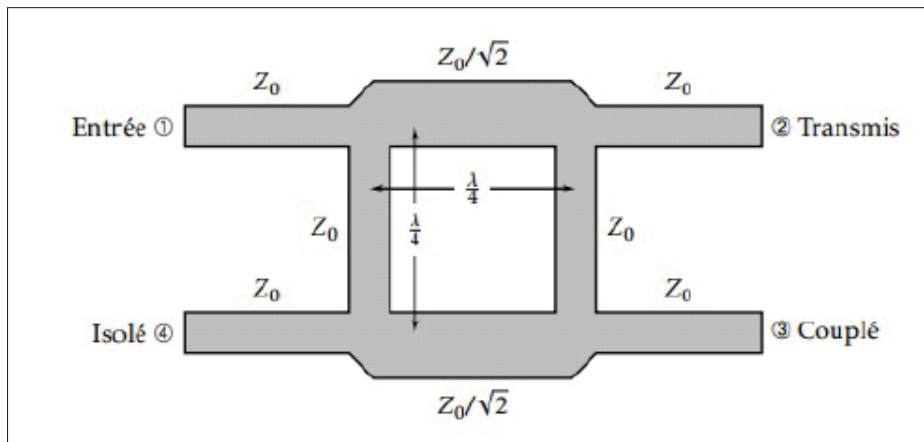


Figure 3.10 Schematic diagram of 3dB hybrid coupler



The S-parameters of an ideal 3dB hybrid coupler are presented below:

$$[S] = \begin{bmatrix} 0 & s_{12} & s_{13} & 0 \\ s_{21} & 0 & 0 & s_{24} \\ s_{31} & 0 & 0 & s_{34} \\ 0 & s_{42} & s_{43} & 0 \end{bmatrix} = \frac{1}{\sqrt{2}} \begin{bmatrix} 0 & 1 & j & 0 \\ 1 & 0 & 0 & j \\ j & 0 & 0 & 1 \\ 0 & j & 1 & 0 \end{bmatrix} \quad (3.5)$$

To ensure the performance described (i.e., coupling and phase shift), the lines must have a length of  $\frac{\lambda}{4}$ , and the impedance of the lines must be as follows:

- Between ports (1,2) and (4,3):  $\frac{Z_0}{\sqrt{2}} = 35.3553\Omega$ .
- Between ports (1,4) and (2,3):  $Z_0 = 50\Omega$ .

### Overview of 3dB hybrid coupler design stage

We synthesize the physical parameters (line width) of microstrip lines with characteristic impedance  $50\Omega$  and  $35.3553\Omega$  at the operating frequency 6GHz. Subsequently, we perform a simulation of the S parameters of the structure. So, we adjust our circuit in order to follow the specification.

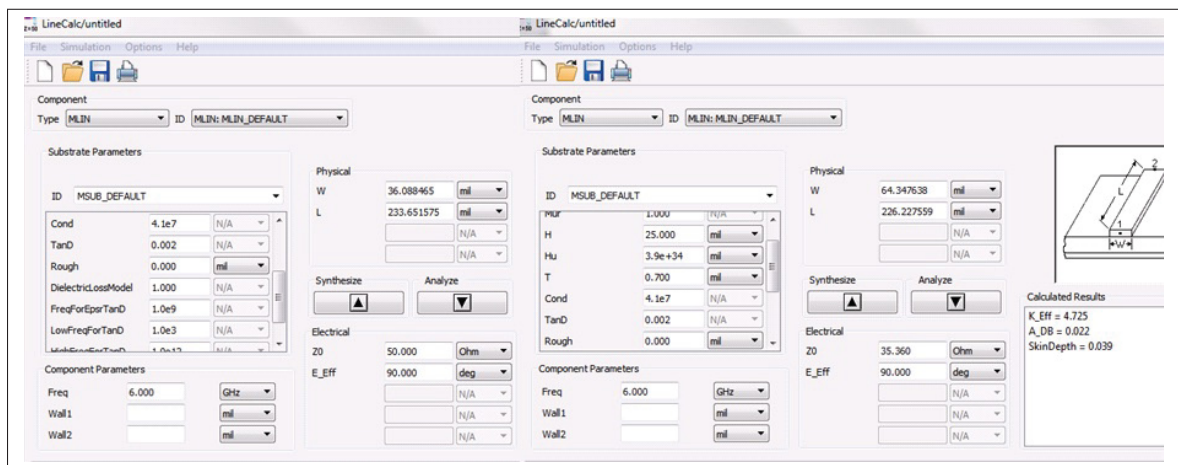


Figure 3.11 Parameters of transmission lines for characteristic impedance  $50\Omega$  and  $35.3553\Omega$  of 3dB hybrid coupler

### Simulation results of 3dB hybrid coupler

Table 3.3 Comparison of 3dB Hybrid Coupler Specification and Simulation Results

Parameters( $s_{ij}$ )	Coupling dB	Dephasor	Adaptation dB	Isolation dB
Specification	3(+/-0.5)	$90^\circ$ (+/-0.5)	$\geq 25$	$\geq 20$
Simulation	3	$86.338^\circ$	24.7	23.8

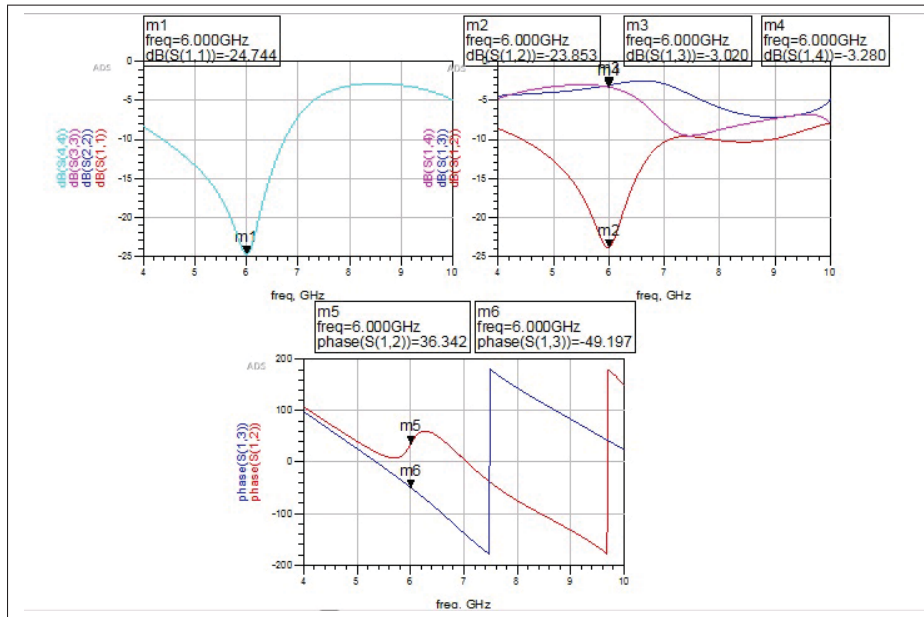


Figure 3.12 Simulation of S-parameters of 3dB hybrid coupler

#### 3.3.1.2 Wilkinson divider/combiner

The proposed APD circuit is divided into two directions: linear and nonlinear. To meet the theoretical requirements, we design a Wilkinson divider/combiner with microstrip line technology using ADS software.

#### Theory of Wilkinson divider/combiner

The Wilkinson divider (3-port) splits an RF signal into two signals of the same amplitude (3dB) and the same phase Pozar (1998). At the same time, the divider is also in combiner mode due to the reciprocity property, allowing it to combine the incoming power to port2 and port3 to output

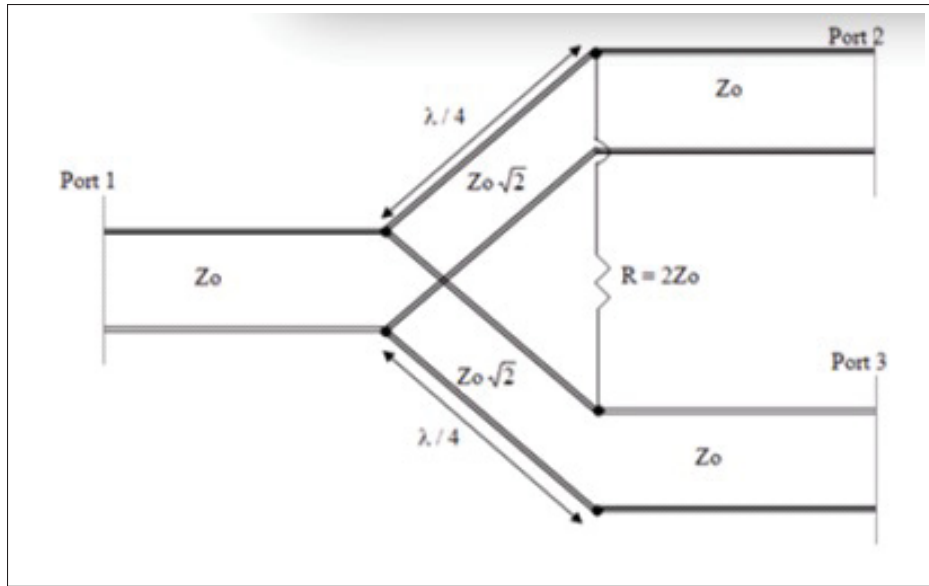


Figure 3.13 Wilkinson divider/combiner

port1. The following [S] matrix shows an ideal Wilkinson divider:

$$[S] = \begin{bmatrix} 0 & \frac{-j}{\sqrt{2}} & \frac{-j}{\sqrt{2}} \\ \frac{-j}{\sqrt{2}} & 0 & 0 \\ \frac{-j}{\sqrt{2}} & 0 & 0 \end{bmatrix} \quad (3.6)$$

Figure 3.13 illustrates the Wilkinson divider/combiner. As can be seen, the main impedance transmission line  $Z_0$  is divided into two lines of characteristic impedance  $Z_0\sqrt{2}$  of length  $\frac{\lambda}{4}$ . Then, a resistor  $R = 2Z_0$  is placed at the end of the lines  $\frac{\lambda}{4}$  which makes it possible to isolate the output ports 2 and 3 by forcing the flow of current through it if the terminal load of port2 and port3 are different, or if the input signals in combiner mode are unbalanced. Therefore, ideally, no current should flow in the resistance. Finally, the last portion of the divider is completed by characteristic impedance lines  $Z_0$  to the output ports.

### Overview of Wilkinson divider/combiner design stage

The LINECALC tool of ADS is used to calculate the physical parameters of the transmission lines, whose characteristics correspond to that of the R03006 substrate. With the characteristic impedance  $50\Omega$  and  $70.71\Omega$  at operating frequency 6GHz of frequency 6GHz of length  $\frac{\lambda}{4}$ .

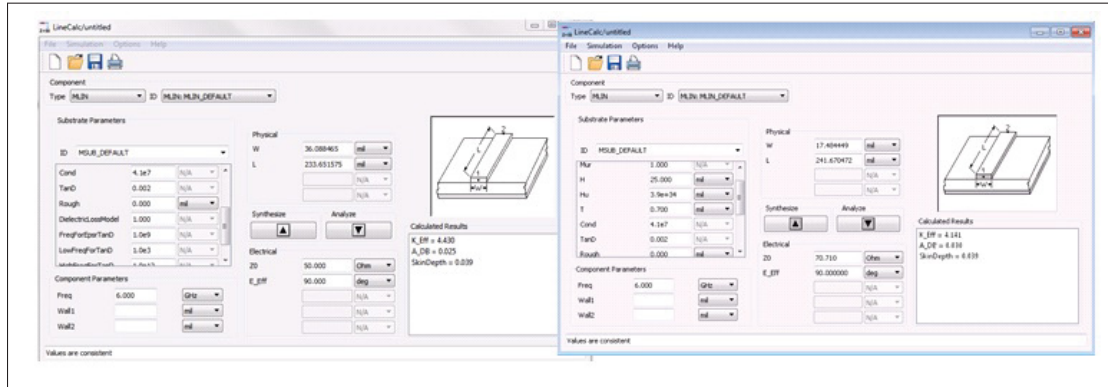


Figure 3.14 Parameters of transmission lines for characteristic impedance  $50\Omega$  and  $70.71\Omega$  of Wilkinson divider/combiner

### Simulation results of Wilkinson divider/combiner

Table 3.4 Comparison of Wilkinson Divider/Combiner Specification and Simulation Results

Parameters( $s_{ij}$ )	Insertion loss dB	Dephasor	Adaptation dB	Isolation dB
Specification	3(+/-0.5)	$0^\circ$ (+/-5)	$\geq 25$	$\geq 25$
Simulation	3	$0^\circ$	35.7	32.3

#### 3.3.2 Characterization and simulation of ADP circuit's nonlinear control branch

The nonlinear control branch, as defined in Figure 3.8, is presented as the GD distortion generator. The GD is built on a balanced structure based on the 3dB model previously described. The structure of the GD is shown in Figure 3.16. In this case, we want to offer nonlinear behaviour for distortion to be created. To do this, we selected Schottky diodes to accomplish the charges that are to be mounted at the hybrid coupler's direct and coupled ports. The circuit surrounding

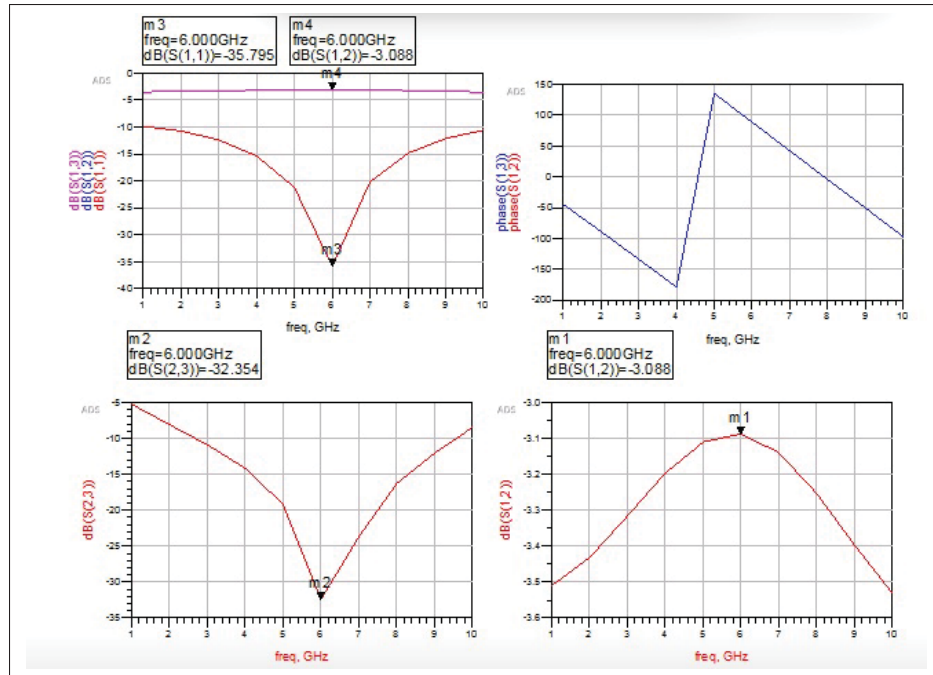


Figure 3.15 Simulation of S-parameters of Wilkinson divider/combiner

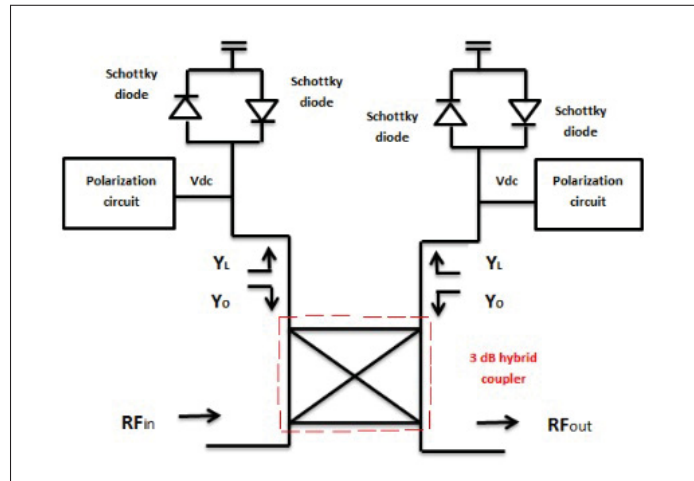


Figure 3.16 Structure of distortion generator (GD)

the Schottky diode and its polarization plays an important role in the GD's output; Hadouej (2013) research presented in detail.

### 3.3.2.1 Simulation of Schottky diode

In this part, we propose observing the DC behaviour of the Schottky diode. The chosen model is the SMS3922 under the SMS392x series of diodes from Skyworks presented in Appendix II, which used a frequency up to 6GHz. This model is provided with its specifications, which allows us to know approximately its real behaviour. The characteristic  $I(v)$  obtained following a DC simulation with ADS software of the diode pair is illustrated in Figure 3.17. We obtain a behaviour close to that indicated in the specifications, with a threshold voltage of around 0.17v. Further, we can distinguish that the region  $0.17v < V_{dc} < 0.35v$  is the nonlinear region of the diode. This nonlinearity is exploited to generate the distortions of odd order at the output of GD. The voltage at the input of the branch is  $V_{total} = V_{RF} + V_{dc}$ . We can choose the bias voltage  $V_{dc}$  typically between 0.1v and 0.45v. This choice, coupled with that of the bias circuit, makes it possible to have a nonlinear behaviour (expansion/compression) in a well-defined input power range. The shape is then controlled by the rest of the linear components to adjust to the shape of the obtained nonlinear response of modelled GaN PA; this step is explained in the next section.

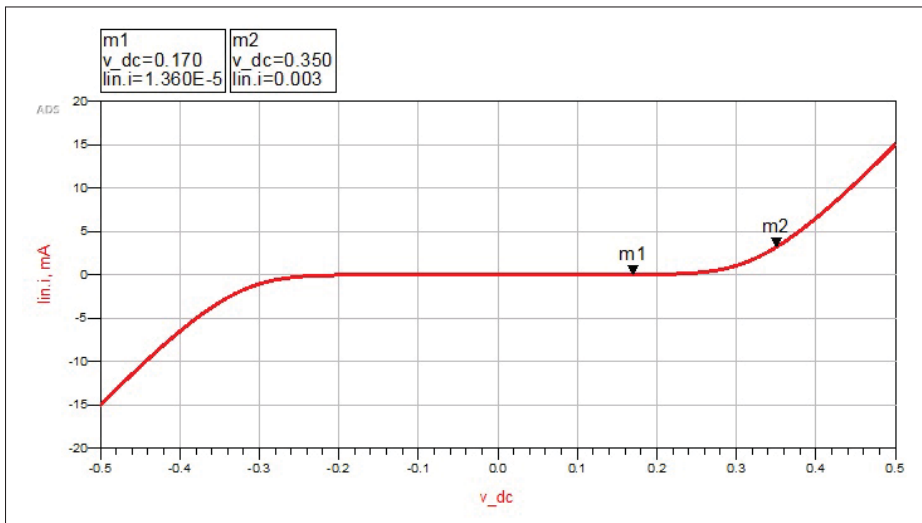


Figure 3.17 Characteristic  $I(V)$  simulation of pair of Schottky SMS 3922 diodes

### 3.3.3 Simulation and linearization results of APD circuit

After presenting and simulating the different APD circuit design components, we propose in this section to simulate the behaviour of the whole circuit of APD with ADS software. The structure of the APD circuit constructed is illustrated in Figure 3.18. To find out how the linearization works correctly, we follow this step:

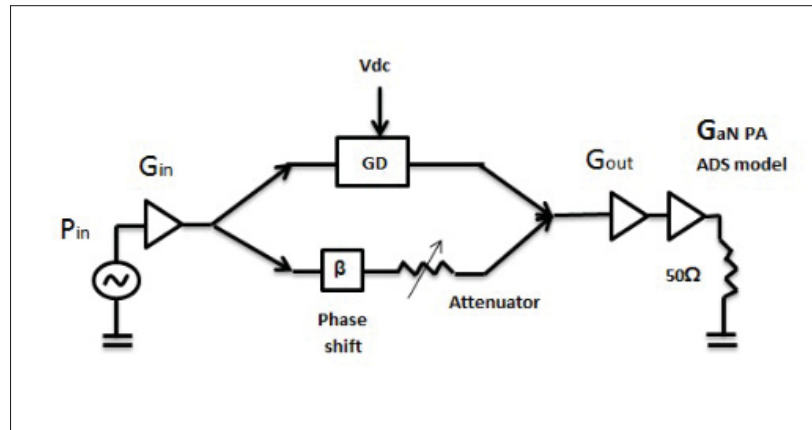


Figure 3.18 Schematic of APD circuit with GaN PA model

- The concept of pre-distortion, as shown in Figure 1.9, shows us that the model of PA is a function of the output of GD. So, the response has to be the same as the obtained nonlinear response of modelled GaN PA. By using the phase-shift value in the linear branch of the proposed APD circuit, the shape obtained by GD is input/output and by GaN PA is output. This can be modified to obtain the same shape of the nonlinear response of the modelled GaN PA, especially in the nonlinear region called the pre-distortion operation region. Our simulation at the  $P_1 dB$  corresponds to input at  $9.8 dBm$ , which also corresponds to an output equal to  $34.7 dBm$ . This matches the same value obtained nonlinear response of the modelled GaN PA presented previously in section 3.1.

The figures bellow show a comparison between the responses of the simulation GaN PA with and without APD.

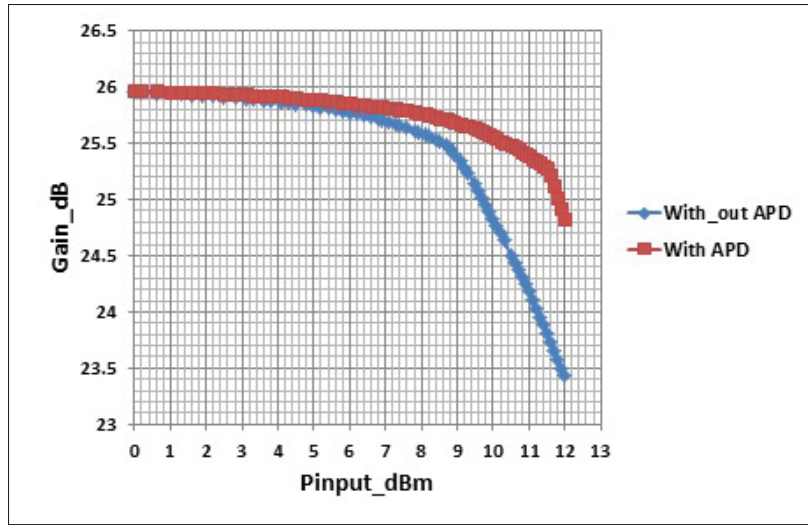


Figure 3.19 Comparison between responses of simulation GaN PA without and with APD (AM/AM)

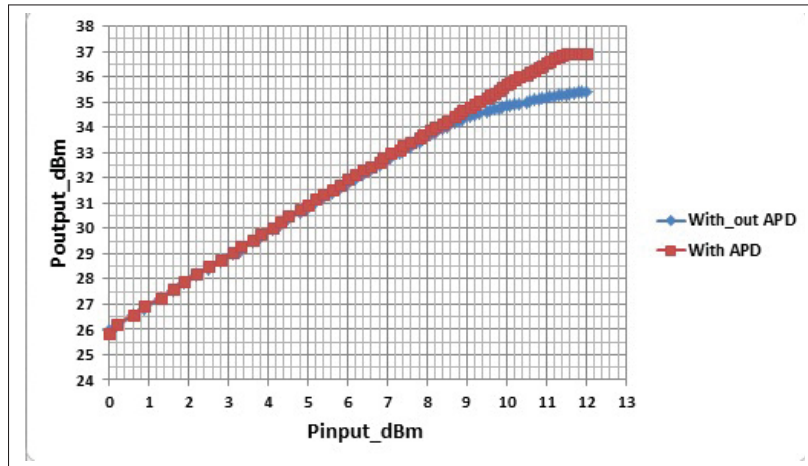


Figure 3.20 Comparison between responses of simulation GaN PA without and with APD (output power)

The results had an impact on improving the linearity of the cascade (APD + GaN PA). Hence, the  $P_1$  dB corresponds to input were increased from 9.8 dBm to 10.5 dBm. Further, the compression gain was reduced from 8.145 dB to 7.1 dB as saturation, and the  $P_1$  dB corresponding to output was then increased from 34.4 dBm to 35.4 dBm or 1 dB of improvement. We noted a decrease in the overall gain of around 1 dB.



Table 3.5 The linearity result of the cascade (APD + GaN PA)

Parameters	Value	Unit
Operation frequency	6	Ghz
$P_1$ dB input	10.5	dBm
$P_1$ dB output	35.4	dBm
$P_{output}$ maximum saturation	36.9	dBm
Compression of gain at saturation	7.1	dB

### 3.4 Proposed digital pre-distortion (DPD) model/Simulink-MATLAB

The proposed linearization techniques are designed to resolve nonlinearization effects, in which pre-distortion (PD) is a method of distorting the signal being sent to the PA. The PD has an inverse transfer characteristic to that of the PA. As a result, we get the characteristic of linearization, as shown in Figure 1.9. Because PA begins to exhibit a memory effect in a wideband signal, complex pre-distortion gain based on (LUT) is able to obtain less than optimal linearization Bache (2015).

We can use a number of different behavioural models when describing how a nonlinear system's input and output are related, and how the memory effect functions, the latter for which the DPD linearization techniques are intended. Polynomial constructs and models based on the Volterra series or their pruned variants are excellent examples of behavioural analysis of PAs and DPD interactive pre-distortion behavioural models. However, the realistic structure and implementation of the DPD algorithm is more complicated when reversing the nonlinear characteristic of PA.

Since memory affects the PA, the DPD must be adaptive and work in a near-loop configuration to compensate for the PA effect. Furthermore, the DPD algorithm is a digital algorithm implemented in the baseband, while PAs are high-frequency RF components. Therefore, up-conversion and down-conversion stages are needed to make the two systems work together. Figure 3.21

shows the proposed schematic baseband DPD with a digital pre-distortion algorithm and power amplifier<sup>1</sup>.

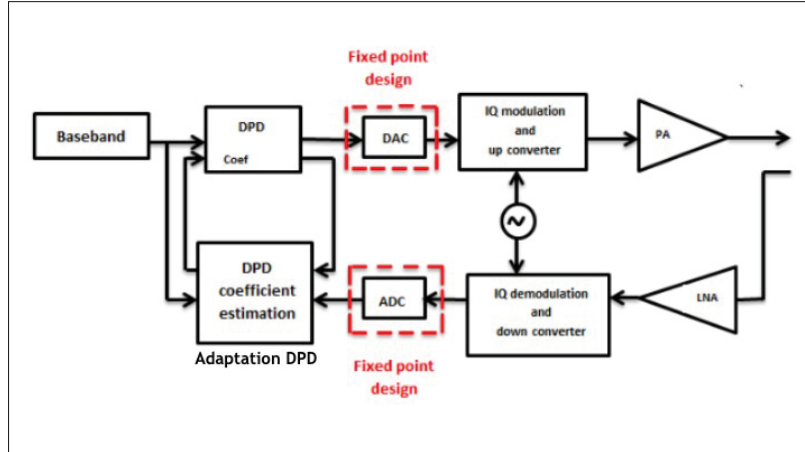


Figure 3.21 Proposed baseband DPD circuit model

The requirements of the proposed DPD model contents are listed below:

- 16 QAM baseband signal.
- Power amplifier with memory effect.
- A/D and D/A converter (as explained in the next section).
- Quadrature modulation and demodulation (up-converter and down-converter).
- Coupler.

### 3.4.1 Workflow of proposed DPD circuit

PA has a memory effect, so RF PA block includes the coefficient matrix of the PA when the Volterra memory effect is selected.

- We propose using a 16 QAM modulation as might be found in a realistic wireless signal generator in baseband with the selected GaN PA. In our model, the processing bandwidth (envelope bandwidth) is about three to five times the Nyquist bandwidth. (Note that the models support bandwidths up to 25 MHz, 100MHz and 1GHz.) A comparison of these

<sup>1</sup> <https://en.wikipedia.org/wiki/Predistortion>

models with various bandwidths is provided in the following section. Additionally, complex baseband measurements of  $I + jQ$  signals are defined or evaluated, as shown in Figure 3.22. Then, we load complex baseband input and output  $I + jQ$  signals into MATLAB.

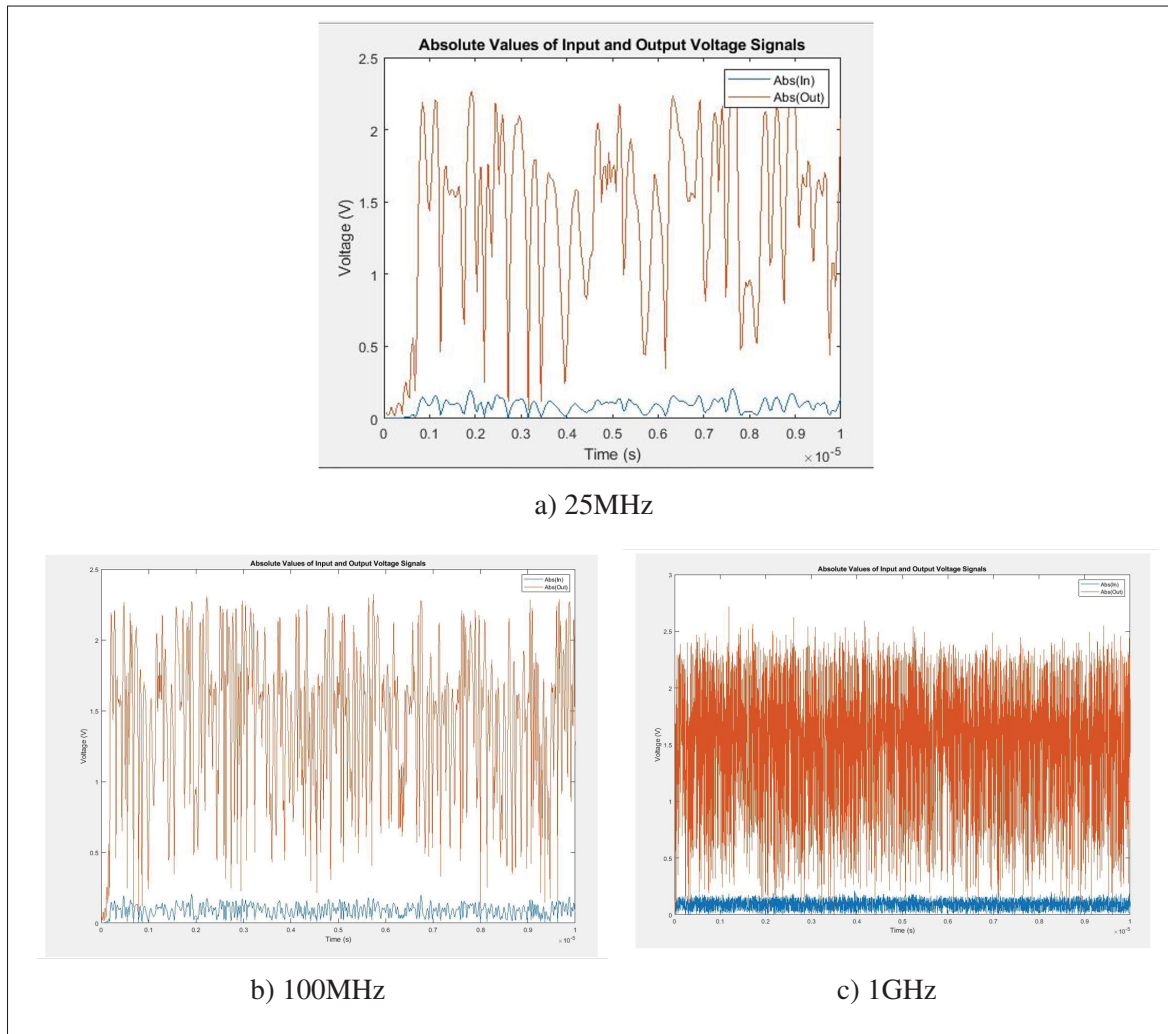


Figure 3.22 Input and output complex measurement of I/Q data for various proposed sample rates (25MHz, 100MHz and 1GHz)

- MATLAB provides a simple fast-fitting procedure (Appendix V). By using previously loaded data from GaN PA with 16 QAM to extract the model coefficients based on the selected value of  $k$  and  $m$ , the better fitting allows the establishment of PA model coefficients so the PA can be inserted into a simulation model. Figure 3.23 presents the absolute value of output and fitting output signals.

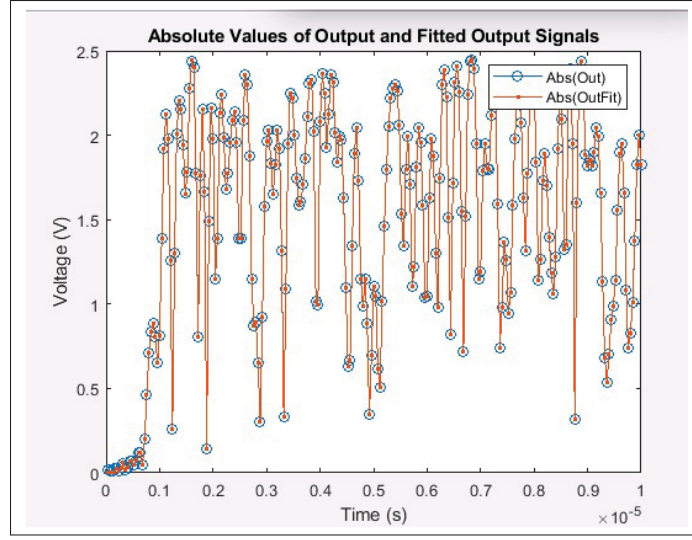


Figure 3.23 Absolute value of output and fitting output signals for sample rate of 25MHz

- The PA behavioral model is based on memory polynomial Liu *et al.* (2013):

$$y_{MP}(n) = \sum_{k=0}^{K-1} \sum_{m=0}^{M-1} a_{km} x(n-m) |x(n-m)|^k \quad (3.7)$$

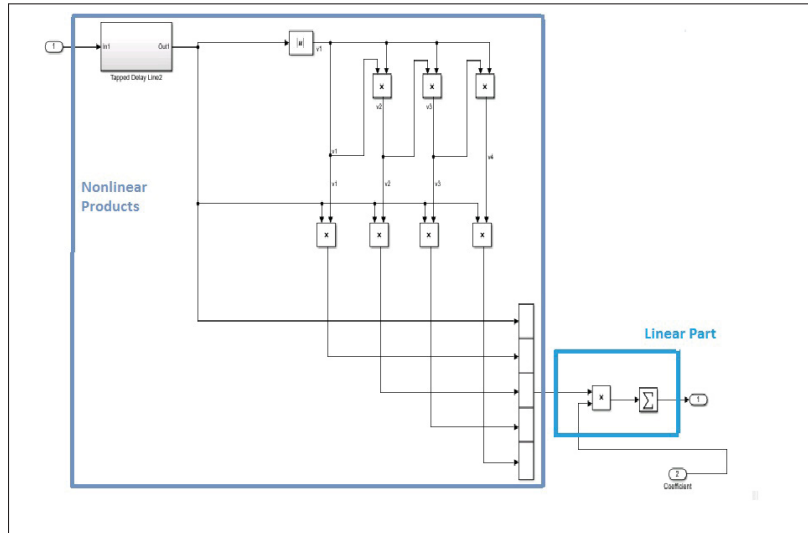


Figure 3.24 Simulation DPD Block

where:

$a$  is the model coefficient.

$k$  is the degree of nonlinearity.

$K$  is the number of degree to which the PA is modeled.

$m$  is the memory depth value.

$M$  is the memory depth of the model.

In the model, as well as the simulation, the DPD block is based on the polynomial memory.

However, adaptive DPD coefficient calculation is called for in this model. It can be a difficult task in the case of hard nonlinearity, since a high-order model is needed. Hence, estimation techniques are required as LMS and RPEM algorithms, as shown in Appendix III Schutz (2014). We can conclude that the RPEM algorithm is more complex than the LMS algorithm. In a feedback loop of the proposed DPD system, the estimation algorithms calculate an error signal, with the error being the difference between the input of measured PA and the input of estimated PA. The algorithm tries to reduce this error to zero and converge on the best approximation of the DPD coefficients. By comparing adaptive DPD algorithms, we can see how RPEM provides a more optimal outcome compared to LMS. In this case, we choose the RPEM algorithm in adaptive DPD in our model.

### 3.4.2 Implementation and linearization results of proposed DPD system

- As explained in section 3.1,  $IIP3$  corresponds to an input of approximately  $23dBm$  and an output of  $36dBm$  (saturation – maximum power).
- To test the capability of the DPD algorithm and linearize the output signal, the PA should be driven near saturation. The proposed DPD operating points are above  $9dBm$ , corresponding to the the input power. Different PAP (back-off input) values are fed into the PA in the simulation model input as (dB gain block) to analyze its behaviour. We propagate PAP equal to  $-17dB$ , giving the input power of the simulation model of around  $9.8dBm$  to apply DPD to the operating point.

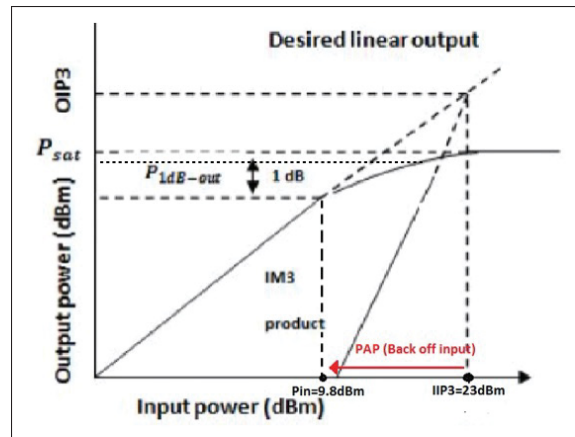


Figure 3.25 DPD operation point

- The PA behavioural model and DPD performance metrics for calculating PA linearity are shown in the following:

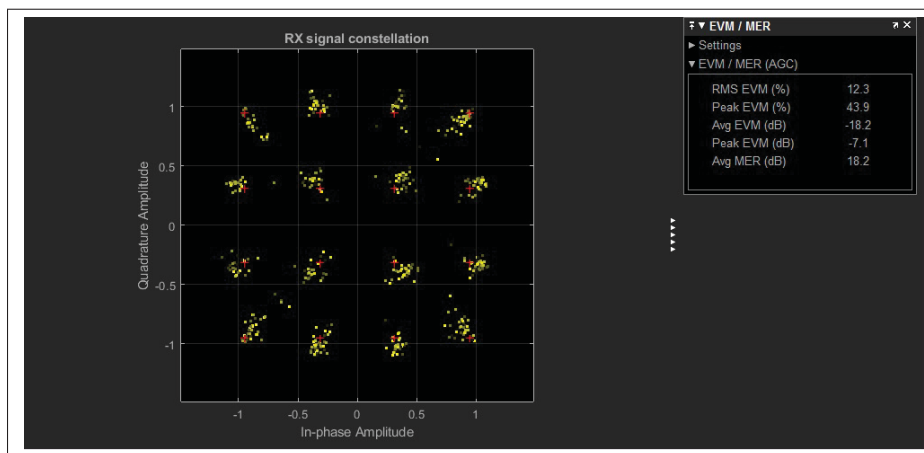


Figure 3.26 EVM without applying DPD algorithm

1. Before the DPD algorithm is enabled, the EVM has an RMS value of 12.3%. Figure 3.26 shows the constellation of the RF transmitter's output signal with a 16 QAM signal. After allowing the DPD algorithm, the RMS value of EVM is reduced to 2%, as shown in Figure 3.27.
2. Figure 3.28 represents the PA spectrum without applying DPD for the suggested sample rates. The nonlinearized PA spectrum signal without applying DPD suffers from significant intermodulation distortion [IMD3]. This can distort the adjacent channels, producing high

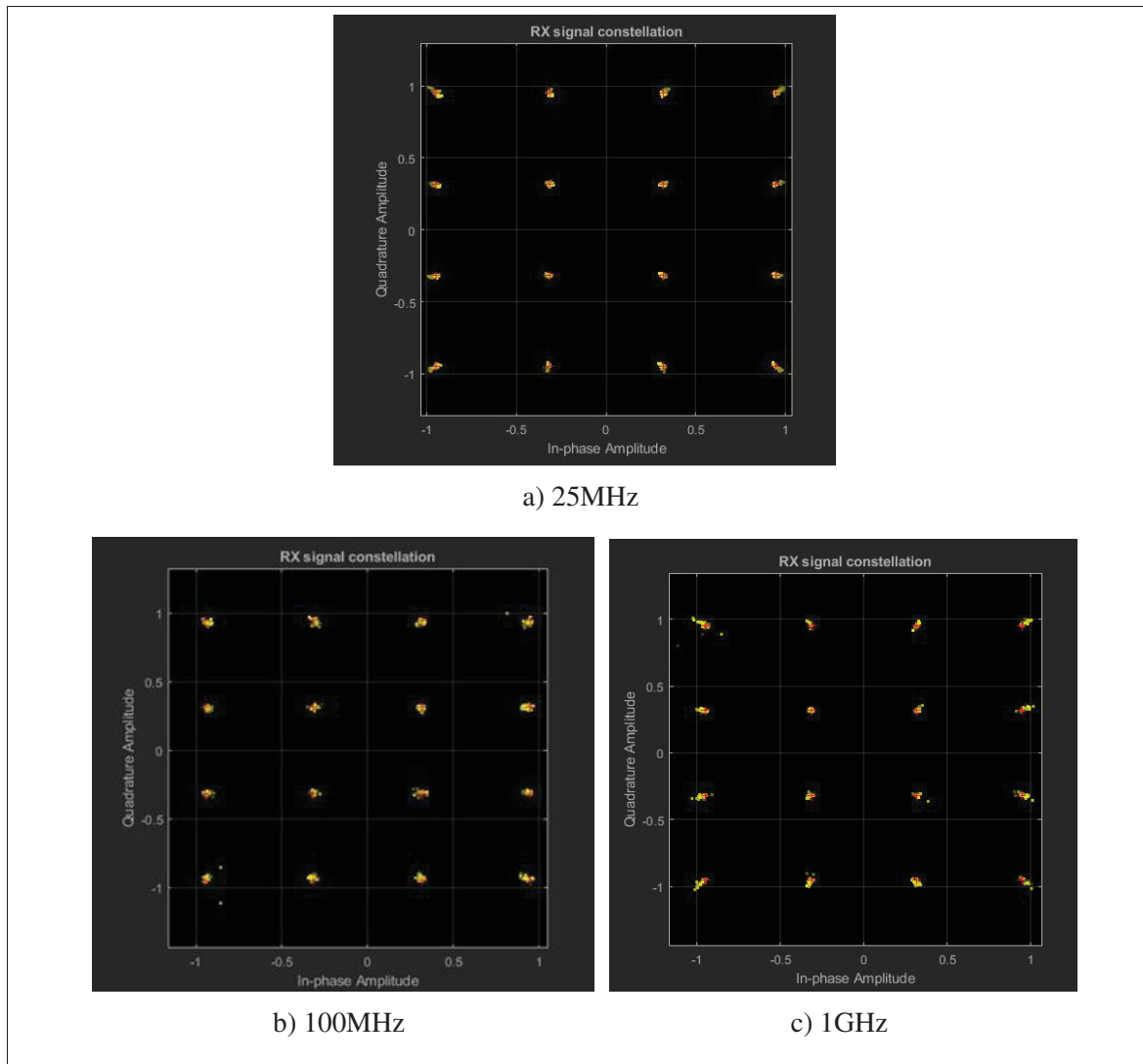


Figure 3.27 EVM with applying DPD technique for various proposed sample rates (25MHz, 100MHz and 1GHz)

rates of intermodulation power of around  $21.7\text{dBc}$ . Additionally, the output shows around  $24\text{dB}$  of gain at the expense of significant spectral regrowth. After the adaptive DPD algorithm is implemented, IMD3 is reduced. The amount of discounted of IMD3 depends on the sample rate amount, as illustrated in Figures 3.29 and 3.30. The relation between ACPR test results with and without DPD for the suggested sample rates are shown in Table 3.6 to determine the degree of nonlinearity and its improvement where ACPR measurement is used.

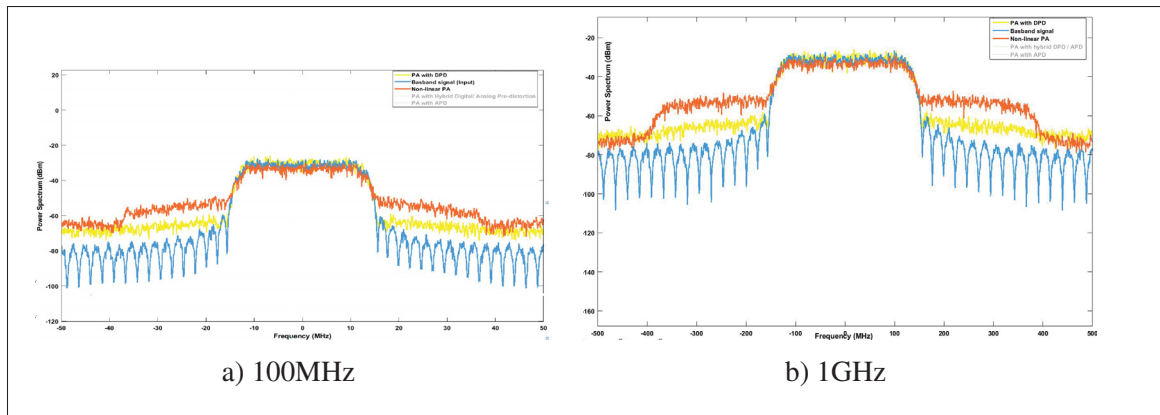


Figure 3.28 Spectrum analyzer for input and output signal of PA with and without applying DPD algorithm for suggested sample rates (100MHz and 1GHz)

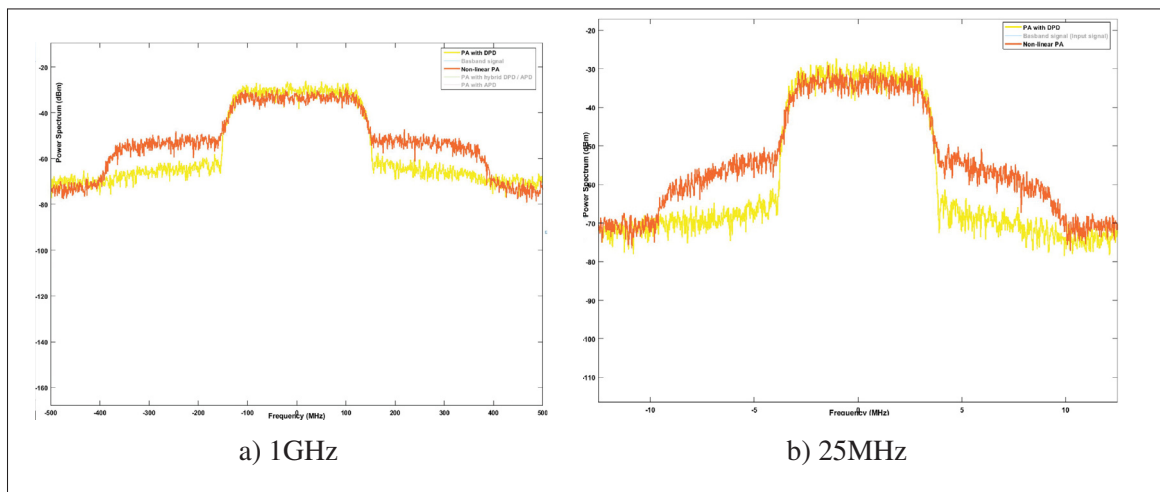


Figure 3.29 Comparison of PA output signal without/with applying DPD technique for bandwidth of 25MHz and 1GHz



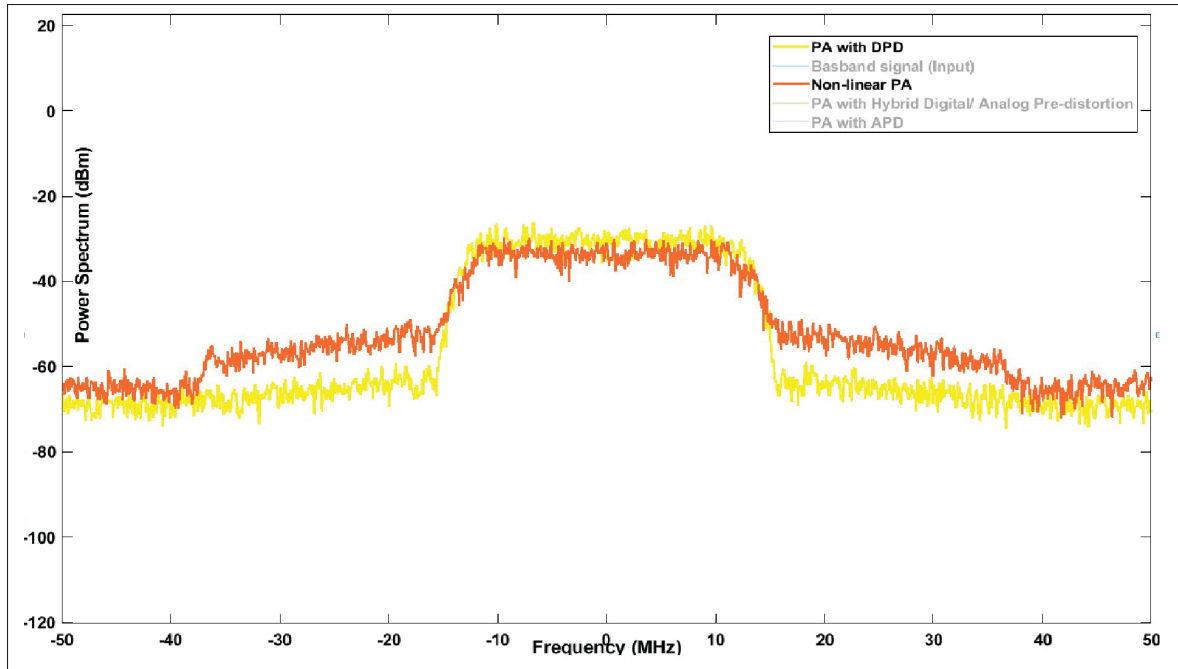


Figure 3.30 Comparison of PA output signal without/with applying DPD technique for bandwidth of 100MHz

Table 3.6 Compression Results of ACPR Improvement and IMD3 Improvement for the Various Suggested Bandwidths

DPD Technique	ACPR Improvement (dB)	IM3 Improvement (dB)	RMS Value of EVM %
Bandwidth of 25MHz	12.7	9.71	2.3
Bandwidth of 100MHz	12.6	9.8	3
Bandwidth of 1GHz	11.6	10.1	<b>3</b>

- The plots of AM / AM and output power before and after DPD are shown in Figures 3.31 and 3.32; we may infer that GaN PA's nonlinear distortion is eliminated after DPD.

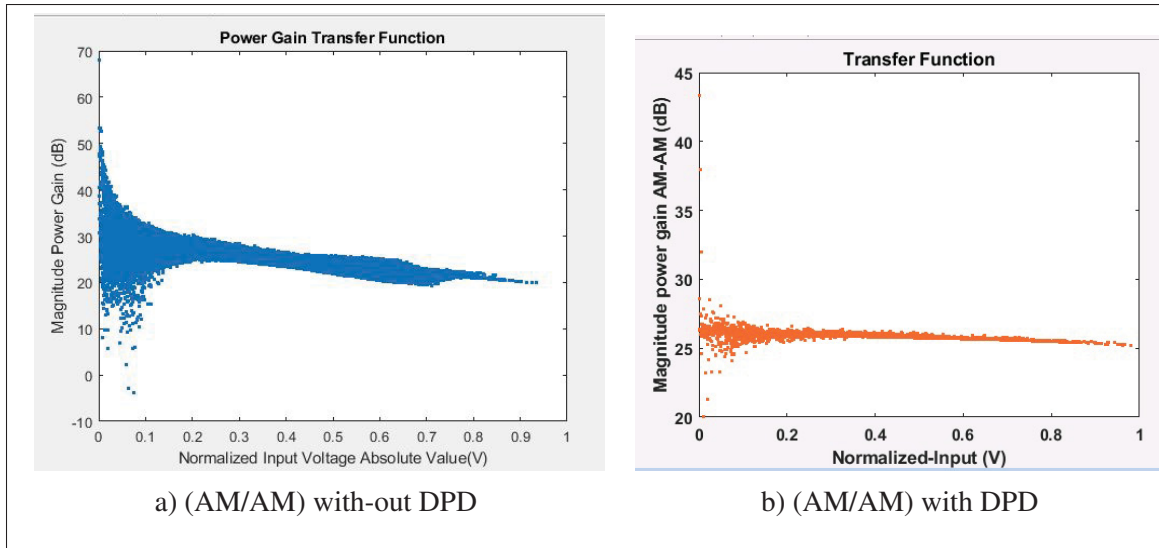


Figure 3.31 (AM/AM) with and without applying DPD

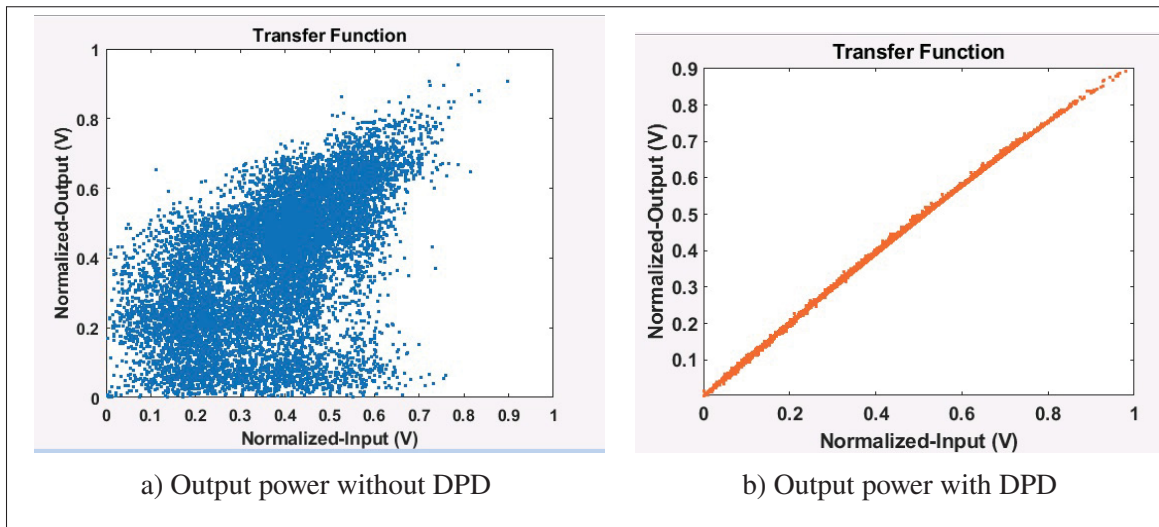


Figure 3.32 Output power (transfer function) with and without applying DPD

### 3.4.3 Hardware requirements

In modern systems, mobile applications need a wideband signal, which requires analog-to-digital converters (ADCs) and digital-to-analog converters (DACs) for higher precision. One option is to use low-precision ADCs and DACs to reduce the system's complexity. Table 3.7 shows

various ADC requirements of devices based on bandwidth, resolution, and power consumption. Generally, these requirements contradict each other: high resolution and high bandwidth suggest more complex hardware that should have low power consumption and high environmental tolerance (noise, temperature, etc.).

Table 3.7 ADC Requirements for Various Applications

Application	Resolution	Bandwidth	Power Consumption
Microcontrollers	Low-Medium	Low-Medium	Low-Medium
Audio	High	Medium	Low
Video	Medium-High	High	Low
Microwave	Medium-High	High	Low
Telecommunication	Medium	High	Low

Figure 3.33 also illustrates the bandwidth-resolution relationship for different applications.

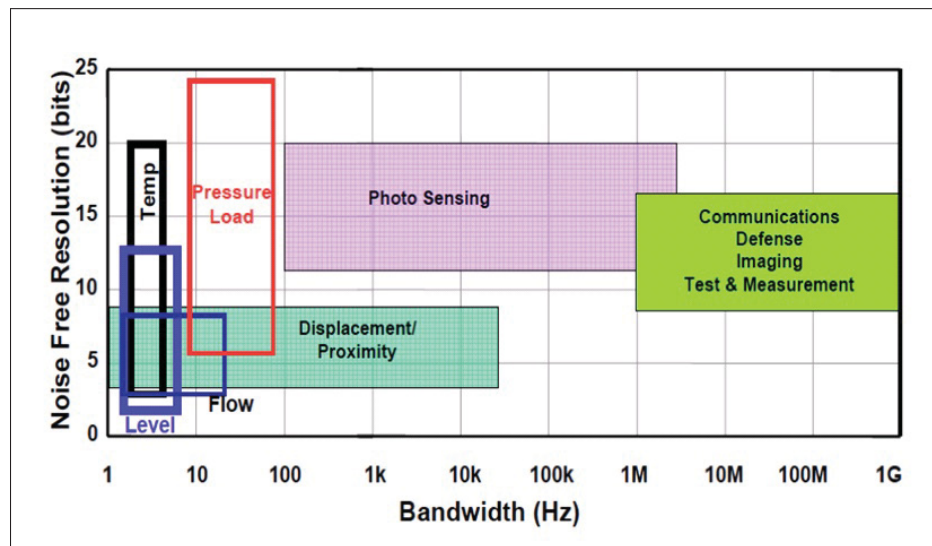


Figure 3.33 Bandwidth/resolution relationship for different applications  
Taken from Tex (2018)

Figure 3.34 illustrates the ideal resolution and bandwidth requirements of ADC and DAC structures.

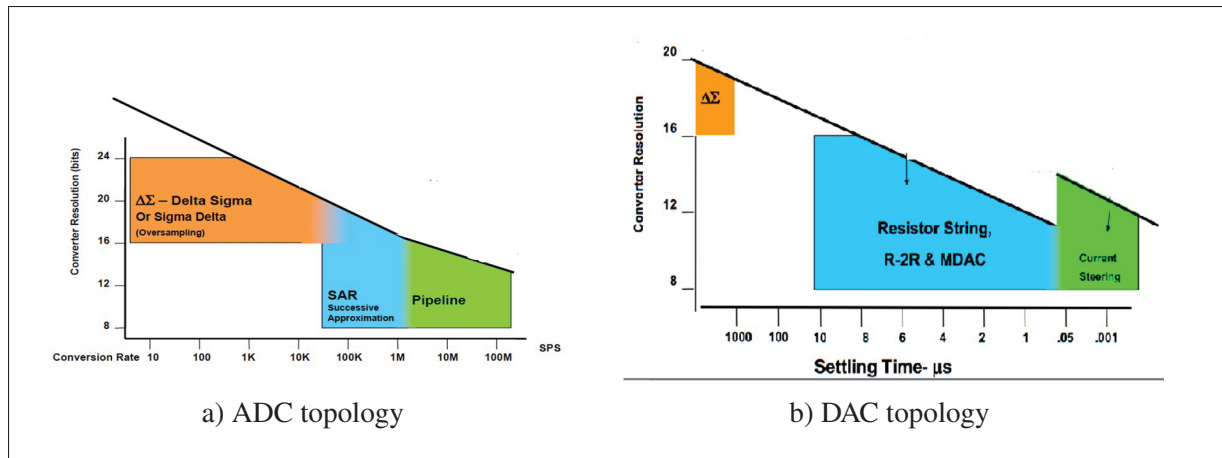


Figure 3.34 Bandwidth/resolution for different topologies of ADC and DAC  
Taken from Tex (2018)

#### 3.4.4 Basics of analog-to-digital converters (ADCs)

Analog-to-digital converters are essential components in digital communication signals in real-time. Analog signals have a continuous sequence of continuous values in the real world, whereas digital signals have a sequence of discrete values, with the signal broken down into sequences depending on the time series or sampling rate. When analog data is used, the computer machine (microcontrollers) cannot read values. This is because digital devices can only see the voltage levels that depend on the ADC resolution and the device's voltage Hoeschele (1994). Its sampling rate and resolution are two essential aspects of ADC:

- ADCs follow a sequence in which an analog signal is converted to digital.
- First, sample the signal by ADCs.
- Then quantify it in order to determine the bit of resolution.
- Finally, set binary values and submit the digital signal to the system.

### Sampling frequency

The ADC sampling rate, known as the sampling frequency, can be linked to the speed of the ADC. The more samples the ADC takes, the higher frequency it can handle.

$$F_s = \frac{1}{T} \quad (3.8)$$

where:

$F_s$  is the sample rate/frequency.

$T$  is the period of the sample or time it takes before sampling again.

When the sampling rate is slow and the signal frequency is high, the ADC cannot reproduce the original analog such that the system can receive incorrect data. The Nyquist theorem demonstrates that the sample rate/frequency must be at least twice as high as the signal's highest frequency to recreate the original signal. In our model, the processing bandwidth (envelope bandwidth) is about three to five times the Nyquist bandwidth Farrow, Shaw, Kim, Juhás & Billinge (2011).

### Bits of resolution (bit depth)

Bits of resolution are important principles to pay attention to, as they substantially determine the number of bits each sample represents. To accurately gauge the voltage level needed by the device, it is necessary to know the bit of resolution. Higher resolution leads to a better dynamic range, enabling converters to better match an analog signal. The resolution depends on the bit length as well as the reference Ball (2001).

$$\text{Width of step (Step size)} = V_{Ref}/N \quad (3.9)$$

$$N = 2^n \quad (3.10)$$

where:

*Step size* is the relation of each level in term of voltage.

$V_{Ref}$  is the voltage reference (ranges of voltages).

$N$  is total level size of ADC.

$n$  is bits of resolution (bit depth).

Table 3.8 illustrates the standard bit depth or length, number of levels, and step size for a ( $5v$ ) reference.

Table 3.8 Standard Bit Depth, Number of Levels and Step Size for  $5v$  Reference

Bit Depth	Levels	Step Size ( $5v$ range)
8 bits	256	19.53 mv
10 bits	1024	4.88 mv
12 bits	4096	1.22 mv
16 bits	65536	76.29 $\mu v$
18 bits	262144	19.07 $\mu v$
20 bits	1048576	4.7 $\mu v$
24 bits	1677216	0.298 $\mu v$

To set the right ADC/DAC in our model, we need to know:

1. What speed is required for ADC/DAC (sampling frequency)?
2. How many Bits of ADC/DAC resolution are needed?

To answer the previous questions, we follow the explanation in detail in the next section.

### 3.4.5 Converting proposed DPD model to fixed-point design

A PA's analog output must be converted in an ADC in order for training to be carried out in digital processors. However, the quality of the signal may degrade during quantization and thus limit the DPD algorithm's performance. To remedy this problem, fixed-point design can be utilized for quantization of feedback input in order to determine the required bit resolution. Converting the DPD algorithm from a floating-point to a fixed-point correctly answers the question of how many bits this algorithm needs by calculating the true dynamic signal range. A

fixed-point tool is available in Simulink/MATLAB. Simulink highlights some of the key features in fixed-point design that can help to convert the ideal floating-point design model to an efficient fixed-point design that meets the constraints of the target hardware. Mathworks fixed-point designer provides a workflow guide to help designers convert the models as follows:

- Preparing the model for fixed-point conversion.
- Collecting the range information of the model.
- Using the provided tool to propose data types.
- Last, applying the chosen data type and then comparing the results with floating-point.

Note that this is a process of trade-off. If the results appear to be good, the proposed word-length will be implemented. Each signal in the entire model is evaluated and collected according to the proposed data type in fixed-point conversion to determine the true dynamic range and suggested word-length at each signal line. The conversion is completed for each model separately with various suggested sample rates. We consider two models with wide-band signal, as presented in section 3.4. The proposed bandwidth (envelope bandwidth) is about three to five times the Nyquist bandwidth. In this case, the target ADC for each model is operated with a high speed clock of 100MHz and 1GHz.

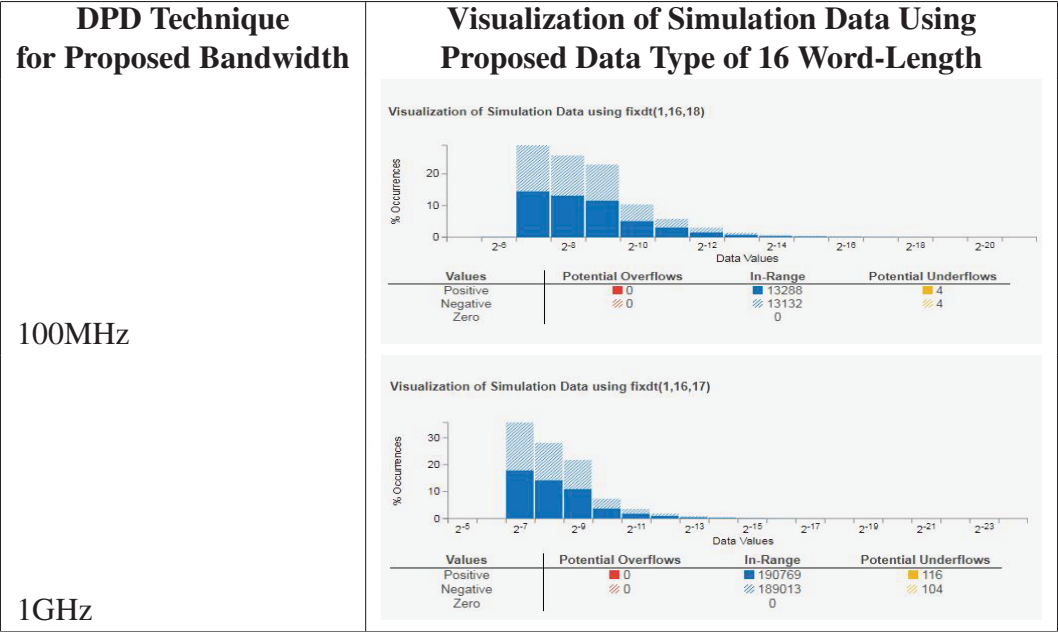
Table 3.9 illustrates each model with different proposed data types and precision results for the target analog-to-digital converter. In viewing the table, we can conclude that by using just the DPD technique, the DPD algorithm will be performed with a longer word-length to achieve lower precision of the target ADC hardware.

Table 3.9 Precision of Target ADC in Each Model for Various Proposed Word-lengths/DPD Technique

<b>DPD Technique</b>	<b>Precision of Target ADC in Each Model for Various Proposed Word-Lengths</b>					
Proposed bandwidth	16 bit	14 bit	12 bit	10 bit	8 bit	6 bit
100MHz	3.8146E-06	1.5258E-5	6.1035E-5	0.000244	0.0009765	0.003906
1GHz	7.62939E-6	3.0517E-5	0.001220	0.000488	0.0019531	0.007812

Also, we can visualize how the data type fits the present study’s design and whether there are potential overflows or underflows as a result of the proposed data type, as shown in Tables 3.10, 3.11, 3.12 and 3.13.

Table 3.10 Visualization of Simulation Data Using Proposed Data Type of 16 bit for Proposed Bandwidth/DPD Model Only



Hence, as shown in Figure 3.35, the 16 bit, 14 bit and 12 bit word-length proposals can successfully convert the suggested 100MHz double floating-point design model to a fixed-point model that satisfies the behavioral requirements.

Also, as shown in Figure 3.36, the 16 bit word-length proposal can successfully convert the suggested 1GHz double floating-point design to a fixed-point model that satisfies the behavioral requirements. As stated earlier, this is a trade-off process, so it must then be determined whether the extra expense is worth the improvement in performance.



Table 3.11 Visualization of Simulation Data Using Proposed Data Type of 12 Bit for Proposed Bandwidth/DPD Model Only

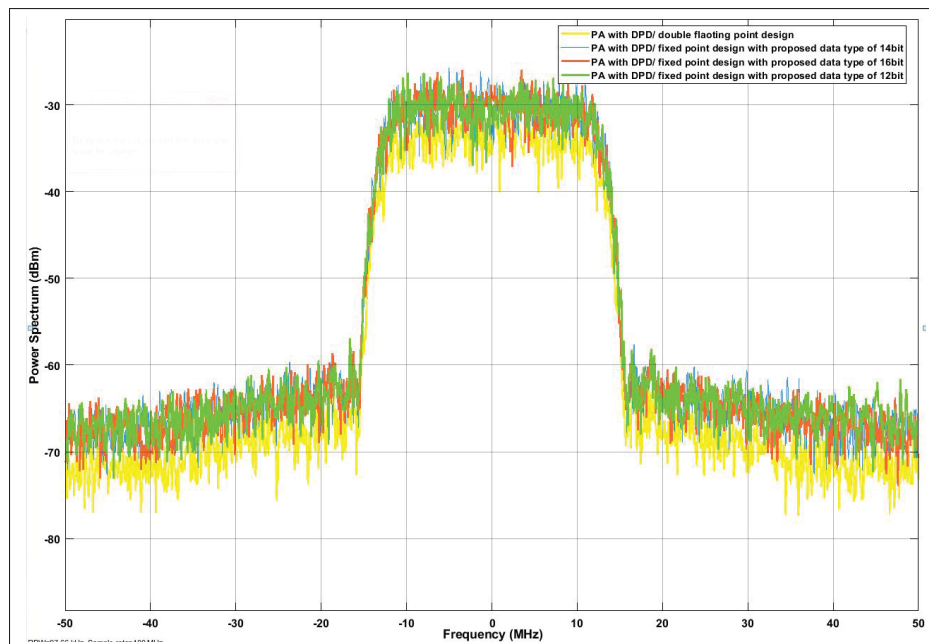
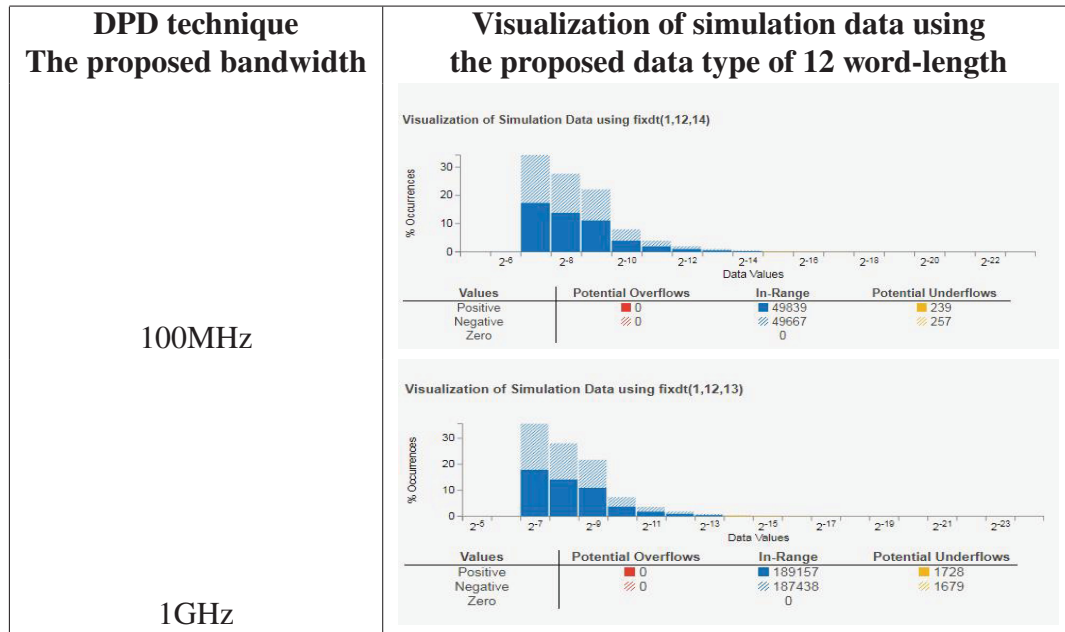


Figure 3.35 Converting suggested 100MHz double floating-point design model to fixed-point mode

Table 3.12 Visualization of Simulation Data Using Proposed Data Type of 10 Bit for Proposed Bandwidth/DPD Model Only

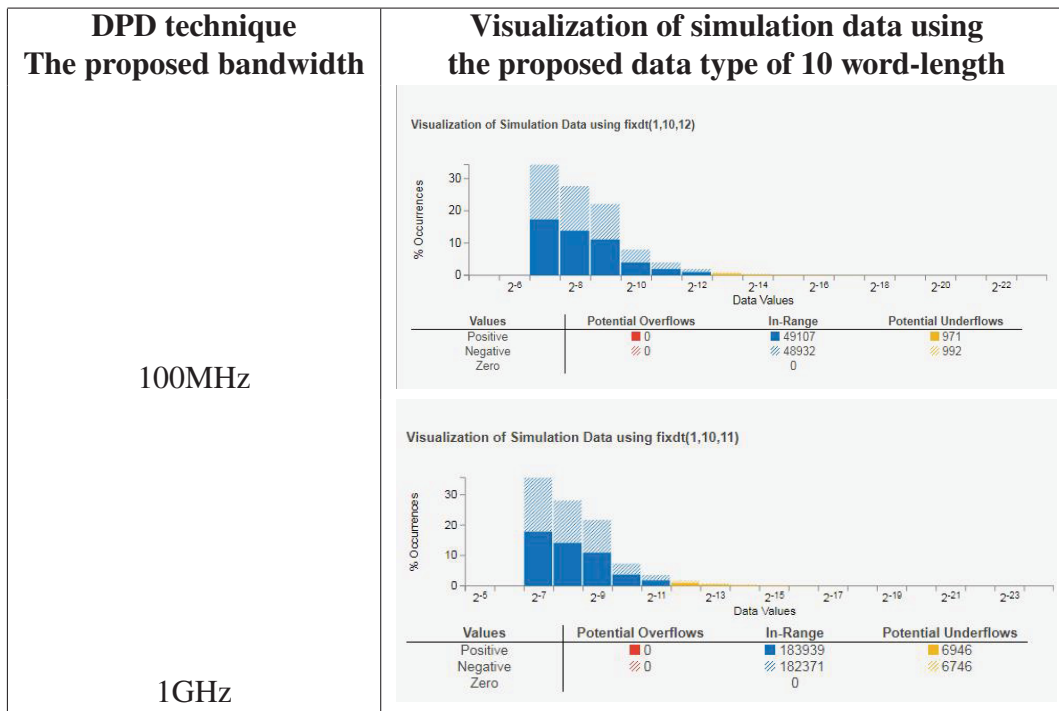
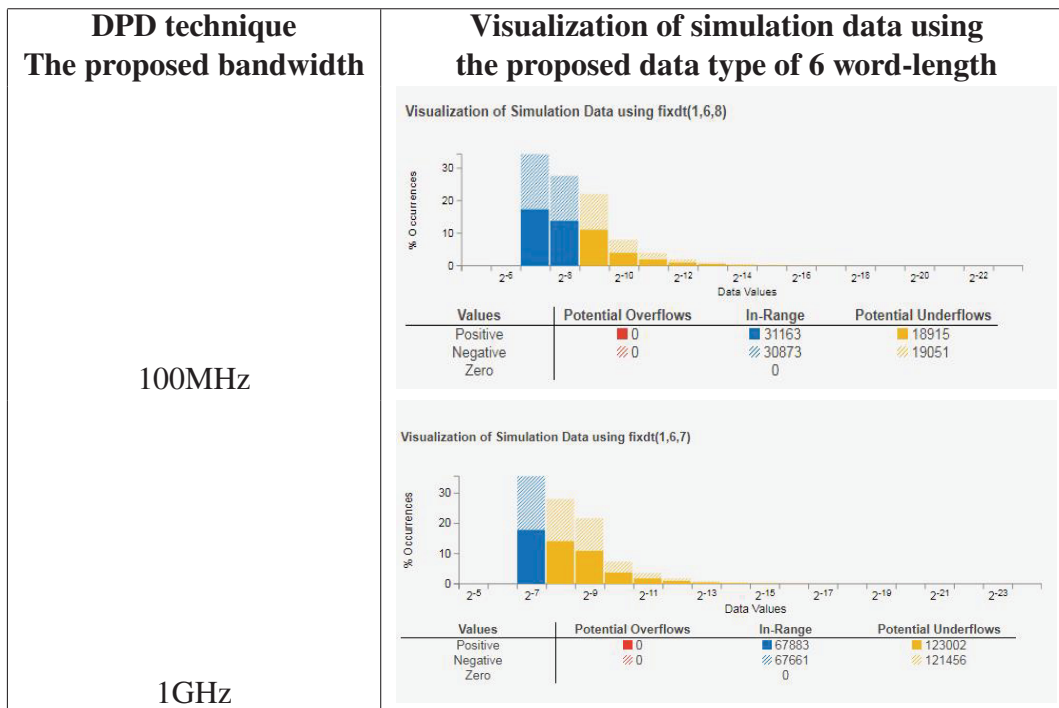


Table 3.13 Visualization of Simulation Data Using Proposed Data Type of 6 Bit for Proposed Bandwidth/DPD Model Only



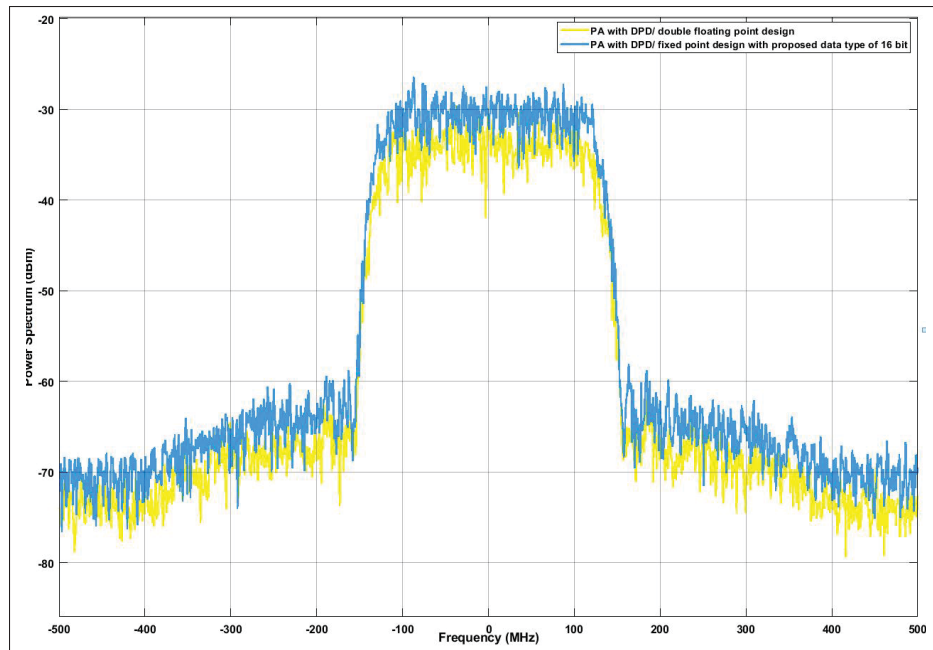


Figure 3.36 Converting suggested 1GHz double floating-point design model to fixed-point model

As stated in the previous section, the right ADC hardware type can be selected depending on the application type, the resolution, and the sample rate. The suggested sample rate of each model and their resulting resolution for the target ADC shown in the previous results help us to choose the right ADC for each model. It appears that Pipeline (high-speed) is the ideal topology for analog-to-digital conversion in our model.

The Digi-key website helps define how many of the selected hardware ADCs exist on the market. The available Pipeline (high-speed) ADC products target the hardware of the suggested model by applying DPD only. These are shown in Table 3.14.

Table 3.14 Pipeline (high-speed) ADCs Available in the Market for Suggested Model with Applying DPD Only

<b>ADCs for the Sample-Rate of 100MHz</b>
ADS52J90ZZE
ADS5295PFPR
ADS5295PFPT
<b>ADCs for the Sample-Rate of 1GHz</b>
ADS54J60IRMPT
ADS54J60IPMP

Table 3.15 Pipeline (high-speed) ADCs for Proposed Hybrid Digital/Analog Pre-Distortion Model

<b>High-speed ADC</b>	<b>Sampling Rate (Per second)</b>	<b>Number of bits</b>	<b>Cost</b>
ADS52J90ZZE	100MHz	14 bit	\$229.94
ADS5295PFPT	100MHz	12 bit	\$127.42
ADS5295PFPR	100MHz	12 bit	\$124.75
ADS54J60IRMP	1GHz	14 bit	\$1139.87
ADS54J60IRMPT	1GHz	14 bit	\$1138.92

### 3.5 Conclusion

Chapter 3 covers the modelling of the selected 6 GHz GaN PAs and obtains its nonlinear model in ADS. Then, by using Simulink/MATLAB, the proposed digital pre-distortion with memory effect is presented and modelled, and its bandwidth and nonlinearity requirements are quantified for the selected PA. Additionally, a comparison of the performance of the proposed DPD with different bandwidths is done. As a result, we found some drawbacks in the proposed method, such as when the bandwidth is increased, the performance is reduced. The simulation model also converts to a fixed-point design to define the number of resolutions needed by the DPD algorithm, which helps select the appropriate ADC and DAC for our model. In the last part of chapter 3 includes a conventional analog-pre-distortion circuit, which is provided in ADS, combined with the PA, and a linearized response is obtained.

The next chapter demonstrates the proposed hybrid approach to both APD and DPD combined. It may lead to the advantages of each of these techniques being captured such that they will complete each other.



## CHAPTER 4

### HYBRID DIGITAL/ANALOG PRE-DISTORTION METHOD

There are complementary advantages and disadvantages in both APD and DPD, so combining them as a means to offset their disadvantages could be a good idea. A combined linearization method is proposed in this thesis called a hybrid digital/analog pre-distortion of the selected GaN PA. The following shows the mathematically proved proposed hybrid digital-analog pre-distortion with the DPD and APD applied in series. Figure 4.1 presents an enlarged diagram of the blocks.

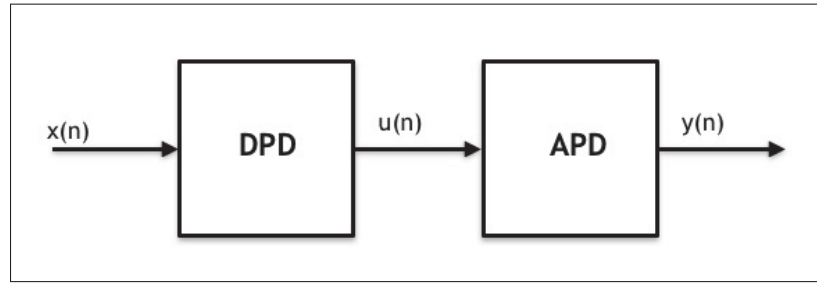


Figure 4.1 Implemented DPD and APD series in proposed model

As APD is a memoryless circuit of nonlinearity, a polynomial model will express it. The polynomial model is the first model, which is conventional Gutierrez *et al.* (1999). This is the easiest way to approximate the characteristic curve of AM-AM and AM-PM. Its function is expressed as:

$$y(n) = \sum_{k=0}^K a_k u(n) |u(n)|^k \quad (4.1)$$

Where:  $x(n)$  is an input signal of DPD,  $u(n)$  and  $y(n)$  represent the input and output signals of APD,  $k$  is the polynomial order, and  $a_k$  is the polynomial complex parameter. The polynomial model is not complicated, but its accuracy is poor.

The DPD model can be any model able to offset the memory effect. In this case, it is baseband DPD.

The relation between  $u(n)$ ,  $x(n)$ , and  $y(n)$  should therefore be:

$$u(n) = f(x(n)) \quad (4.2)$$

$$y(n) = h(u(n)) = \sum_{k=0}^K a_k u(n) |u(n)|^k \quad (4.3)$$

By replacing formula (4.2) with formula (4.3), we get:

$$y(n) = \sum_{k=0}^K a_k f(x(n)) |f(x(n))|^k \quad (4.4)$$

Where:  $f(x(n))$  is a DPD function, containing both memory effect and non-linearity.

There are no useful properties, as the  $y(n)$  expression is very complex. Therefore an engineering method is needed to simplify the expressions.

First, the nonlinearity section of  $f(n)$  is defined as  $e(n)$ . Hence,  $u(n)$  could be expressed as:

$$u(n) = bx(n) + e(x(n)) \quad (4.5)$$

Where:  $b$  is a constant, and  $e(x(n))$  includes the quiescent nonlinearity and memory effect of DPD models.

Substituting (4.5) for (4.3), the results are:

$$\begin{aligned} y(n) &= h(bx(n) + e(n)) \\ &= \sum_{k=0}^K a_k (bx(n) + e(n)) |bx(n) + e(n)|^k \end{aligned} \quad (4.6)$$



Since  $y(n)$  is a nonlinear invariant time formula, we can use distributive law and the error caused by  $y(n)$ , in which case  $y(n)$  will be:

$$\begin{aligned} y(n) &= h(bx(n)) + h(e(n)) + e'(n) \\ &= b^{K+1} \sum_{k=0}^K a_k(x(n))|x(n)|^k + \sum_{k=0}^K a_k(e(n))|e(n)|^k + e'(n) \end{aligned} \quad (4.7)$$

Where:  $e'(n)$  is an error in the law on linear distributions.

Since  $b$  is a constant and valued at approximately one, the first term of  $y(n)$  is precisely the APD model. The second and third terms are the nonlinearity memory effect polynomial, which can be represented by a DPD model, including a memory effect polynomial model (MP).

Therefore for both APD and DPD, the entire system can be written in a sequence form. The DPD technique employed in this study is the DPD baseband, and the concept of the linearization method proposed is:

$$y(n) = \sum_{m=0}^{M-1} \sum_{k=0}^K d_{k_m} x(n-m)|x(n-m)|^k + \sum_{k=0}^K a_k x(n)|x(n)|^k \quad (4.8)$$

The baseband DPD model is the first term in Eqn. 4.8. The second part is a memoryless polynomial that is used to characterize the circuit of APD. From Eqn. 4.8, it is evident that when the memory effect is set to zero, the expression of the APD formula is the same as the DPD formula.

The APD coefficients are specially designed to account for quiescent nonlinearity. The DPD coefficients are determined to eliminate both memory and quiescent nonlinearity effects. The DPD and APD will work together to compensate ACPR.



#### 4.1 Comparison of results between hybrid approach, DPD only, and APD only

The proposed hybrid approach is used for the various bandwidths, as suggested when applying DPD only in Chapter 3. Here, we compare the results between the proposed hybrid digital/analog pre-distortion, the suggested DPD only, and the conventional ADP only.

For the different proposed wide-bands for DPD only, APD only, and hybrid digital/analog pre-distortion, Table 4.1 shows the compression effects of ACPR and IMD3 improvement.

The compression of the spectrum analyzer for the different proposed wide-bands for DPD only, APD only, and hybrid digital/analog pre-distortion can be seen in Figures 4.2, 4.3, and 4.4.

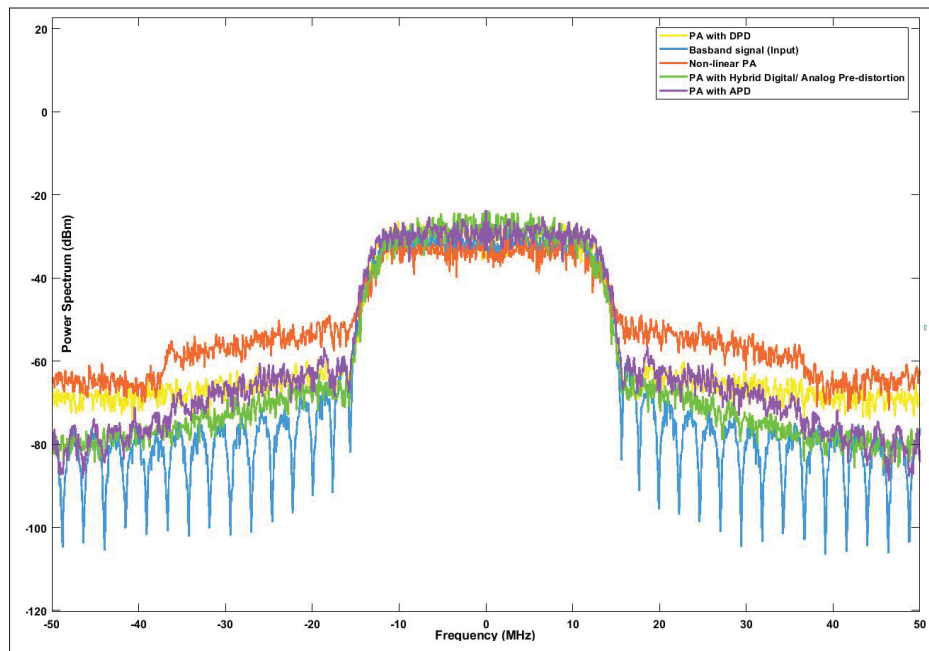


Figure 4.3 Spectrum analyzer for baseband signal, nonlinear PA applying pre-distortion methods (APD, DPD, and hybrid approach) for signal envelope bandwidth of 100MHz

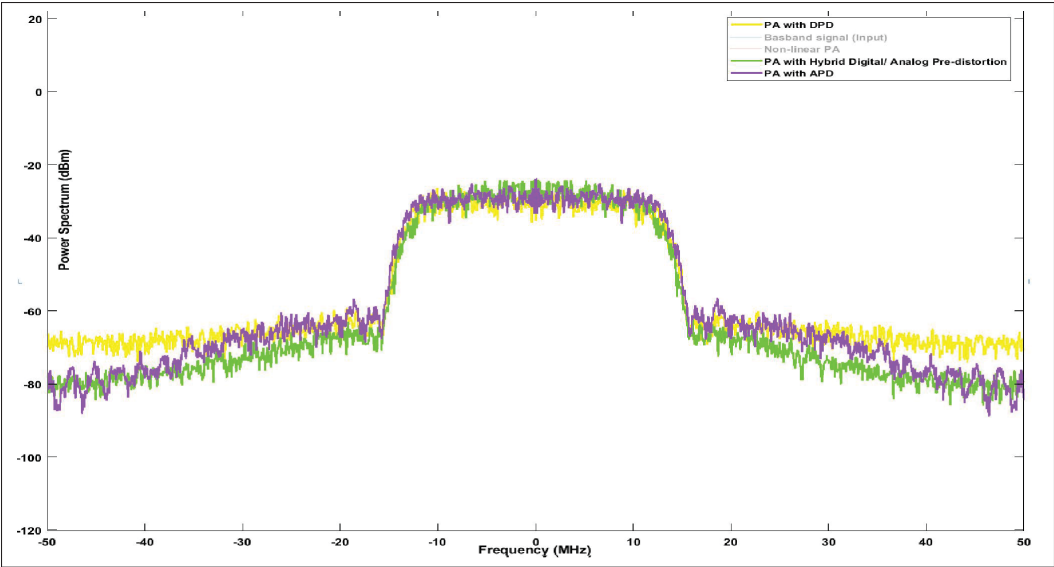


Figure 4.4 Spectrum analyzer for applying pre-distortion methods (APD, DPD, and the hybrid approach) for signal envelope bandwidth of 100MHz

Table 4.1 Compression Results Between DPD Only, APD Only, and Hybrid Digital/Analog Pre-Distortion (ACPR and IMD3 Improvement)

Pre-Distortion Technique	ACPR Improvement (dBc)		IMD3 (dB)	
	100MHz	1GHz	100MHz	1GHz
Signal bandwidth	100MHz	1GHz	100MHz	1GHz
DPD only	12.6	11.6	9.8	10.1
APD only	14.32	12.7	8.08	9
Hybrid digital/analog pre-distortion	20.76	19.59	1.64	1.75

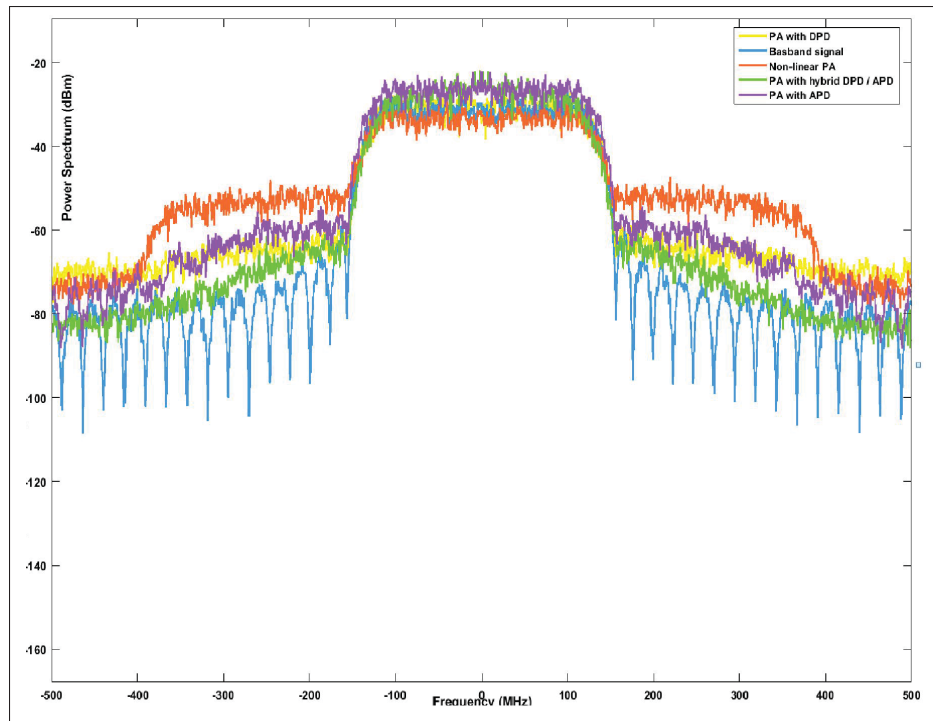


Figure 4.5 Spectrum analyzer for baseband signal and nonlinear PA, applying pre-distortion methods (APD, DPD, and hybrid approach) for signal envelope bandwidth of 1GHz

As can be seen in the results above, the proposed hybrid digital/analog pre-distortion can combine the advantages of both pre-distortion techniques (APD and DPD). In the suggested bandwidths, the proposed hybrid approach achieves the best improvement of ACPR and IMD3 where they are suppressed.

Converting the hybrid digital/analog pre-distortion model from floating-point design to fixed-point design is done by following the implementation steps of converting the DPD model only, as explained in section 3.4.5.

Table 4.2 illustrates the resultant models of 100MHz and 1GHz with different proposed data types giving the same precision for the target ADC. From this, we can visualize how the data type fits the proposed design and whether there are potential overflows or underflows as a result

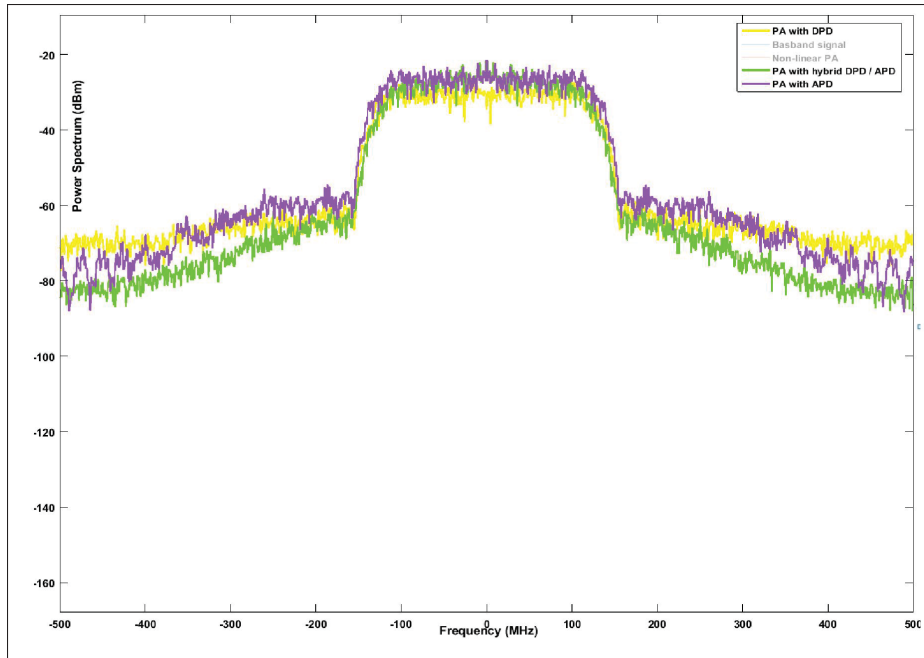


Figure 4.6 Spectrum analyzer for applying pre-distortion methods (APD, DPD, and hybrid approach) for signal envelope bandwidth of 1GHz

of the proposed data type. Tables 4.3 presents a comparison between the DPD model only that was shown from Tables 3.10 to 3.13 and the hybrid digital/analog pre-distortion model.

Table 4.2 Precision of Target ADC in Proposed Hybrid Digital/Analog Pre-Distortion Model for Various Proposed Word-Lengths

Hybrid Digital/Analog Pre-distortion Method	Precision of Target ADC for Various Proposed Word-Lengths					
Proposed bandwidths	16 bit	14 bit	12 bit	10 bit	8 bit	6 bit
100MHz/ 1GHz	2.3841e-7	9.5367e-7	3.8146e-6	1.5258e-5	6.1035e-5	0.0002447

Table 4.3 Visualization of Simulation Using Proposed data type for Target ADCs with Proposed Bandwidth of 100MHz/Hybrid Digital/Analog Pre-Distortion Model



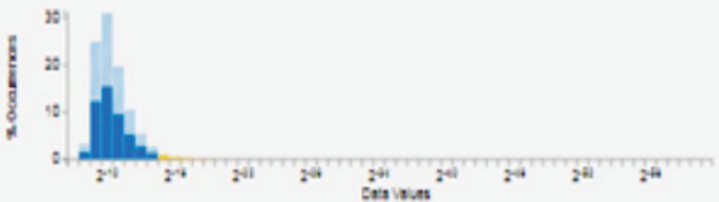
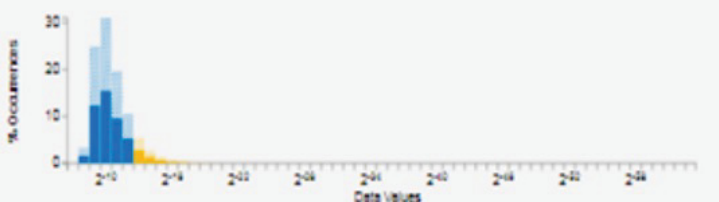
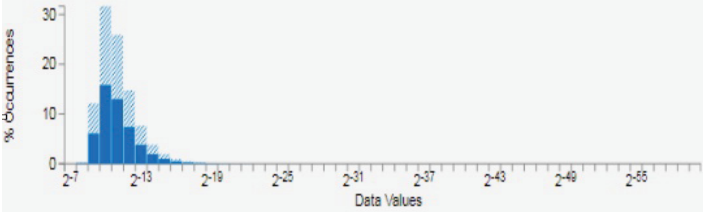
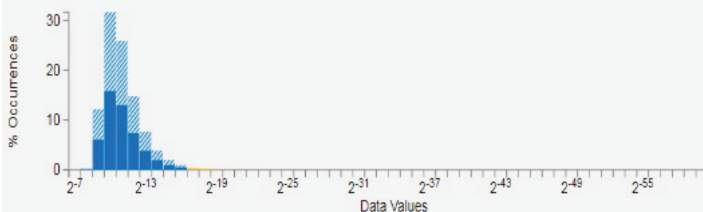
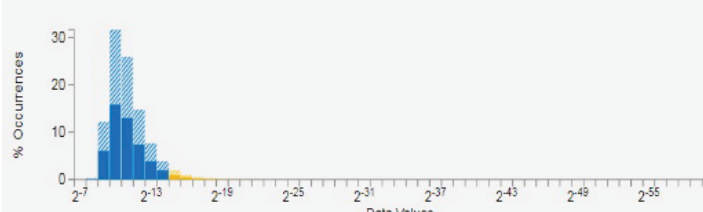
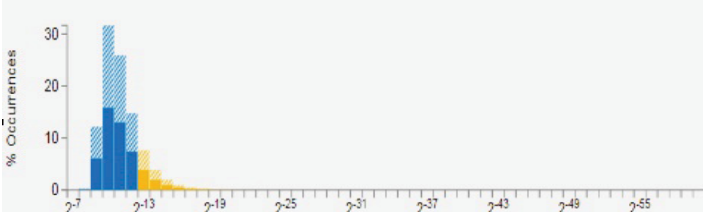
Proposed data type	Visulazation of Simulation Data for Target ADC in Proposed Hybrid Digital/Analog Pre-Distortion model
16 bit	<p data-bbox="646 510 1174 541">Visualization of Simulation Data using fixdt(1,16,22)</p> 
10 bit	<p data-bbox="646 825 1239 856">Visualization of Simulation Data using fixdt(1,10,16)</p> 
8 bit	<p data-bbox="646 1140 1222 1171">Visualization of Simulation Data using fixdt(1,8,14)</p> 
6 bit	<p data-bbox="646 1455 1206 1486">Visualization of Simulation Data using fixdt(1,6,12)</p> 

Table 4.4 Visualization of Simulation Using Proposed Data Type for Target ADCs with Proposed Bandwidth of 1GHz/Hybrid Digital/Analog Pre-Distortion Model

Proposed Date Type	Visulazation of Simulation Data for Target ADC in Proposed Hybrid Digital/Analog Pre-Distortion Model
16 bit	<div>Visualization of Simulation Data using fixdt(1,16,22)</div> 
10 bit	<div>Visualization of Simulation Data using fixdt(1,10,16)</div> 
8 bit	<div>Visualization of Simulation Data using fixdt(1,8,14)</div> 
6 bit	<div>Visualization of Simulation Data using fixdt(1,6,12)</div> 



As a result, we can conclude that by using the hybrid approach, the DPD algorithm will be performed with lower word-length (as low as 8 bit) to achieve lower precision of the target ADC hardware.

Based on the Digi-key website, we can define how many of the selected hardware ADCs exist on the market. The available Pipeline (high-speed) ADC products target the hardware of the suggested model by applying hybrid digital/analog pre-distortion, as shown in Table 4.5.

Table 4.5 Pipeline (high-speed) ADCs Available in the Market for Proposed Hybrid Digital/Analog Pre-Distortion Model

<b>ADCs for Sample-Rate of 100MHz</b>
ADC08100CIMTC/NOPB-ND
AD9288BSTZ-100-ND
AD9287ABCPZ-100-ND
AD9283BRSZ-100-ND
ADC08100CIMTCX/NOPB-ND
ADC08100CIMTC-ND
AD9283BRS-100-ND
AD9283BRS-RL100-ND
AD9283BRSZ-RL100TR-ND,AD9283BRSZ-RL100CT-ND, AD9283BRSZ-RL100DKR-ND
AD9287BCPZRL7-100CT-ND, AD9287BCPZRL7-100DKR-ND
<b>ADCs for Sample-Rate of 1GHz</b>
ADC08D1000CIYB/NOPB-ND
ADC08D1020CIYB/NOPB-ND
ADC081000CIYB/NOPB-ND
ADC08D1000CIYB-ND

Table 4.6 Pipeline (high-speed) ADCs for Proposed Hybrid Digital/Analog Pre-Distortion Model

<b>High-speed ADC</b>	<b>Sampling Rate (Per second)</b>	<b>Number of bits</b>	<b>Cost</b>
AD9288BSTZ-100-ND	100MHz	8 bit	\$35.4
AD9287ABCPZ-100-ND	100MHz	8 bit	\$44.18
ADC081000CIYB/NOPB	1GHz	8 bit	\$189.04
ADC08D1000CIYB/NOPB	1GHz	8 bit	\$507.7
ADC08D1020CIYB/NOPB	1GHz	8 bit	\$633.95

## 4.2 Conclusion

This chapter presented the proposed hybrid digital/analog pre-distortion of the selected GaN PA based on a conventional analog pre-distortion and memory polynomial DPD for the proposed wide-band signals. The proposed hybrid method can combine the advantages of both of the pre-distortion techniques (APD and DPD) for the suggested wide-band signals. The results obtained show excellent agreement with the wide-band signals proposed and the hybrid approach proposed, achieving the strongest ACPR and IMD3 enhancement where they are suppressed. In addition, the bits resolution of the target ADC in the proposed model is reduced as low as 8 bit as Figure 4.7 is illustrated the sample rate as function of resolution bits. The achieved results are proved by reducing the hardware requirements. Overall, the DPD algorithm enables a shortening of word-lengths, thus saving both energy consumption and area requirement upon implementation.

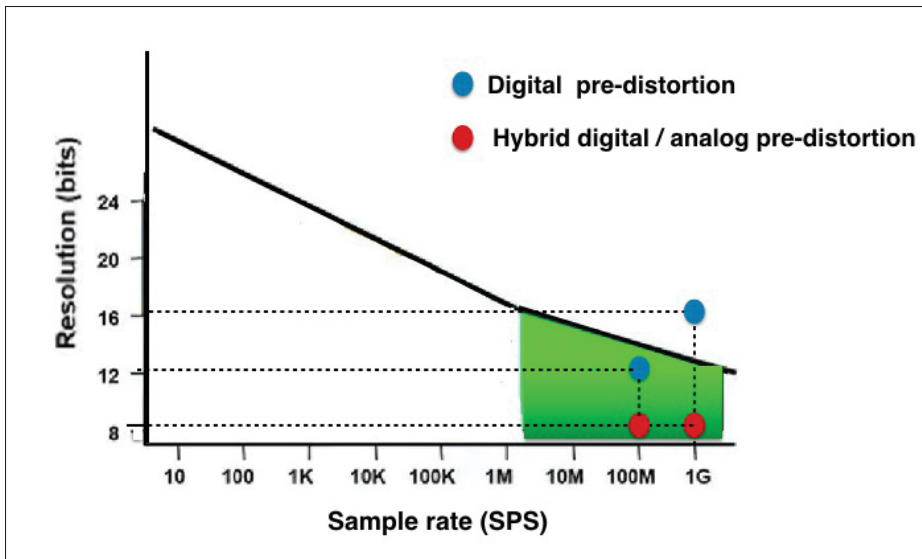


Figure 4.7 Sample rate as function of resolution bits of the target (high-speed ADC) in the proposed model with applying DPD only and Hybrid digital/ analog pre-distortion

## CONCLUSION AND RECOMMENDATIONS

### Conclusion

Wireless technologies have undergone rapid growth both in business and production in recent years, along with smartphones and wireless network devices. However, wireless systems require a wide-band signal and a high sample rate. This has become a significant issue due to increases both in power consumption and system complexity, leading to a subsequent increase in hardware requirements. In these systems, power amplifiers are the primary contributors to energy consumption at the transmission stage, with PAs being the source of the signal distortion. Fortunately, pre-distortion methods are well-suited as linearization techniques.

The main objective of the present work was to combine the advantages of both analog pre-distortion (APD) and digital pre-distortion (DPD) linearization techniques to create the proposed hybrid approach of the selected GaN PA. In so doing, better linearization performance was achieved. At the same time, there was a reduction in hardware requirements by using low-precision ADCs and DACs. This led to the DPD algorithm being performed with a shorter word-length, as well as providing a higher sample rate for the entire DPD algorithm.

The proposed conventional (APD) circuit is suggested Hadouej (2013) in ADS software, where the linearization response of the selected GaN PA with its inverse function is obtained. A baseband digital pre-distortion method with memory effect was also proposed with various wide-band signals, which were designed and modeled using Simulink/MATLAB in double-precision floating-point design to give us the ideal numerical behavior. Our results provide evidence that the drawback of the DPD technique is obvious in the wide-band signal, causing low linearization performance. To account for the right hardware of our model, Simulink highlighted some features in the fixed-point design to convert the ideal floating-point design model that meets the constraints of the target hardware. This step is required as, in a practical system, the PA's analog output must convert in an ADC to allow training to be conducted using digital processing. This

is done with a fixed-point tool in order to determine how many bits of resolution are needed for the DPD.

By applying just the DPD technique, our findings indicated that the DPD algorithm performed with a longer word-length achieved lower precision of the target ADC hardware of each suggested wide-band signal. The broad implication of the present research is that it would be warranted to combine the previous proposed conventional APD and the proposed BB-DPD methods to create the suggested hybrid approach of the selected GaN PA.

To the best of our knowledge, this is the first report aiming to study how to achieve lower hardware requirements by reducing the resolution bits in the target hardware in the hybrid digital/analog pre-distortion system. The present findings confirm the advantages of each of these techniques and show that they complete each other. Overall, our results demonstrate a strong effect of the hybrid approach to achieve better linearization performance of the suggested wide-band signals for the improvement IMD3, the ACPR and to reduce the resolution bits as low as 6 bit and 8 bit of the target ADC. Certainly, there is evidence here that the system's complexity can be reduced, leading to savings in the area. It may also help to reduce the carbon footprint of wireless communication systems.

**Future work**

- Interesting research questions for future research can be derived from the implementation of this study in a real-world system. The analog pre-distortion circuit and the selected GaN PA should first be fabricated. When both circuits are combined into a single chip/circuitry design using a multilayer LTCC technology substrate where the components of the resistors and capacitors (RC) are embedded within the LTCC substratum, this would be a new approach. In addition, applying the real-time circuit with the proposed DPD would create lead to an outcome similar to that provided by the proposed hybrid approach of this study.
- Future research could examine the proposed whole system with the right hardware for each proposed model in order to capture the results in a real-world system.



## APPENDIX I

### SELECTED GAN POWER AMPLIFIER

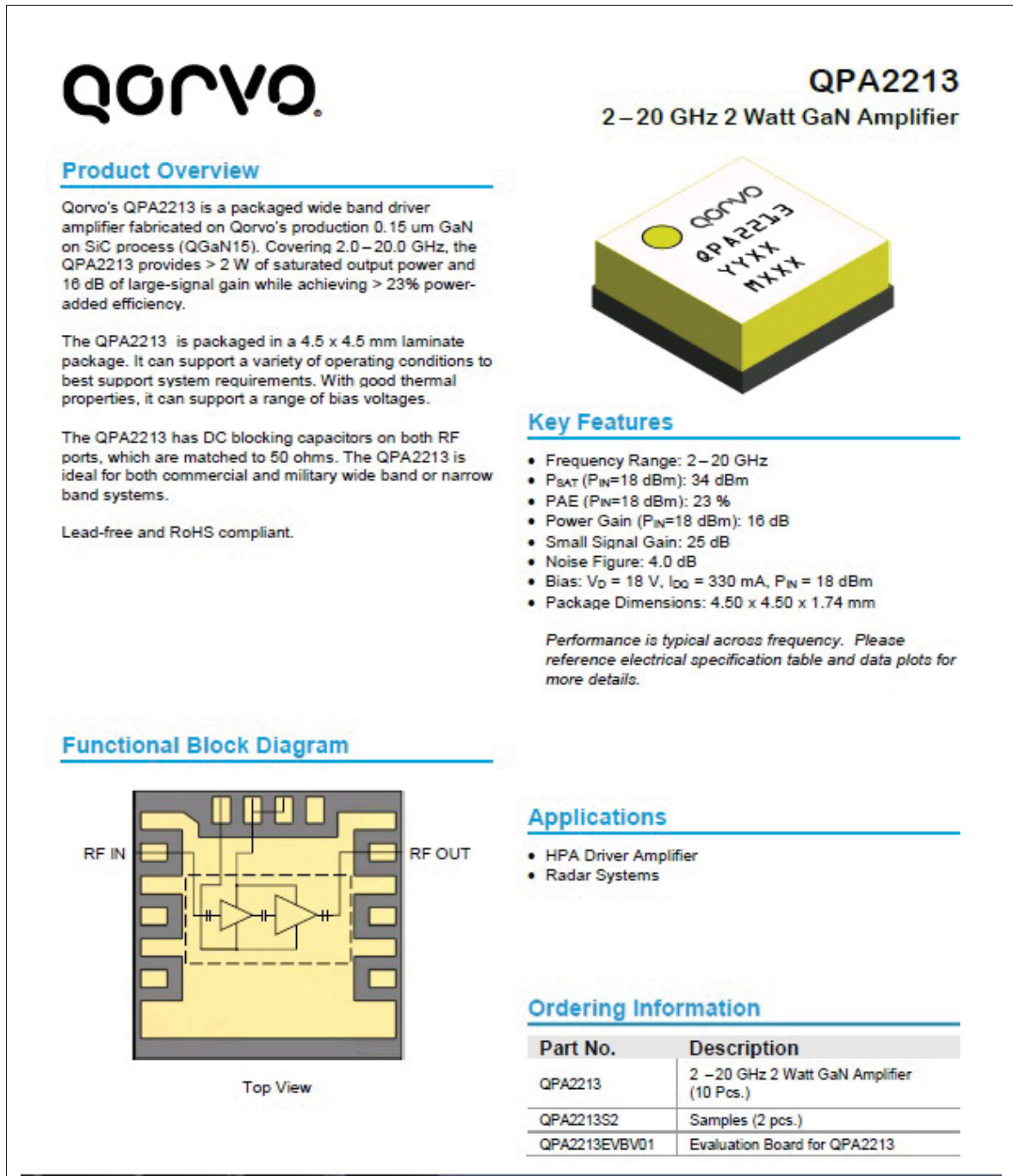


Figure-A I-1 Data Sheet of QPA2213 2-20GHz 2Watt GaN Amplifier



**QPA2213**  
2 – 20 GHz 2 Watt GaN Amplifier

### Electrical Specifications

Parameter		Min	Typ	Max	Units
Operational Frequency		2		20	GHz
Output Power ( $P_{IN}=18$ dBm)	2 GHz		34.2		dBm
	6 GHz		35.5		dBm
	10 GHz		34.2		dBm
	15 GHz		34.0		dBm
	20 GHz		33.3		dBm
Power Added Efficiency ( $P_{IN}=18$ dBm)	2 GHz		36.9		%
	6 GHz		22.5		%
	10 GHz		23.6		%
	15 GHz		21.5		%
	20 GHz		20.4		%
Small Signal Gain	2 GHz		25.3		dB
	6 GHz		26.0		dB
	10 GHz		24.8		dB
	15 GHz		22.9		dB
	20 GHz		21.4		dB
Input Return Loss	2 GHz		18		dB
	6 GHz		16		dB
	10 GHz		12		dB
	15 GHz		14		dB
	20 GHz		29		dB
Output Return Loss	2 GHz		7		dB
	6 GHz		15		dB
	10 GHz		19		dB
	15 GHz		19		dB
	20 GHz		26		dB
Noise Figure	2 GHz		7.6		dB
	6 GHz		4.4		dB
	10 GHz		3.2		dB
	15 GHz		4.0		dB
	20 GHz		5.3		dB
IMD3 ( $P_{OUT}/\text{Tone}=27$ dBm) (100 MHz tone spacing)	2 GHz		-23.0		dBc
	6 GHz		-21.7		dBc
	10 GHz		-21.9		dBc
	15 GHz		-21.4		dBc
	20 GHz		-19.8		dBc
$P_{OUT}$ Temp. Coeff. (85 °C to 25 °C, $P_{IN} = 18$ dBm))			-0.006		dB/°C
Sm. Sig. Gain Temp. Coefficient (85 °C to -40 °C)			-0.043		dB/°C

Test conditions, unless otherwise noted:  $T = 25$  °C,  $V_D = 18$  V,  $I_{DD} = 330$  mA

Figure-A I-2 Electrical Specification of QPA2213 2-20GHz 2Watt GaN Amplifier



## APPENDIX II

### SCOTTKY DIODE SMS392X SERIES OF DIODES



**SKYWORKS**

**DATA SHEET**

**SMS392x Series: Surface-Mount General-Purpose Schottky Diodes**

**Applications**

- High volume commercial detectors, mixers, switches, and digital pulse forming systems

**Features**

- Tight parameter distribution
- Available as singles and dual series pairs
- 100 percent DC tested
- Packages rated MSL1, 260 °C per JEDEC J-STD-020



Skyworks Green™ products are compliant with all applicable legislation and are halogen-free. For additional information, refer to Skyworks *Definition of Green™*, document number SQ04-0074.



Four surface-mount Schottky diodes are shown in different packages: SOT-23, SC-79, SC-88, and SOD-882.

**Description**

The SMS3922, SMS3923, and SMS3924 series of 8, 20, and 70 V rated, low-cost plastic packaged Schottky diodes are designed for general purpose use in RF applications. All diodes are fully characterized, including SPICE model parameters, and deliver tight parameter distribution, which minimizes performance variability.

Wiring configurations include singles and dual series pairs. The SMS392x series of diodes may be used at frequencies up to 6 GHz.

Table 1 describes the various packages and marking of the SMS392x series.

Figure-A II-1 Data Sheet of SCOTTKY Diode SMS392X Series

## DATA SHEET • SMS392x SCHOTTKY DIODES

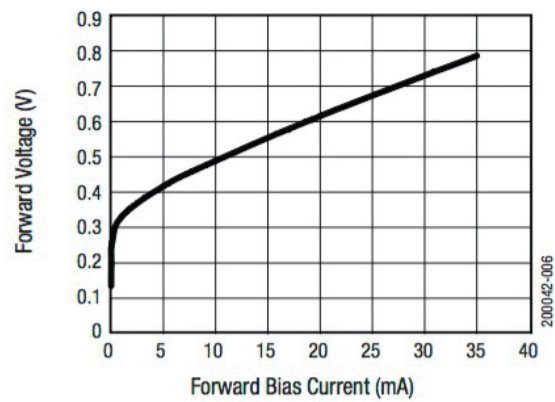
**Figure 6. SMS3923-081LF Series Forward Voltage vs Forward Bias Current**

Figure-A II-2 SMS392X Series Forward Voltage vs Forward Bias Current

## APPENDIX III

### LMS AND RPEM ALGORITHM

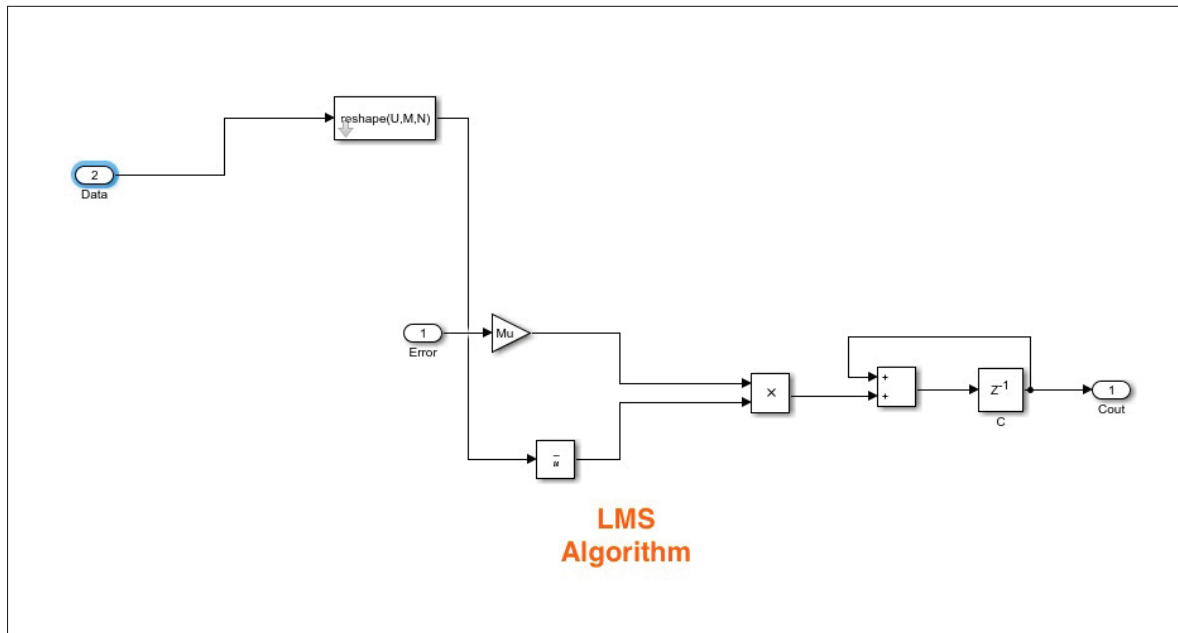


Figure-A III-1 LMS Algorithm/ Matlab-Simulink

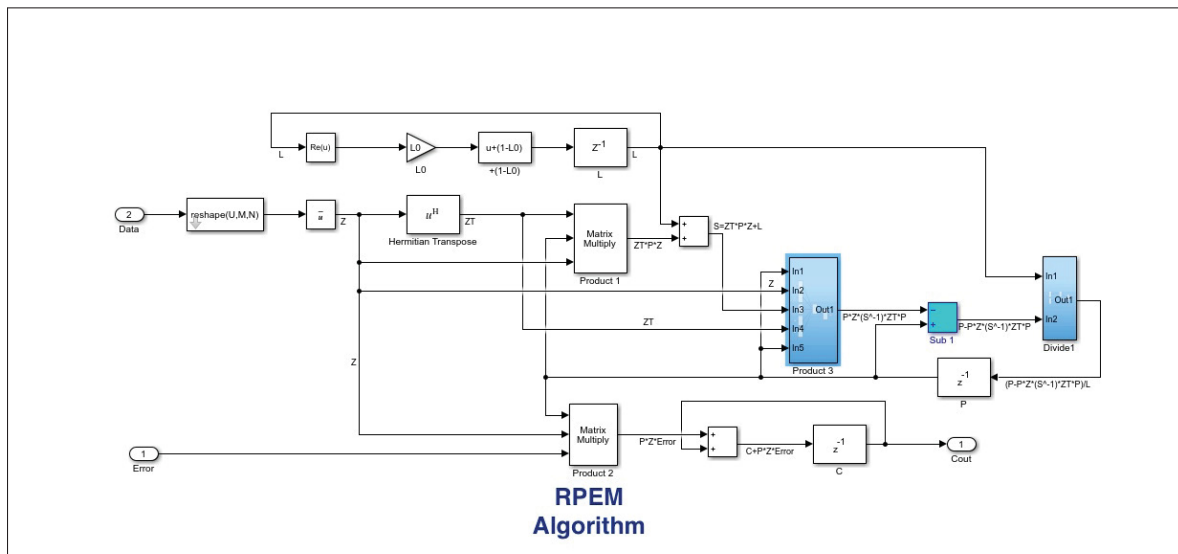


Figure-A III-2 RPEM Algorithm/ Matlab-Simulink



## APPENDIX IV

## CONVERTING DPD SIMULINK MODEL TO FIXED-POINT DESIGN MODEL

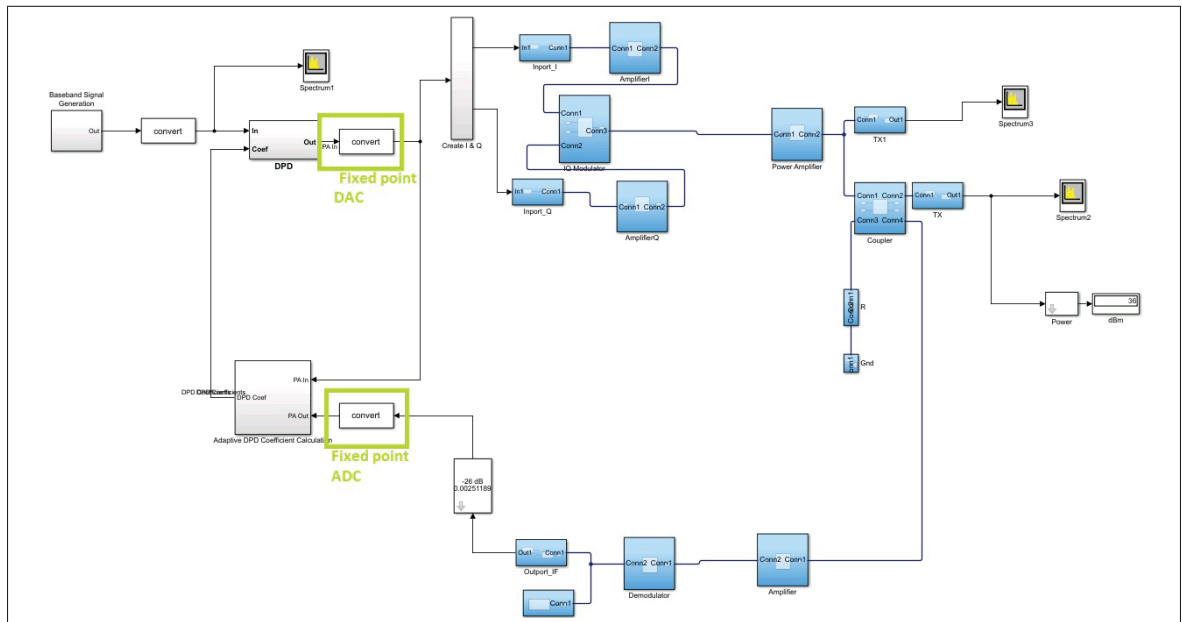


Figure-A IV-1 Converting DPD Simulink model to fixed-point design model/  
Matlab-Simulink



## APPENDIX V

### SIMPLE FAST-FITTING PROCEDURE/ MATLAB-CODE

```
1 function varargout =amp_helper(proc,varargin)
2 %   %AMP_HELPER
3 % Helper function to perform various functionality for power amp example.
4 % Each of the cases below returns a single variable.
5 %
6 % coefficientMatrix =
7 %   amp_helper('coefficientFinder',x,y,memLen,degLen,modType)
8 %
9 % outputSignal =
10 %   amp_helper('signalGenerator',x,coefMat,modType)
11 %
12 % signalError =
13 %   amp_helper('errorMeasure',x,y,coefMatFit,modType)
14 %
15
16 % Copyright 2017 The MathWorks, Inc.
17
18 % Check number of outputs
19 nargoutchk(1, 1)
20
21
22 switch proc
23 case 'coefficientFinder'
24     % Procedure to compute the coefficient matrix given input and
25     % output signals, memory length, degree, and model type
26
27     % modType
28     %   memPoly:   Memory polynomial
29     %   ctMemPoly: Cross-term memory polynomial
30
31     % Check number of inputs and assign values
32     narginchk(6,6)
33     x      = varargin{1};
34     y      = varargin{2};
35     memLen = varargin{3};
36     degLen = varargin{4};
37     modType = varargin{5};
38
39     % Length of input vector
40     xLen = length(x);
41     x = x(:);
42     y = y(:);
43
```

```

44 % Compute input variable term for each entry in coefficient matrix
45 switch modType
46 case 'memPoly'
47     xrow = reshape((memLen:-1:1)' + (0:xLen:xLen*(degLen-1)),1,[]);
48     xVec = (0:xLen-memLen)' + xrow;
49     xPow = x.*(abs(x).^(0:degLen-1));
50     xVec = xPow(xVec);
51 case 'ctMemPoly'
52     absPow = (abs(x).^(1:degLen-1));
53     partTop1 = reshape((memLen:-1:1)' + (0:xLen:xLen*(degLen-2)), ...
54         1,[]);
55     topPlane = reshape( ...
56         [ones(xLen-memLen+1,1), ...
57         absPow((0:xLen-memLen)' + partTop1)].', ...
58         1,memLen*(degLen-1)+1,xLen-memLen+1);
59     sidePlane = reshape(x((0:xLen-memLen)' + (memLen:-1:1)).', ...
60         memLen,1,xLen-memLen+1);
61     cube = sidePlane.*topPlane;
62     xVec = reshape(cube,memLen*(memLen*(degLen-1)+1), ...
63         xLen-memLen+1).';
64 end
65
66 % Use MATLAB \ operator to generate a least-squares solution to the
67 % overdetermined problem. Reshape xTerms where a row is each term
68 % of the coefficient matrix expanded along columns at a particular
69 % instant of time.
70 coef = xVec\y(memLen:xLen);
71 % Output coefficient matrix (coefMat)
72 varargout{1} = reshape(coef,memLen,numel(coef)/memLen);
73
74 case 'signalGenerator'
75     % Generate output signal for narrowband power amplifier using an
76     % input signal
77
78     % Check number of inputs and assign values
79     narginchk(4,4)
80     x = varargin{1};
81     coefMat = varargin{2};
82     modType = varargin{3};
83

```



```

84      % Handle setup constants
85      [memLen, numCols] = size(coefMat);
86      memLenM1 = memLen-1;
87      coefReshaped = reshape(coefMat,1,memLen*numCols);
88      xLen = length(x);
89      y = zeros(xLen,1);
90
91      % modType
92      %   memPoly:   Memory polynomial
93      %   ctMemPoly: Cross-Term memory
94      switch modType
95      case 'memPoly'
96          degLen = numCols;
97          for timeIdx = memLen:xLen
98              % Common input variable entry terms for all rows in
99              % coefficient matrix
100             xTerms = zeros(1,memLen*degLen);
101             xTime = x(timeIdx-(0:memLenM1));
102             xTerms(1,1:memLen) = xTime;
103             for degIdx = 2:degLen
104                 degIdxM1 = degIdx-1;
105                 startPos = degIdxM1*memLen+1;
106                 endPos = startPos+memLenM1;
107                 xTerms(1,startPos:endPos) = ..
108                     xTime.*(abs(xTime).^degIdxM1);
109             end
110             y(timeIdx) = coefReshaped*xTerms(:);
111         end
112     case 'ctMemPoly'
113         degLen = round((numCols-1)/memLen)+1;
114         degLenM1 = degLen-1;
115         for timeIdx = memLen:xLen
116             % Common input variable entry terms for all rows in
117             % coefficient matrix
118             xTime = x(timeIdx-(0:(memLenM1)));
119             xRow = [1 zeros(1,numCols-1)];
120             for powIdx = 1:degLenM1
121                 startPos = 2+memLen*(powIdx-1);
122                 endPos = startPos+memLenM1;
123                 xRow(startPos:endPos) = abs(xTime).^powIdx;
124             end

```

```

125         % Generate all individual terms for output signal
126 -       xTerms = xTime(:)*xRow;
127         % Multiply each term by appropriate coefficient
128 -       y(timeIdx) = coefReshaped*xTerms(:);
129 -     end
130         % Output generated output signal
131 -     end
132     varargout{1} = y;
133
134 - case 'errorMeasure'
135     % Compute coefMat and output signal error measures
136
137     % Check number of inputs and assign values
138 -     narginchk(5,5)
139 -     x          = varargin{1};
140 -     y          = varargin{2};
141 -     CoefMat = varargin{3};
142 -     modType   = varargin{4};
143
144 -     memLen = size(CoefMat,1);
145 -     y_prediction = zeros(size(y));
146 -     y_prediction(:) = amp_helper('signalGenerator', ...
147 -         x, CoefMat, modType);
148 -     M = abs(y(memLen:end));
149 -     difference = abs(y(memLen:end)-y_prediction(memLen:end))./M;
150
151     % Output error measure (errSig)
152 -     varargout{1} = std(difference)*100;
153 - end
154
155 - end % [EOF]

```

## APPENDIX VI

### CALCULATING THE COEFFICIENT OF PA/ MATLAB-CODE

1	%% Read and visualize measured PA input/output data	
2	load('maaaaa.mat')	
3	datarate = 1000000000;	
4	Tstep = 1/datarate;	
5	%% Plot PA input/output measurements	
6	numDataPts = length(iii);	
7	plot((1:numDataPts)*Tstep, abs(iii),	...
8	(1:numDataPts)*Tstep, abs(ooo))	
9	legend('Abs(In)', 'Abs(Out)', 'Location', 'northeast')	
10	xlabel('Time (s)')	
11	xlim([0 1e-5])	
12	ylabel('Voltage (V)')	
13	title('Absolute Values of Input and Output Voltage Signals')	
14		
15	%% plot PA power transfer function	
16		
17	TransferPA = abs(ooo./iii);	
18	plot(abs(iii./0.25), 20*log10(TransferPA), '.')	
19	xlabel('Normalized Input Voltage Absolute Value(V)')	
20	ylabel('Magnitude Power Gain (dB)')	
21	title('Power Gain Transfer Function')	
22	%% PLOT PA output vs input	
23	Pin = abs (iii./0.25);	
24	Pot = abs(ooo./3);	
25	plot((Pin), (Pot), '.')	
26	xlabel('Normalized Voltage-Input (V)')	
27	ylabel('Normalized Voltage-Output (V)')	
28	title('Transfer Function')	
29	%% Determine PA Block coefficient matrrix from measured signals	
30	memLen = 3;	
31	degLen = 7;	
32	numDataPts = length(iii);	
33	halfdatapts = round(numDataPts/2);	
34		

35	%% The helper function supports the possibility to chose different memory models	
36	modType = 'memPoly';	
37	%% plot fitting results	
38	Coff = amp_helper('coefficientFinder',	...
39	iii(1:halfdatapts), ooo(1:halfdatapts), memLen, degLen, modType);	
40		
41	[errSig] = amp_helper('errorMeasure', iii, ooo, Coff, modType);	
42	disp(['Signal standard deviation = ' num2str(errSig) '%'])	
43		
44	Pout_fit = amp_helper('signalGenerator',	...
45	iii, Coff, modType);	
46	plot((1:numDataPts)*Tstep1, abs(ooo), 'o-',	...
47	(1:numDataPts)*Tstep1, abs(Pout_fit), 'b-')	
48	xlabel('Time (s)')	
49	ylabel('Voltage (V)')	
50	xlim([0 1e-5])	
51	legend('Abs(Out)', 'Abs(OutFit)', 'Location', 'northeast')	
52	title('Absolute Values of Output and Fitted Output Signals')	
53	%% To visualize both the measured output signal and the fitted output	
54	%signal, plot the time-domain output voltage (We also plot the magnitude of the power transfer function):	
55		
56	TransferPA_fit = abs(Pout_fit./ooo(:));	
57	plot(abs(iii), 20*log10(TransferPA), 'o',	...
58	abs(iii), 20*log10(TransferPA_fit), 'b-')	
59	xlabel('Input Voltage Absolute Value(V)')	
60	ylabel('Magnitude Power Gain (dB), Phase Power Gain')	
61	legend('Abs Gain', 'Abs Gain Fit', 'Location', 'northeast')	
62	title('Power Gain Transfer Function')	

```

63
64 %% Improve Fitting with Memory Polynomial Model Including Cross Terms
65 % We now determine the fitted coefficient matrix from the input and output
66 % characteristics by using a different approach that includes leading and
67 % lagging memory cross terms.
68 %We use the same helper function, but we use a different model type.
69 - modType = 'ctMemPoly';
70 - Coff = amp_helper('coefficientFinder', ...
71     iii(1:halfdatapts),ooo(1:halfdatapts),memLen,degLen,modType);
72
73 - [errSig] = amp_helper('errorMeasure', ...
74     iii, ooo, Coff, modType);
75 - disp(['Signal standard deviation = ' num2str(errSig)])
76 - Pout_fit = amp_helper('signalGenerator', ...
77     iii, Coff, modType);
78 - plot((1:numDataPts)*Tstep1, abs(ooo), 'o-', ...
79     (1:numDataPts)*Tstep1, abs(Pout_fit), '-.')
80 - xlabel('Time (s)')
81 - ylabel('Voltage (V)')
82 - xlim([0 1e-5])
83 - legend('Abs(Out)', 'Abs(OutFit)', 'Location', 'northeast')
84 - title('Absolute Values of Output and Fitted Output Signals')
85
86 - %%
87 - TransferPA_fit = abs(ooo./iii(:));
88 - plot(abs(iii./0.25), 20*log10(TransferPA), 'o', ...
89     abs(iii./0.25), 20*log10(TransferPA_fit), '-')
90 - xlabel('Normalized Input Voltage Absolute Value(V)')
91 - ylabel('Magnitude Power Gain (dB)')
92 - legend('Abs Gain', 'Abs Gain Fit', 'Location', 'northeast')
93 - title('Power Gain Transfer Function')
94
95 %% % At last, we save the coefficient matrix of the PA model that we will
96 % import and use in RF Blockset for simulation at the system-level.
97 %
98
99 - save('maaaaa.mat', 'Coff')

```

## APPENDIX VII

### POWER GAIN TRANSFER FUNCTION AND ITS FITTING

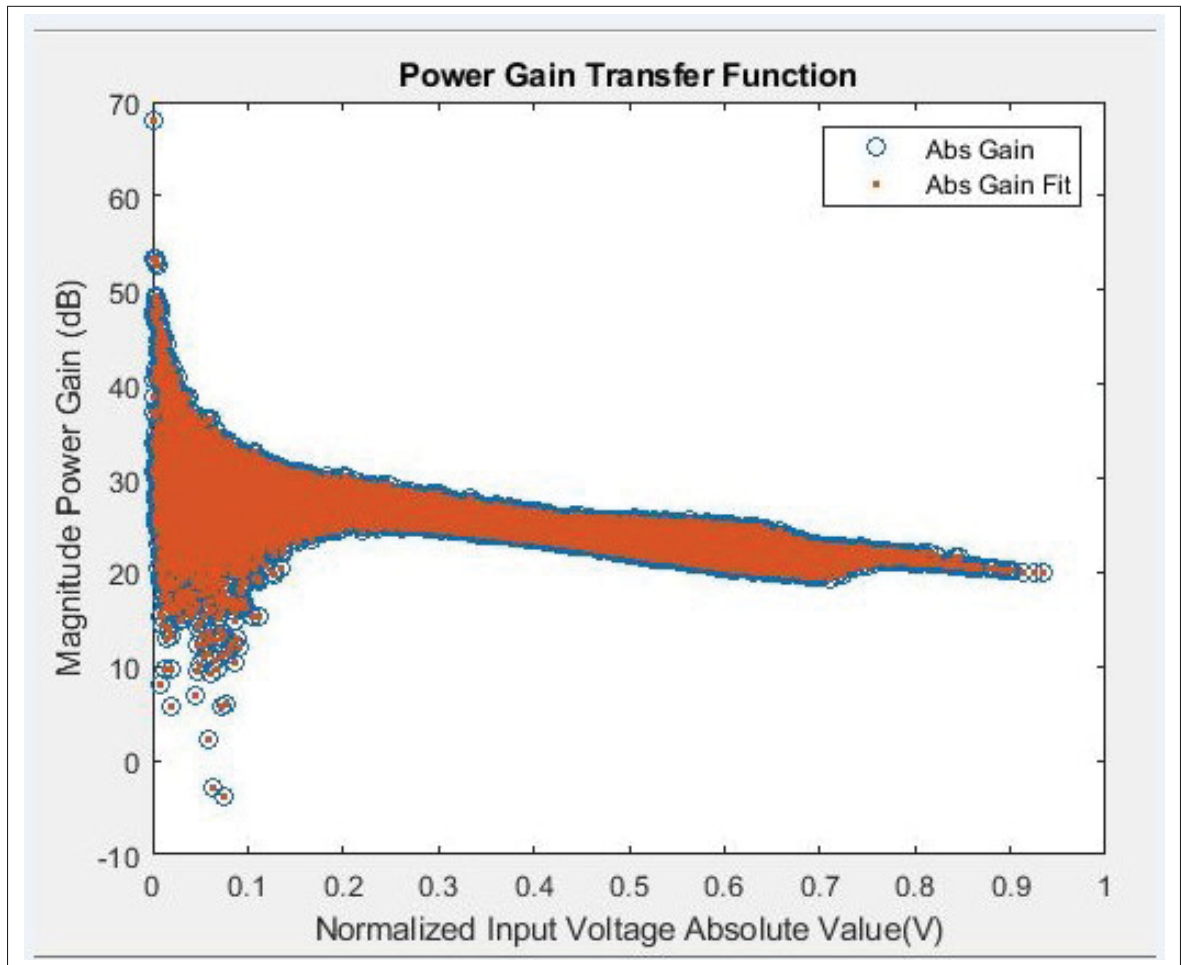


Figure-A VII-1 Power gain transfer function and its fitting with memory effect





## BIBLIOGRAPHY

- Abi Hussein, M., Bohara, V. A. & Venard, O. (2012). On the system level convergence of ILA and DLA for digital predistortion. *2012 International Symposium on Wireless Communication Systems (ISWCS)*, pp. 870–874.
- Aguilar-Lobo, L. M., Garcia-Osorio, A., Loo-Yau, J. R., Ortega-Cisneros, S., Moreno, P., Rayas-Sánchez, J. E. & Reynoso-Hernández, J. A. (2014). A digital predistortion technique based on a NARX network to linearize GaN class F power amplifiers. *2014 IEEE 57th International Midwest Symposium on Circuits and Systems (MWSCAS)*, pp. 717–720.
- Ai, B., Yang, Z.-x., Pan, C.-y., Tang, S.-g. & Zhang, T.-t. (2007). Analysis on LUT based predistortion method for HPA with memory. *IEEE transactions on broadcasting*, 53(1), 127–131.
- Aschbacher, E. & Rupp, M. (2003). Modelling and identification of a nonlinear power-amplifier with memory for nonlinear digital adaptive pre-distortion. *2003 4th IEEE Workshop on Signal Processing Advances in Wireless Communications-SPAWC 2003 (IEEE Cat. No. 03EX689)*, pp. 658–662.
- Bache, M. (2015). *Digital Predistortion Linearization of Power Amplifier for X-band Radar System*. (Master's thesis, NTNU).
- Ball, S. (2001). Analog-to-digital converters. *Embedded Systems Programming*, 10–25.
- Barradas, F. M., Cunha, T. R., Lavrador, P. M. & Pedro, J. C. (2014). Polynomials and LUTs in PA behavioral modeling: A fair theoretical comparison. *IEEE Transactions on microwave theory and techniques*, 62(12), 3274–3285.
- Bortoni, R., Noceti Filho, S. & Seara, R. (2002). On the design and efficiency of class A, B, AB, G, and H audio power amplifier output stages. *Journal of the Audio Engineering Society. Audio Engineering Society*, 50, 547-563.
- Braithwaite, R. N. (2015). A comparison of indirect learning and closed loop estimators used in digital predistortion of power amplifiers. *2015 IEEE MTT-S International Microwave Symposium*, pp. 1–4.
- Chang, S.-L. & Ogunfunmi, T. (1998). LMS/LMF and RLS Volterra system identification based on nonlinear Wiener model. *ISCAS'98. Proceedings of the 1998 IEEE International Symposium on Circuits and Systems (Cat. No. 98CH36187)*, 5, 206–209.
- Cho, M. (2016). *Analog predistortion for improvement of RF power amplifier efficiency and linearity*. (Ph.D. thesis, Georgia Institute of Technology).

- Colantonio, P., Giannini, F. & Limiti, E. (2009). *High efficiency RF and microwave solid state power amplifiers*. John Wiley & Sons.
- Costa, E., Midrio, M. & Pupolin, S. (1999). Impact of amplifier nonlinearities on OFDM transmission system performance. *IEEE Communications Letters*, 3(2), 37–39.
- Ding, L., Zhou, G. T., Morgan, D. R., Ma, Z., Kenney, J. S., Kim, J. & Giardina, C. R. (2004). A robust digital baseband predistorter constructed using memory polynomials. *IEEE Transactions on communications*, 52(1), 159–165.
- Farrow, C. L., Shaw, M., Kim, H., Juhás, P. & Billinge, S. J. (2011). Nyquist-Shannon sampling theorem applied to refinements of the atomic pair distribution function. *Physical Review B*, 84(13), 134105.
- Ghorbani, A. & Sheikhan, M. (1991). The effect of solid state power amplifiers (SSPAs) nonlinearities on MPSK and M-QAM signal transmission. *1991 Sixth International Conference on Digital Processing of Signals in Communications*, pp. 193–197.
- Guo, Y. & Cavallaro, J. R. (2002). A novel adaptive pre-distorter using LS estimation of SSPA non-linearity in mobile OFDM systems. *2002 IEEE International Symposium on Circuits and Systems. Proceedings (Cat. No. 02CH37353)*, 3, III–III.
- Gutierrez, H., Gard, K. & Steer, M. B. (1999). Spectral regrowth in microwave amplifiers using transformation of signal statistics. *1999 IEEE MTT-S International Microwave Symposium Digest (Cat. No. 99CH36282)*, 3, 985–988.
- Hadouej, T. (2013). *Linéarisation par pré-distorsion cubique d'un tube à ondes progressives en bande C*. (Ph.D. thesis, École de technologie supérieure).
- Hoeschele, D. F. (1994). *Analog-to-digital and digital-to-analog conversion techniques*. Wiley New York.
- Hsia, C., Kimball, D. F. & Asbeck, P. M. (2011). Effect of maximum power supply voltage on envelope tracking power amplifiers using GaN HEMTs. *2011 IEEE Topical Conference on Power Amplifiers for Wireless and Radio Applications*, pp. 69–72.
- Imai, N., Nojima, T. & Murase, T. (1989). Novel linearizer using balanced circulators and its application to multilevel digital radio systems. *IEEE transactions on microwave theory and techniques*, 37(8), 1237–1243.
- Iwamoto, M., Williams, A., Chen, P.-F., Metzger, A. G., Larson, L. E. & Asbeck, P. M. (2001). An extended Doherty amplifier with high efficiency over a wide power range. *IEEE Transactions on Microwave Theory and Techniques*, 49(12), 2472–2479.



- Katz, A. & Dorval, R. (2012). Linearizing high power amplifiers (with emphasis on predistortion and GaN devices). *2012 IEEE Topical Conference on Power Amplifiers for Wireless and Radio Applications*, pp. 33–36.
- Katz, A., Wood, J. & Chokola, D. (2016). The evolution of PA linearization: From classic feedforward and feedback through analog and digital predistortion. *IEEE Microwave Magazine*, 17(2), 32–40.
- Keith, B. (2017). GaN Breaks Barriers—RF Power Amplifiers Go Wide and High. Consulted at <https://www.analog.com/en/applications/technology/gan.html>.
- Kenington, P. B. (2000). *High linearity RF amplifier design*. Artech House, Inc.
- Liu, Y.-J., Zhou, J., Chen, W. & Zhou, B.-H. (2013). A robust augmented complexity-reduced generalized memory polynomial for wideband RF power amplifiers. *IEEE Transactions on Industrial Electronics*, 61(5), 2389–2401.
- Madero-Ayora, M., Barataud, D., El Dine, M. S., Neveux, G., Nebus, J.-M., Reina-Tosina, J., Allegue-Martinez, M. & Crespo-Cadenas, C. (2011). Baseband digital predistortion of a 10 W GaN power amplifier. *2011 41st European Microwave Conference*, pp. 341–344.
- Mathews, V. J. & Sicuranza, G. (2000). *Polynomial signal processing*. John Wiley & Sons, Inc.
- Mkadem, F. & Boumaiza, S. (2011). Physically inspired neural network model for RF power amplifier behavioral modeling and digital predistortion. *IEEE Transactions on Microwave Theory and Techniques*, 59(4), 913–923.
- Morgan, D. R., Ma, Z., Kim, J., Zierdt, M. G. & Pastalan, J. (2006). A generalized memory polynomial model for digital predistortion of RF power amplifiers. *IEEE Transactions on signal processing*, 54(10), 3852–3860.
- Nordsjo, A. (2002). An algorithm for adaptive predistortion of certain time-varying nonlinear high-power amplifiers.
- Pozar, D. M. (1998). *Microwave engineering*, johnwiley & sons. Inc., New York, 367–368.
- Pozar, D. M. (2000). *Microwave and RF design of wireless systems*. John Wiley & Sons.
- Pozar, D. M. (2005). *Microwave engineering* 3rd ed., ma john wiley & sons. Inc.
- Raich, R., Qian, H. & Zhou, G. T. (2004). Orthogonal polynomials for power amplifier modeling and predistorter design. *IEEE transactions on vehicular technology*, 53(5), 1468–1479.

- Rapp, C. (1991). Effects of HPA-nonlinearity on a 4-DPSK/OFDM-signal for a digital sound broadcasting signal. *ESASP*, 332, 179–184.
- Santella, G. & Mazzenga, F. (1998). A hybrid analytical-simulation procedure for performance evaluation in M-QAM-OFDM schemes in presence of nonlinear distortions. *IEEE Transactions on Vehicular Technology*, 47(1), 142–151.
- Schutz, K. (2014). Adaptive DPD Design. Consulted at <https://www.mathworks.com/matlabcentral/fileexchange/45890-adaptive-dpd-design>.
- Srirattana, N., Raghavan, A., Heo, D., Allen, P. E. & Laskar, J. (2005). Analysis and design of a high-efficiency multistage Doherty power amplifier for wireless communications. *IEEE Transactions on Microwave Theory and Techniques*, 53(3), 852–860.
- Tarver, C. & Cavallaro, J. R. (2017). Digital predistortion with low-precision ADCs. *2017 51st Asilomar Conference on Signals, Systems, and Computers*, pp. 462–465.
- Texas Instruments. (2018). Choose the right A/D Converter for your application. Consulted at <https://www.ti.com>.
- Tomé, P. M., Barradas, F. M., Cunha, T. R. & Pedro, J. C. (2018). Hybrid analog/digital linearization of GaN HEMT-based power amplifiers. *IEEE Transactions on Microwave Theory and Techniques*, 67(1), 288–294.
- Walt, D. (2016). Gauging the state of GaN power amplification. Consulted at <https://www.analog.com/en/technical-articles/gauging-the-state-of-gan-power-amplification.html>.
- Wikipedia. (2020). Predistortion. Consulted at <https://en.wikipedia.org/wiki/Predistortion>.
- Woo, W., Miller, M. D. & Kenney, J. S. (2005). A hybrid digital/RF envelope predistortion linearization system for power amplifiers. *IEEE Transactions on Microwave Theory and Techniques*, 53(1), 229–237.
- Wu, H.-J., Xia, J., Zhai, J.-F., Tian, L., Yang, M.-S., Zhang, L. & Zhu, X.-W. (2012). A wideband digital pre-distortion platform with 100 MHz instantaneous bandwidth for LTE-advanced applications. *2012 Workshop on Integrated Nonlinear Microwave and Millimetre-Wave Circuits*, pp. 1–3.
- Xie, X. (2017). *Combined linearization of both analog and digital pre-distortion for broadband radio over fiber transmission*. (Ph.D. thesis, Concordia University).